ABSTRACT

ROUSE, JILLIAN GRACE. Effects of Mechanical Stimuli on Biological Interactions with Amino Acid-Derivatized Fullerenes at the Tissue and Cellular Levels. (Under the direction of Dr. Nancy A. Monteiro-Riviere).

Engineered nanomaterials have structural features with at least one dimension in the 1–100 nm range. Because of their small size, nanoparticles possess unique chemical, mechanical, electrical, optical, magnetic, and biological properties that make them ideal candidates for a variety of novel commercial and medical applications. Particularly, carbon-based nanomaterials such as fullerenes, nanotubes, and nanowires are considered key elements in the development of new nano-applications with the potential to be used in everything from biomedicine and drug delivery systems to nanoelectronics and energy conservation mechanisms. Relatively unknown, however, is how exposure to nanoscale particles effects normal biological functions and processes. A major focus of recent toxicological research has begun to investigate the interactions between the biological environment and engineered nanoparticles and to determine appropriate safety standards that should be considered when interacting with nanomaterials. The purpose of this research is to investigate how fullerene-based amino acids interact with the biological environment both at the tissue and cellular levels and to identify factors, such as mechanical stimulation, that increase these interactions.

The functionalization of a fullerene (C_{60}) with such complexes as amino acids has the potential to provide greater interaction between fullerenes and the biological environment yielding potential new medical and pharmacological applications. In an attempt to understand the biological activity of functionalized C_{60}, human epidermal keratinocytes (HEK) were exposed to fullerene-based amino acid (Baa) solutions ranging in concentrations of 0.4–

0.00004 mg/mL. Results showed that cell viability decreased and proinflammatory cytokine production increased after 48 h for Baa concentration of 0.4 and 0.04 mg/mL. These results indicate that concentrations lower than 0.04 mg/mL initiate less cytokine activity and maintain cell viability and, thus, may be considered safe for use in new nano-applications.

In order to investigate the relationship between mechanical stressors and nanoparticle exposure at the tissue level, a flexing apparatus was designed to simulate repetitive wrist motion. Dermatomed porcine skin was fixed to the flexing device and topically dosed with 33.5 mg/mL of a fullerene substituted phenylalanine derivative (Baa-Lys(FITC)-NLS). Skin was flexed for 60 or 90 min or left unflexed (control). Percutaneous absorption was assessed using a flow-through diffusion cell system for 8 h and 24 h. Confocal microscopy was used to visualize penetration of the fluorescent nanoparticles and TEM was used to detect the fullerene within skin at the ultrastructural level. Skin flexed for 60 and 90 min depicted dermal penetration at 8 h, whereas Baa-Lys(FITC)-NLS did not penetrate into the dermis of unflexed skin until 24 h. TEM analysis revealed nanoparticle localization within the intercellular spaces of the stratum granulosum, suggesting that penetration of the derivatized fullerene occurs through intercellular lipid moieties. These results suggest that external factors, such as a repetitive flexing motion and the associated mechanical stressors, can influence interactions that occur between nanoparticles and skin.

To investigate the effects of mechanical stimulation on cellular interactions with nanoparticles, HEK were grown on flexible membrane plates, dosed with 0.04 mg/mL of Baa-Lys(FITC)-NLS, and exposed 10% cyclic tensile strain for 4 h or 8 h. Cellular proliferation, membrane integrity, and cytokine release were monitored over a 24 h time period. Although the results of this study indicated that treatment with Baa-Lys(FITC)-NLS

and mechanical strain decreased cell proliferation, decreased membrane integrity, and increased the release of proinflammatory cytokines, it was not clear as to whether these responses were caused by the direct effects of mechanical stimulation or the ability of mechanical stimulation to increase cellular interactions with the fullerene nanoparticles. Further studies are needed to establish a relationship between mechanical strain and nanoparticle interactions at the cellular level.

EFFECTS OF MECHANICAL STIMULI ON BIOLOGICAL INTERACTIONS WITH AMINO ACID-DERIVATIZED FULLERENES AT THE TISSUE AND CELLULAR LEVELS

by

JILLIAN GRACE ROUSE

A thesis submitted to the Graduate Faculty of
North Carolina State University
In partial fulfillment of the
Requirements for the Degree of
Master of Science

BIOMEDICAL ENGINEERING

Raleigh, North Carolina

2007

APPROVED BY:

Dr. Nancy A. Monteiro-Riviere Chairman of Advisory Committee	Dr. Elizabeth G. Loboa Co-Chairman of Advisory Committee

Dr. Peter L. Mente
Advisory Committee

BIOGRAPHY

Jillian Grace Rouse was welcomed into the world on March 20, 1983 by her loving parents Gary and Patsy Rouse and older sisters Jennifer and Jessica. She grew up in Clinton, North Carolina and after graduating from Clinton High School earned a Bachelor of Science degree in Biomedical Engineering from North Carolina State University in May of 2005. She joined Dr. Nancy A. Monteiro-Riviere's lab in the Center for Chemical Toxicology Research and Pharmacokinetics in June of 2005 and continued her education at N.C. State University to pursue a master's degree in Biomedical Engineering.

ACKNOWLEDGEMENTS

I would like to thank my advisor, Dr. Nancy A. Monteiro-Riviere, for her guidance and support and for allowing me the opportunity to learn the value of scientific research while working in her lab. I would also like to thank Dr. Elizabeth G. Loboa and Dr. Peter L. Mente for serving on my advisory committee and for their continuous mentorship and guidance throughout my undergraduate- and graduate-level biomedical engineering education. This research was made possible by funding provided by the National Academies Keck Future Initiative (NAKFI) Grant and the US EPA-STAR program #RD-83171501-0.

I am especially grateful to the staff of the Center for Chemical Toxicology Research and Pharmacokinetics, with special thanks to Al Inman, Dr. Jessica Ryman-Rasmussen, and Jim Brookes. Their knowledge, expertise, and willingness to help were instrumental in helping me accomplish my goals. I am grateful for their patience and support while training me in the many techniques used in my research. I would also like to thank Dr. Susan Bernacki and Dr. Ruwan Sumanasinghe for their assistance in the Cell Mechanics Lab.

Finally, I would like to thank my family for their unfailing love and support. My parents, Gary and Patsy, for allowing me to follow my dreams and supporting me while doing it. My sisters and brother, Jennifer, Jessica, and Josh, for providing endless friendship and love. Robby, for encouraging me to follow my heart and for always keeping me in his prayers. Garrison, for providing the joy and happiness that only a baby nephew can. And finally, Charlie and Wally, for their endless energy that brightens every day and never ceases to make me smile!

TABLE OF CONTENTS

LIST OF FIGURES ..... **vii**

CHAPTER 1: INTRODUCTION **1**

CHAPTER 2: LITERATURE REVIEW **4**

1. SKIN 4
2. MODELS IN DERMATOLOGICAL RESEARCH 12
3. ROUTES OF PENETRATION AND ABSORPTION 15
4. DERMATOTOXICITY 16
5. MECHANOTRANSDUCTION 20
6. NANOTECHNOLOGY 22
7. REFERENCES 28

CHAPTER 3: FULLERENE-BASED AMINO ACID INTERACTIONS WITH HUMAN EPIDERMAL KERATINOCYTES **38**

1. INTRODUCTION 40
2. MATERIALS AND METHODS 43
   - 2.1 Baa Synthesis 43
   - 2.2 Cell Culture 43
   - 2.3 Dose Response 44
   - 2.4 Time Response 44
   - 2.5 Cytokine Assay 45
   - 2.6 TEM 45
   - 2.7 Statistical Analysis 46
3. RESULTS 46
   - 3.1 Dose Response and HEK Viability 46
   - 3.2 Time Response and Cytokine Expression 47
   - 3.3 TEM 49
4. DISCUSSION 52
5. REFERENCES 55

CHAPTER 4: EFFECTS OF MECHANICAL FLEXION ON THE PENETRATION OF FULLERENE AMINO ACID-DERIVATIZED PEPTIDE NANOPARTICLES THROUGH SKIN **58**

1. INTRODUCTION 60
2. MATERIALS AND METHODS 61
2.1 Baa-Lys(FITC)-NLS Synthesis 61
2.2 Animal Care 63
2.3 Flexing Apparatus 63
2.4 Flow-Through Diffusion Cell System 63
2.5 Confocal Microscopy 64
2.6 Transmission Electron Microscopy 65
2.7 Dynamic Light Scattering 65
2.8 Cryo-TEM 65
3. RESULTS 66
3.1 Penetration of Baa-Lys(FITC)-NLS 66
3.2 TEM 69
3.3 Dynamic Light Scattering 69
3.4 Cryo-TEM 70
4. DISCUSSION 71
5. REFERENCES 75
CHAPTER 5: EFFECTS OF CYCLIC STRAIN ON AMINO ACID-DERIVATIZED FULLERENE PEPTIDE NANOPARTICLE INTERACTIONS WITH HUMAN EPIDERMAL KERATINOCYTES 78
1. INTRODUCTION 79
2. MATERIALS AND METHODS 82
2.1 Baa-Lys(FITC)-NLS Synthesis 82
2.2 Cell Culture 83
2.3 Baa-Lys(FITC)-NLS Treatment 83
2.4 Mechanical Strain 84
2.5 Cell Proliferation Assay 84
2.6 Membrane Integrity Assay 85
2.7 Cytokine Assay 86
2.8 Statistical Analysis 86
3. RESULTS 86

4. DISCUSSION 90
5. REFERENCES 94
CHAPTER 6: CONCLUSIONS 97

LIST OF FIGURES

Figure 2.1. Generalized stress-strain curve for human excised skin tested in uniaxial tension. The low modulus region of the curve represents the straightening of the wavy collagen fibers and the stretching of elastic fibers, while the linear region corresponds to the stretching of collagen fibers within cross-linked collagen fibrils. The final yield (failure) region is a reflection of failure of the collagen fibrils, which results in loss of fibrillar structure (*adapted from* Silver *et al.*, 2003). 11

Figure 3.1. Effect of Baa on HEK viability. Mean viability (±SEM) of MTT 48 h after exposure to Baa. Histogram with different letters (A, B, C, D) denote mean values that are statistically different at $p < 0.05$. 47

Figure 3.2. IL-8 release in HEK exposed to Baa. Mean IL-8 concentration (±SEM) increases with exposure time. Histogram with different letters (A, B, C) denote mean values that are statistically different at $p < 0.05$. 48

Figure 3.3. Mean IL-6 concentration (±SEM). Histogram with different letters (A, B) denote mean IL-6 values that are significantly different at $p < 0.05$. 48

Figure 3.4. Mean IL-1β concentration (±SEM). Histogram with different letters (A, B) denote mean values that are significantly different at $p < 0.05$. 49

Figure 3.5. TEM micrograph depicting intracytoplasmic vacuole localization of 0.04mg/mL Baa (arrows) after 24 h (unstained). 50

Figure 3.6. TEM micrograph that shows the localization of 0.4 mg/mL Baa (arrows) after 24 h (post-stained)..... 50

Figure 3.7. TEM micrograph of necrotic HEK as a result of 48 h exposure to 0.4 mg/mL Baa (arrows) (post-stained). 51

Figure 3.8. TEM micrograph of HEK treated with 0.4 mg/mL Baa (arrows) for 48 h (post-stained). 51

Figure 4.1. Schematic representation of Bucky amino acid (Baa)..... 61

Figure 4.2. Calculated structure of Baa-Lys(FITC)-NLS showing the special relationship between the C_{60}. 62

Figure 4.3. Confocal scanning microscopy images of intact skin dosed with Baa-Lys(FITC)-NLS for 8 h. Top row: confocal-DIC channel image shows an intact stratum corneum (SC) and underlying epidermal (E) and dermal layers (D). Middle row: Baa-Lys(FITC)-NLS fluorescence channel (green) and con focal-DIC channel shows fullerene penetration through the epidermal and dermal layers of skin. Bottom row: fluorescence

intensity scan showing Baa-Lys(FITC)-NLS penetration. All scale bars represent 50 μm. 67

Figure 4.4. Confocal scanning microscopy images of skin dosed with Baa-Lys(FITC)-NLS for 24 h. Top row: confocal-DIC channel image shows an intact stratum corneum (SC) and underlying epidermal (E) and dermal layers (D). Middle row: Baa-Lys(FITC)-NLS fluorescence c hannel (green) and confocal-DIC channel shows fullerene penetration through the skin. Bottom row: fluorescence intensity scan of Baa-Lys(FITC)-NLS. All scale bars represent 50 μm. 68

Figure 4.5. Unstained transmission electron microscopy image of Baa-Lys(FITC)-NLS (arrows) localization at 24 h in skin flexed for 90 min. The fullerenes are present within the intercellular space of the stratum granulosum cell layer (shown by the arrows). The scale bar represents 300 nm. 69

Figure 4.6. Plot of the fraction of aggregates for Baa-Lys(FITC)-NLS as a function of solution concentration. Average aggregate size = 40 nm (▫), 250 nm (●), and 800 nm (■)..... 70

Figure 4.7. Vitreous ice cryo-TEM micrograph of the large aggregates (a) and small aggregates (b) formed by Baa-Lys(FITC)-NLS in PBS buffer (1.0 mg.mL-1 @ pH = 7) 71

Figure 5.1. Calculated structure of Baa-Lys(FITC)-NLS showing the special relationship between the C60..... 83

Figure 5.2. HEK proliferation, corresponding to LDH content in the medium of lysed cells. Histogram with different letters (A, B, C) denote fluorescence values that are significantly different at $p < 0.05$..... 87

Figure 5.3. LDH release by HEK was monitored throughout the 24 h time period and used as an indicator of cell membrane integrity. Histogram with different letters (A, B) denote fluorescence values that are significantly different at $p < 0.05$ 88

Figure 5.4. IL-8 release in HEK exposed to Baa-Lys(FITC)-NLS and mechanical strain. Histogram with different letters (A, B, C) denote mean values that are statistically different at $p < 0.05$..... 89

Figure 5.5. IL-6 release in HEK exposed to Baa-Lys(FITC)-NLS and mechanical strain. Histogram with different letters (A, B, C) denote mean values that are statistically different at $p < 0.05$..... 89

Figure 5.6. IL-1β release in HEK exposed to Baa-Lys(FITC)-NLS and mechanical strain. Histogram with different letters (A, B, C) denote mean values that are statistically different at $p < 0.05$..... 90

CHAPTER 1: INTRODUCTION

Over the past decade, there has been rapid development of nanotechnology and an emergence of a broad spectrum of nanomaterial applications. Nanomaterials have at least one structural dimension in the 1-100 nanometer range and, because of their small size, have unique physiochemical properties and functions. Particularly, carbon-based nanomaterials such as fullerenes, nanotubes, and nanowires are considered key elements in the development of new nano-applications with the potential to be used in everything from biomedicine and drug delivery systems to nanoelectronics and energy conservation mechanisms. Large-scale production of engineered nanoparticles, increased exposure of manufacturers and consumers to nanomaterials, and the development of nano-applications involving biological interactions have raised concerns about the threat of adverse health effects in humans and the potential for environmental damage. Currently, there is little information regarding the safety of nanoparticle use; however, a major focus of recent toxicological research has begun to investigate the interactions between the biological environment and engineered nanoparticles and to determine appropriate safety standards that should be considered when interacting with nanomaterials.

Nanoparticle exposure can occur through oral, dermal, inhalation, and injection routes, all of which could potentially initiate an adverse biological response. Because of its large surface area, skin is one of the principle portals of nanoparticle entry, providing an environment within the avascular epidermis where particles can lodge and not be susceptible to phagocytotic removal (Monteiro-Riviere and Inman 2006). Additionally, alteration of the structural organization of the upper layers of skin during standard physiological processes could compromise the barrier function of the epidermis and lead to increased permeability of

particles (Tinkle *et al.* 2003). Therefore, when evaluating health and safety issues of nanomaterial use, cutaneous exposure and any associated factors that increase exposure should be considered.

The studies presented in this thesis describe the interactions that occur between a fullerene-derivatized amino acid, Baa, and the biological environment both at the tissue and cellular levels. Additionally, the effects of physiologically relevant tensile forces on the penetration of Baa through intact skin and the cellular uptake of Baa by human epidermal keratinocytes (HEK) are presented. Bucky amino acid (Baa) is a nanoscale C_{60} sphere with an attached phenylalanine amino acid derivative. Its biological interactions are of particular interest due to the fullerene's potential for use as a vehicle for therapeutic agents in drug delivery systems (Yang *et al.*, 2007b). However, as presented in Chapter 3, Baa is potentially cytotoxic to *in vitro* cell cultures. The reported findings describe the response of HEK to exposure of a range of Baa concentrations under normal cell culture conditions and present the evidence that some concentrations of Baa are capable of initiating an inflammatory response *in vitro*.

Chapter 4 reports the ability of Baa conjugated with a nuclear localization sequence (NLS) label and a fluorescein isothiocyanate (FITC) marker to penetrate intact skin. These results showed that exposure of Baa-Lys(FITC)-NLS dosed skin to repetitive mechanical flexing increased the rate and depth of nanoparticle penetration. Results of this study are the first to relate physiologically relevant mechanical stimuli to nanoparticle penetration through intact skin. Since stresses and strains at the tissue level are mechanotransduced to individual cells, a separate investigation, which is presented in Chapter 5, was conducted to determine the effects of cyclic tensile strain on HEK interactions with Baa-Lys(FITC)-NLS. Similarly

to the results found at the tissue-level, these findings indicate that mechanical stimulation influences nanoparticle interactions with the biological environment and, therefore, should be considered when identifying risks associated with nanoparticle exposure. Additionally, these results are important for the potential application of Baa in drug delivery systems, especially those involving transepidermal delivery.

The findings reported in this thesis give insight into the interactions that occur between fullerenes and the biological environment at the tissue and cellular levels. Moreover, the results indicate that mechanical stimuli associated with normal physiological activity can affect these biological interactions. These concepts are important factors to consider in the development of nanoparticle applications with biological implications and in the construction of new health and safety regulations for nanoparticle use. The research presented herein is pivotal for the advancement of a developing nano-world.

CHAPTER 2: LITERATURE REVIEW

1. SKIN

Skin is the largest organ of the body and, in addition to its primary function as a barrier for protection of the internal biological milieu from the external environment, has a variety of roles in the maintenance of physiological homeostasis. Skin, for example, prevents dehydration by minimizing unnecessary water loss, assists in thermoregulation by aiding in the constriction and dilation of blood vessels, provides support for internal organs, and participates in the synthesis of vitamin D. The anatomical structure, biological functions, and chemical composition of skin are important in its ability to serve as a protective barrier and contribute to the rate and extent of percutaneous absorption (Monteiro-Riviere, 2001a).

Anatomically, skin is comprised of two principal components: a stratified, avascular epidermis and the underlying dermis. The epidermis is further classified into layers called the stratum corneum, stratum lucidum, stratum granulosum, stratum spinosum, and stratum basale. Together, these cell layers function to anchor the epidermis to the underlying dermis, to replenish cells that are naturally sloughed off from the surface epidermis, and to form a permeability barrier that protects the internal biological environment from the external milieu. The dermis consists of a dense irregular network of collagen, elastic, and reticular fibers that provides mechanical support for the tissue. An extensive network of capillaries, nerves, and lymphatics also located in the dermis facilitate the exchange of metabolites between blood and tissues, fat storage, protection against infections, and tissue repair. Below the dermis is the hypodermis, which anchors skin to underlying muscle or bone by loose connective tissue of collagen and elastic fibers (Monteiro-Riviere, 2001a, 2004, 2006; Taylor *et al.*, 2006).

The epidermis

The epidermis is derived from ectoderm and consists of stratified squamous keratinized epithelium. The thickness and number of stratified layers varies among mammalian species and anatomical location. In general, porcine skin in the thoracolumbar area is an acceptable model for percutaneous absorption studies and has an epidermal thickness of about 52 μm and a stratum corneum thickness of about 12 μm (Monteiro-Riviere, 2004). The avascular epidermis continuously undergoes an orderly process of proliferation, differentiation, and keratinization to replenish the epidermis as stratum corneum cells are naturally sloughed from the skin's surface (Monteiro-Riviere, 2006).

Keratinocytes are the predominate cell type of the epidermis, accounting for approximately 80% of the cell population (Monteiro-Riviere, 2004). These cells originate in the stratum basale and, upon mitosis, undergo a continual differentiation process, known as keratinization. During this process, the epidermal cells migrate upward, increase in size, and produce differentiation products such as tonofilaments, keratohyalin granules, and lamellated bodies. Epidermal layers are easily identified by distinct differences in cell morphology and differentiation products that result due to keratinization. The remaining group of epidermal cells, known as nonkeratinocytes, consists of melanocytes, Langerhans cells, and Merkel cells and do not participate in the process of keratinization (Smack, *et al.*, 1994).

The stratum basale is the layer of skin located closest to the dermis and is comprised of a single layer of columnar or cuboidal cells that are attached to the overlying stratum spinosum cells and to adjacent basale cells by desmosomes and to the underlying basement membrane by hemidesmosomes. Desmosomes are small, localized adhesion sites that mediate direct cell-to-cell contact by providing anchoring sites for intermediate filaments of

the cellular cytoskeletons. Hemidesmosomes, on the other hand, function to provide strong attachment sites between the intermediate filaments of cells and the extracellular matrix of the underlying basal lamina (Taylor *et al.*, 2006). In addition to their role in synthesizing the basement membrane, basale cells also function as stem cells to continuously produce keratinocytes that subsequently undergo keratinization. Immature keratinocytes of the stratum basale are capable of engaging in the synthesis of keratin, which are later assembled into keratin filaments called tonofilaments. Other nonkeratinocytes cells are also present in the stratum basale. Merkel cells are closely associated with nerve fibers and function as mechanoreceptors capable of relaying sensory information to the brain. Additionally, melanocytes, which produce and secrete melanin and provide protection from ultraviolet irradiation, reside near the basement membrane and are responsible for transferring melanin to surrounding keratinocytes.

The stratum spinosum or "prickle cell layer" is located above the stratum basale and consists of several layers of irregularly shaped polyhedral cells. Tight junctions and desmosomes connect adjacent cells and the underlying stratum basale. Additionally, Langerhans cells, important for the skin's immune response, are found in this epidermal layer. This layer is morphologically distinguished from other epidermal layers by the presence of tonofilaments. As keratinocytes mature and move upward through this layer, the cells increase in size and become flattened in a plane parallel to the surface of the skin. Keratinocytes within the upper part of the stratum spinosum begin to produce keratohyalin granules and lamellar bodies, which are distinctive features of the cells in the stratum granulosum.

The next epidermal layer, the stratum granulosum, contains several layers of flattened cells positioned parallel to skin's surface. The numerous granules that are present in the cells of this layer contain precursors for the protein filaggrin, which is responsible for the aggregation of keratin filaments present within the cornified cells of the stratum corneum. These granules fuse with the cell membrane and secrete their contents via exocytosis into the intercellular spaces between the stratum granulosum and stratum corneum layers. The lipid contents of the granules then form the intercellular lipid component of the stratum corneum barrier.

Present only in areas of thick skin, such as the palms of the hands and soles of the feet, is a subdivision of the stratum corneum called the stratum lucidum. This epidermal layer is a thin, translucent layer of cells devoid of nuclei and cytoplasmic organelles. These cells are keratinized and contain a viscous fluid, eleidin, which is analogous to keratin.

The stratum corneum is the outermost layer of the epidermis and its composition and organization significantly contribute to the skin's permeability barrier. The stratum corneum consists of terminally differentiated cells arranged in multicellular stacks perpendicular to the surface of the skin. The cells are devoid of nuclei and cytoplasmic organelles and are almost completely filled with keratin filaments. The interlocking columns of cells are embedded in a structured lamellar matrix that consists of specialized lipids secreted from the granules of the stratum granulosum cells. This barrier functions to restrict the penetration of hydrophilic substances and large entities through the skin and to prevent excess loss of body fluids (Mackenzie, 1975; Menton, 1976; Monteiro-Riviere, 1991, 2001a, 2001b, 2006; Smack, 1994; Taylor *et al.*, 2006).

The dermis

Collagen, elastic, and reticular fibers embedded in an amorphous ground substance of proteoglycans create a network of dense connective tissue that makes up the dermis. Fibroblasts, mast cells, and macrophages are the predominate cell types found in the dermis; however, plasma cells, fat cells, chromatophores, and extravasated leukocytes are often also present. The more superficial layer of the dermis, the papillary layer, lies immediately beneath the basement membrane and contains a less dense, irregular framework of type I and type III collagen molecules and elastic fibers. This region also contains blood and lymphatic vessels that serve but do not enter the epidermis and nerve processes that either terminate in the dermis or penetrate into the epidermis. Fingerlike protrusions of the dermal connective tissue into the underside of the epidermis are called dermal papillae. Likewise, epidermal ridges are similar protrusions of the epidermis into the dermis. Increased mechanical stress on the skin increases the depth of the epidermal ridges and length of the dermal papillae, thus, creating a more extensive interface between the dermis and epidermis. The reticular layer of the dermis lies beneath the papillary layer. This layer is substantially thicker than its superficial layer and is characterized by thick bundles of mostly type I collagen, coarser elastic fibers and fewer cells (Monteiro-Riviere, 1991, 2001a, 2001b, 2006).

The hypodermis

The hypodermis is superficial fascia that lies below the skin and helps to anchor the dermis to underlying muscle and bone. It is comprised of connective tissue containing a loose arrangement of collagen and elastic fibers that allows for flexibility and free movement of the skin over the underlying structures (Monteiro-Riviere, 2006).

Skin appendages

Hair follicles, associated sebaceous glands, arrector pili muscles, and sweat glands are appendageal structures commonly found in skin. Hairs are produced by hair follicles and are keratinized structures derived from epidermal invaginations that traverse the dermis and may extend into the hypodermis. Although skin penetration through a hair follicle still requires a compound to traverse the stratum corneum, follicles represent regions of greater surface areas and can, therefore, contribute to increased transdermal absorption (Monteiro-Riviere, 2004). Connective tissue at the base of the hair follicle provides an attachment site for the arrector pili muscle, which upon contraction not only erects the hair but also assists in emptying the sebaceous glands. Sebaceous glands release their secretory product, sebum, into ducts that empty into the canal of the hair follicle. Sebum is an oily secretion that acts as an antibacterial agent. Apocrine and eccrine sweat glands are also located in skin and function to produce secretions involved in communication and thermoregulation, respectively (Monteiro-Riviere *et al.*, 1993).

Material Properties of Skin

Skin is generally classified as a viscoelastic material, and its response to mechanical deformation involves both a viscous component associated with energy dissipation and an elastic component associated with energy storage. The viscous component of skin is responsible for its creep characteristics, or the tissue's tendency to deform in a time-dependent manner. In part, the water, proteins, and macromolecules (specifically the glycosaminoglycans) located in the dermis are responsible for the viscous aspects of skin deformation (Agache *et al.*, 1980). These constituents contribute to the dissipation of energy by promoting sliding of collagen fibrils during their alignment with the direction of the

applied force. The elastic behavior of skin is important in ensuring shape recovery after deformation and is largely the result of collagen and elastic fiber density and orientation (Silver, 1987; Dunn and Silver, 1983).

Biomechanical testing reveals that the stress-strain behavior of skin occurs in three phases (Silver, 1987), as shown in Figure 2.1. During the initial portion of the stress-strain curve, up to strains of about 30%, collagen fibril alignment occurs and the collagen network offers little resistance to deformation. However, viscous movement of the collagen fibrils through the amorphous ground substance and the resistance of elastic fibers act to dissipate much of the applied energy (Oxlund *et al.*, 1988). Thus, the initial response of skin to mechanical loading displays highly viscoelastic properties. Collagen fibrils begin to offer resistance to deformation between strains of 30% and 60%, and the linear region of the stress-strain curve corresponds to the stretching of cross-linked collagen fibers. Finally, the yield region is a reflection of failure of the collagen fibrils, which results in loss of fibrillar structure (Silver *et al.*, 2001).

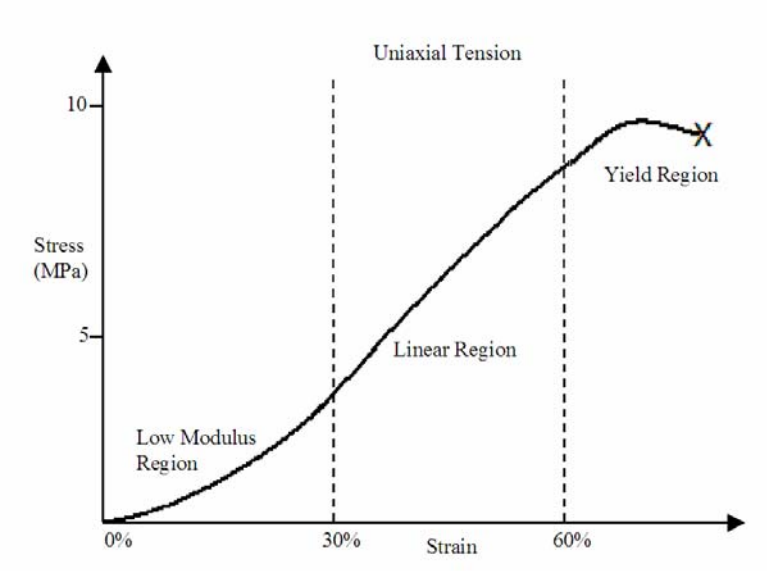

Figure 2.1. Generalized stress-strain curve for human excised skin tested in uniaxial tension. The low modulus region of the curve represents the viscoelastic nature of skin, while the linear region corresponds to the elasticity of the collagen fibers. The yield (failure) region is a reflection of the failure of the collagen fibrils, (adapted from Silver *et al.*, 2003).

The slope of the linear region of the stress-strain curve is an estimate of the Young's modulus, or stiffness, of skin. Many studies have determined that biomechanical properties such as Young's modulus are dependent on age. Specifically, these studies have shown that the elasticity and stretchability of skin significantly diminishes after the age range of 30-45, apparent by the elevated Young's modulus of an older population (Agache *et al.*, 1980; Grahame and Holt, 1969).

Skin Permeability

The structure of the stratum corneum has previously been described using a brick and mortar model with layers of corneocytes embedded in a lipid matrix (Elias, 1983). This structure supports the protective barrier functionality of the stratum corneum by both preventing excessive fluid loss and hindering percutaneous penetration. Many compounds, however, are capable of permeating skin via various penetration routes. The steady-state flux

or rate of diffusion, J_s, of compounds across skin can be predicted using Fick's law of diffusion (Scheuplein, 1967, Scheuplein and Blank, 1971):

$$J_s = \frac{DP\Delta C}{\delta} \qquad \textit{Equation 1}$$

where, D is the diffusion constant or diffusivity of the specific penetrant, P is the partition coefficient between the membrane surface and the external solution, δ is the membrane thickness, and ΔC is the concentration gradient across the membrane. The diffusion constant for a compound is dependent on its actual mechanism of diffusion (i.e. intercellularly versus intracellularly) and is a parameter of its physiochemical characteristics such as molecular size, structure, and solubility in the membrane. The partition coefficient can be a measure of the hydrophobicity of the penetrant and reflects its ability to gain access to the lipid membrane. A variety of factors can affect percutaneous absorption, including: the physiochemical properties of the penetrant (Feldmann and Maibach, 1970), regional variations in epidermal thickness (Maibach *et al.*, 1971; Skinner and Kilgore, 1982), interspecies differences (Bartek *et al.*, 1972), and the use of surfactants and other penetration enhancers (Cooper *et al.*, 1985). In addition, anatomic and physiological changes associated with aging and disease and differences in vascular anatomy and blood flow can contribute to skin permeability (Monteiro-Riviere, 2004). It is important to consider the effects of all of these factors when conducting *in vitro* tests to model penetration and absorption.

2. MODELS IN DERMATOLOGICAL RESEARCH

Isolation of an animal's organs, tissues, and/or cells is often used as an alternative to whole animal testing in scientific research. Specifically, in dermatotoxicological research, keratinocytes are used as *in vitro* models for testing the cutaneous toxicity of chemicals,

drugs, metals, and pesticides (Bernstein and Vaughan, 1999). Cutaneous penetration and absorption of potential toxicants is modeled using porcine skin and flow-through diffusion cell systems (Bronaugh and Stewart, 1985; Bronaugh 2006). With appropriate construction of the physical and chemical *in vitro* environments, these alternatives have the ability to serve as accurate and reliable models in biomedical research.

Porcine skin as a model for human skin

The basic architecture of skin is similar in all mammals. However, differences exist between species and within various anatomical regions of the same species in the thickness of the epidermal and dermal layers, hair density and follicle arrangement, structural composition, and vascular supply. Porcine skin is frequently used as a model for dermatotoxicological research because of its morphological (Meyer *et al.*, 1978; Montanga and Yun, 1964; Monteiro-Riviere, 1986; Monteiro-Riviere and Stromberg, 1985), histochemical (Meyer *et al.*, 1986; Woolina *et al.*, 1991), biochemical, and physiological similarities to human skin. Most importantly for percutaneous absorption studies are the similarities between hair density, epidermal thickness, and stratum corneum lipid properties. Other likenesses between pig and human skin include: epidermal turnover kinetics, carbohydrate biochemistry, vasculature, and ratio between dosing site area to total body mass (Monteiro-Riviere, 1991; Monteiro-Riviere and Riviere, 1996; Monteiro-Riviere, 2001b). These similarities make porcine skin, particularly from the thoracolumbar region, an ideal model for human skin for use in cutaneous penetration and absorption studies.

Flow-through diffusion cell system

The flow-through diffusion cell system is a well-established *in vitro* method for evaluating skin absorption of chemical compounds. Dermatomed skin is placed in a chamber that permits exposure of the top surface of the skin to the environment and the underlying dermal side to constantly perfused fluid that is maintained at physiological temperature and pH. The perfusate serves as a nutritional buffer that helps preserve skin viability during the absorption study. Additionally, the receptor fluid may be collected and the penetrant concentration monitored to determine the rate and extent of skin absorption (Bronaugh and Stewart, 1985). It is important that throughout the study environmental and experimental conditions, such as dose, temperature, humidity, and perfusate composition, are regulated because it has been shown that these parameters can influence percutaneous absorption (Chang and Riviere, 1991).

Cell culture

Keratinocytes are the primary cellular constituent of the epidermis and are typically used in *in vitro* dermatotoxicology studies as an alternative to whole animal testing. Keratinocytes have been harvested from a number of mammalian species including humans (Liu and Karasek, 1978; Liu *et al.*, 1979), mice (Fusenig and Worst, 1975), and pigs (Hengge *et al.*, 1996). For biological modeling of human phenomena, the use of human epidermal keratinocytes has obvious advantages in that it reduces the need for extrapolation of data. However, due to the aforementioned similarities between porcine and human skin, pig keratinocytes are also an acceptable model and are often used in dermatotoxicological studies (Allen *et al.*, 2001b).

3. ROUTES OF PENETRATION AND ABSORPTION

The primary barrier against the passage of foreign hydrophilic substances into the skin is the stratum corneum. The stratum corneum consists of 10-15 layers of nonviable, protein rich cells surrounded by an extracellular lipid matrix. The intercellular lipid lamellae, composed mainly of ceramides, cholesterol, and fatty acids, are primarily responsible for restricting the passage of aqueous entities through the skin (Wertz, 2004*)*. The importance of the lipid moieties in barrier function has been demonstrated by the removal of lipids from the stratum corneum, which subsequently results in an increased penetration of compounds (Hadgraft, 2001; Monteiro-Riviere *et al.*, 2001).

The stratum corneum serves as the rate-limiting barrier to percutaneous absorption because the underlying epidermal layers are much more aqueous in nature and, thus, allow the passage of substances to occur more easily. Once penetration through the epidermis occurs, there is little resistance to diffusion, and substances have access to systemic circulation via absorption into the blood and lymphatic vessels located in the dermis. Additionally, keratinocytes possess metabolizing enzymes that interact with the diffused compound and produce metabolites that can easily be absorbed by cutaneous vasculature (Monteiro-Riviere, 2001a; Riviere, 1990; Bronaugh *et al.*, 1989).

In general, penetration through the stratum corneum can potentially occur via four routes depending on the physiochemical properties of the compound. These pathways include two transappendageal routes (through hair follicles and sweat glands), the intercellular route, and the intracellular route (Scheuplein, 1967). Penetration through the follicular regions and sweat glands most likely occurs through aqueous pores that are created by the appendages that allow the passage of some small polar compounds. Chemicals and other nonionzable,

lipid soluble molecules penetrate the stratum corneum primarily via the lipid-containing intercellular spaces. Thus, substances that modify the lipid matrix of the upper epidermis, such as penetration enhancers, can alter the kinetics of penetration. Some hydrophilic substances are capable of traversing the stratum corneum barrier by passing directly through individual corneocytes, i.e. intracellular penetration (Monteiro-Riviere, 2001a).

There are several factors that can affect percutaneous absorption. Soaps and detergents, for example, are routinely applied to the surface of the skin, but can cause damaging affects by removing intercellular lipids. Furthermore, some organic solvents are capable of partitioning into the intercellular lipid pathway of the stratum corneum and altering its lipophilicity (Monteiro-Riviere, 2004*)*. External mechanical stimuli may also alter the structural organization of the upper epidermal layers by disrupting desmosomal cellular attachments. Tinkle *et al.*, 2003 discovered that repetitive flexing of skin increased the penetration of micro-sized particles into the epidermis. This phenomenon is thought to contribute to the increased absorption of beryllium and zirconium microparticles found in volcanic soil leading to a higher prevalence of podoconiosis among people walking barefoot through the African rift valleys (Frommel *et al.*, 1993). These factors could affect percutaneous absorption by altering the ability of the stratum corneum to serve as a protective barrier.

4. DERMATOTOXICITY

Cytotoxic substances capable of traversing the stratum corneum barrier can potentially initiate a toxic response in the skin. Some irritants perturb the skin's barrier by extracting the intercellular lipids while others are capable of completely digesting and destroying the viable cell layers of the epidermis. In other cases, epidermal cells are affected

and an immunological response is elicited. Immunological and inflammatory processes are mediated by cytokines, which are polypepetide messenger molecules capable of altering cellular functions by initiating autocrine and paracrine signaling cascades (Nickoloff, 1991). In addition to typical immune cells (e.g. Langerhans cells, lymphocytes, mast cells), keratinocytes also assist in cytokine production and are a major contributor to the epidermal immunological and inflammatory response (Monteiro-Riviere, 2001a).

Keratinocyte Mediation of Skin Irritation/Inflammation

As discussed above, keratinocytes differentiate from the basal layer and undergo keratinization to form the stratified layers of the epidermis. In response to an injury, a cytotoxic substance, or under certain pathological conditions, however, keratinocytes are capable of undergoing an alternative pathway that results in cellular activation. Once activated, keratinocytes initiate a myriad of responses that are essential in orchestrating events necessary for the repair of the injured tissue. Activated keratinocytes, for example, are hyperproliferative, migratory, augment their cytoskeleton, change the levels of cell surface receptors, and produce components of the basement membrane. Additionally, they produce and secrete cytokines that modify the actions of neighboring keratinocytes and assist in the signaling of the immune response (Freedberg *et al.*, 2001). Although different toxicants elicit various responses in keratinocytes, several studies have shown cytokine release by HEK in response to ultraviolet irradiation (Granstein *et al.*, 1987; Urbanski *et al.* 1990), psoriasis (Nickoloff, 1991), jet fuel exposure (Allen *et al.*, 2000, Allen *et al.*, 2001a, Allen *et al.*, 2001b, Chou *et al.*, 2003 and Monteiro-Riviere *et al.*, 2003), multi-walled carbon nanotube exposure (Monteiro-Riviere *et al.*, 2005), and sulfur mustard (Arroyo *et al.*, 1999; Lardot *et al.*, 1999).

Both the α and β forms of the cytokine interleukin-1 (IL-1) are present in the cytoplasm of keratinocytes and are the most common initiator of keratinocyte activation (Hauser *et al.*, 1986; Kupper *et al.*, 1986; Mizutani *et al.*, 1991; Kupper and Groves, 1991). Unstimulated keratinocytes normally contain large amounts of preformed and biologically active IL-1α, and upon injury, these sentinel molecules are quickly released and recognized by surrounding cells. IL-1β, however, is present in keratinocytes in its biologically inactive form, pro-IL-1β, and requires the action of exogenous proteases to convert to its active form (Mizutani *et al.*, 1991). Once released, activated IL-1 acts as a paracrine signal to slow the circulation of lymphocytes in the bloodstream (Cartwright *et al.*, 1995; Romero *et al.*, 1997), allowing phagocytic cells to extravasate and migrate to the site of injury. IL-1 also acts as an autocrine signal to activate keratinocytes causing them to proliferate, migrate, and express an activation-specific set of genes. Keratinocyte proliferation and migration are important for re-epithelization of injured skin (Kupper, 1990; Chen *et al.*, 1995).

IL-1 induces the production of tumor necrosis factor-α (TNF-α), which is a cytokine that is important for the induction and maintenance the keratinocyte activation cycle (Nickoloff and Turka, 1993; Chabot-Fletcher *et al.*, 1994). TNF- α is a proinflammatory cytokine that can initiate many systemic effects, such as fever and shock. In healthy skin, low levels of pre-formed TNF-α are localized in the outermost epidermal keratinocytes (Kolde, *et al.* 1992). In response to UV light, chemical irritants, allergens, tumor promoters, and infections, it is likely that this TNF-α is released and made available to neighboring keratinocytes for activation of the cytokine cascade (Nickoloff and Turka, 1993). Once induced, TNF-α acts as a potent stimulator for other proinflammatory cytokines, such as IL-8 and IL-6 (Nickoloff *et al.*, 1991).

Interleukin-8 (IL-8) is a proinflammatory cytokine that is not present in normal skin. Upon induction by IL-1 and TNF-α, keratinocytes can release IL-8, which in turn serves as a chemotactic and activation factor for neutrophils and T lymphocytes. In addition, IL-8 can trigger keratinocyte proliferation. In psoriatic skin lesions, keratinocyte hyperproliferation is at least partially caused by increased production of IL-8 that results in a self-perpetuating abnormal transformation of epidermal keratinocytes (Nickoloff, 1991; Nickoloff *et al.*, 1991). Several studies have also reported the ability of keratinocytes to produce IL-8 in response to chemical irritants (Allen *et al.*, 2000, 2001a, 2001b; Chou *et al.*, 2003)

In addition to IL-8, IL-6 is a proinflammatory cytokine that is produced by a variety of cells, including keratinocytes. Production and secretion of IL-6 is upregulated in response to IL-1 and TNF-α. IL-6 contributes to the epidermal hyperplasia of psoriatic lesions and the activation of T cells, macrophages, and neutrophils that are infiltrated into the tissue during the immune response (Grossman *et al.*, 1989, Mizutani *et al.*, 1989).

IL-10 is considered an anti-inflammatory cytokine because of its role in immune suppression and function as a negative regulator of the irritation response (Grone *et al.*, 2002; Berg *et al.*, 1995). In monocytes and macrophages, for example, IL-10 has been shown to inhibit the production of IL-1 and TNF-α (de Waal Malefyt *et al.*, 1991; Fiorentino et al, 1991). These primary cytokines have synergistic roles in inflammatory processes and pathways and are important for inducing secondary mediators, such as IL-8 and IL-6. Thus, inhibition of IL-1 and TNF-α can have negative consequences for the induction of the cytokine cascade and for the recruitment of chemokines. IL-10 is also produced in UV-irradiated keratinocytes and is likely responsible for the systemic suppression that occurs after UV radiation exposure (Enk and Katz, 1992; Rivas and Ulrich, 1992).

In addition to the cytokines described above, there are many other cell signaling molecules, growth-promoting factors, and environmental cues that participate in and help regulate the inflammation/irritation response in skin. IL-1, TNF-α, IL-8, IL-6, and IL-10 are a few of the important cytokines that can be monitored *in vitro* and serve as biochemical markers of inflammation.

5. MECHANOTRANSDUCTION

Mechanobiology is the study of a cell's biological response to mechanical loads and the mechanotransduction mechanisms used in transforming the loads into signaling cascades and cellular events (Wang and Thampatty, 2006; Ingber, 1998). Naturally, tissues are exposed to a variety of mechanical loads, including: tensile forces applied to the tendons of the musculoskeletal system during locomotion, compressive loads applied to cartilage and bone during walking and exercise, shear stresses and pressure applied to vasculature during blood flow, and tensile, compressive, and shear forces applied to dermal tissue (Wang and Thampatty, 2006). Both exogenous and endogenous mechanical stimuli are transmitted to the cellular level. The magnitude, direction, and distribution of the mechanical stimuli can elicit a wide variety of cellular responses to maintain tissue homeostasis, including growth, differentiation, migration, and apoptosis (Barkhausen *et al.* 2003; Chen *et al.*, 1997; Huang and Ingber, 1999; Kaspar *et al.*, 2000; Loboa *et al.*, 2004; Sumanasinghe *et al.* 2006).

External forces applied to the epidermis include normal forces that occur as a result of compression or tensile stretching of skin and shear forces that result from friction. These forces are transmitted through the epidermis to the dermis and underlying subcutaneous tissues and result in the stretching of collagen fibrils. Internal dermal forces are directed approximately along Langer's lines and exist as passive tension in the collagen fibrils. These

forces are augmented by active cellular tension that occurs between collagen-fibroblast and fibroblast-fibroblast cytoskeleton attachment sites (Grinnell, 2000). Together, the externally applied forces and internal passive forces are transduced into a biochemical response in the cell cytosol and nucleus that result in the activation of secondary messengers (Silver *et al.*, 2003).

Cells in mechanically activate environments are involved in mechanochemical processes that involve both cell-cell and cell-extracellular matrix (ECM) interactions. The ability of these cells to transduce mechanical forces appears to occur through integral membrane proteins, such as β-integrins, that up-regulate the production of protective cytoskeletal proteins (D'Addario *et al.*, 2001). Additionally, mechanical stimulation causes a conformational change in G protein-linked receptors (Vandenburgh, 1992) and triggers activation of stretch-activated ion channels (Yang and Sachs, 1993). These cellular changes induced by mechanical stimulation may activate protein kinase C (PKC)-related signal transduction pathways that increase the secondary messengers cyclic adenosine monophosphate (cAMP) and prostaglandin E_2 (PGE_2). In turn, PGE_2 and cAMP are capable of altering gene expression that is responsible for protein synthesis and cellular proliferation activities.

Studies done to investigate the effects of mechanical stimulation in cultured keratinocytes show that in response to cyclic tensile strain keratinocytes increase cell proliferation, DNA synthesis, elongation, and protein synthesis (Takei, *et al.* 1997). Yano et al, 2004 verified that mechanical stretching of keratinocytes induces proliferative signals that could contribute to the normal hyperproliferative nature of the epidermis. Others attribute strain-induced proliferation to increased production and release of IL-1 (Takei et al, 1998;

Lee *et al.*, 1997). Lee *et al.*, 1997 related increased IL-1 release to transient plasma membrane injury that occurs in response to cellular strain. These results suggests that mechanical stimulation could transiently increase the permeability of individual cellular membranes and lead to increased cellular uptake of surrounding ions. Additionally, these findings could have profound implications on the ability of drugs and other particle-like entities to enter cells.

6. NANOTECHNOLOGY

The terms nanotechnology and nanoscience refer to processes involved in the creation of matter with dimensions in the 1-100 nanometer range and the manipulation of these materials to develop structures, devices, and systems that have new properties and functions based on their small size (The Royal Society, 2004). At the nanoscale level, materials exhibit unique physical, chemical, and biological properties that differ from properties of their bulk material counterparts. In addition to a larger surface area per unit mass, nanoparticles have increased chemical reactivity and demonstrate the ability to create new chemical forms of common chemical elements. As a result, nanoscale materials exhibit better magnetic properties, electrical and optical activity, and structural integrity (Cassee *et al.*, 2002; Oberdorster, 1996; Oberdorster *et al.*, 2005b; Huang *et al.*, 2004; Yang and Watts, 2005). These unique properties make possible the development of novel applications that improve upon the quality and efficacy of existing products, such as the use of nanoparticles for the creation of high performance batteries and carbon nanotubes for lighter yet more durable sporting equipment.

In addition, the increased reactivity of nanomaterials may facilitate, and possibly exacerbate, interactions that occur with biological and environmental systems. Although the

unique properties of nanoparticles provide great potential for the development of techniques to improve water, soil, and air quality and to diagnose, treat and possibly cure medical ailments, the mechanisms of action for these nanomaterials are not fully understood. Therefore, there is an inherent risk associated with the introduction of nanoparticles into biological or ecological environments. Risk assessments and safety regulations that address nanoparticle manufacturing and consumer processes are needed to protect against adverse reactions to nanoparticle exposure (Colvin, 2003; Holsapple *et al.*, 2005; Oberdorster *et al.*, 2005a).

Engineered Nanoparticles

Engineered nanoparticles are those that are intentionally produced in a laboratory or industrial setting and exclude the wide range of natural and anthropogenic particulates, such as those from pollen, viruses, automobiles, and diesel-powered engines (Colvin, 2003; Kittelson, 1998; Biswas and Wu, 2005). Engineered nanoparticles can be manufactured in a variety of forms, most commonly as fullerenes (C_{60} and nanotubes), quantum dots, metal oxides, and nanowires (Terrones and Terrones, 2003). Additionally, these nanostructures can be conjugated to peptides and other molecules to alter the reactivity and functionalization of the original particle (Yang *et al.*, 2007a, 2007b).

Fullerenes are a family of carbon allotropes that exist as a hollow sphere, ellipsoid, or tube. Spherical fullerenes that are composed of carbon atoms arranged in a stable, soccer ball-like formation are called Buckminsterfullerenes. Commonly, Buckminsterfullerenes are referred to as Bucky balls or simply fullerenes. The C_{60} molecules were discovered in 1985 and named after the American architect Richard Buckminster Fuller (Kroto *et al.*, 1985;

Kroto *et al.*, 1992). Spherical fullerenes structures can also contain more or less than sixty carbon atoms; however, C_{60} is the most common naturally occurring fullerene.

Nanotubes are cylindrical fullerenes that can exist as single-walled or multi-walled hollow tubes. These structures are typically 2-10 nanometers in diameter and vary in length from nanometers to millimeters. Nanotubes have unique electronic properties due to the quantum confinement of electrons perpendicular to the nanotube axis, which constrains the propagation of electrons longitudinally along the axis (Charlier and Issi, 1998). Additionally, carbon nanotubes demonstrate high mechanical strength capable of withstanding repetitive bending and twisting without catastrophic failure (Terrones and Terrones, 2003).

Quantum dots and metal oxides are other commonly engineered nanoparticles. Quantum dots are semiconductor nanocrystals that consist of a colloidal core surrounded by one or more surface coatings. Because of their unusually intense and photostable fluorescence, quantum dots have great potential for use as diagnostic and imaging agents. Metal oxides, such as titanium dioxide and zinc oxide, are often used in sunscreens and cosmetic products because of their ability to absorb ultraviolet light and to protect skin against sunburn or genetic damage (Jaiswal and Simon, 2004).

Biological Interactions

Nanoparticle interactions have been shown to be dependent on a variety of factors, including size and structure of the nanoparticle, agglomeration state, crystal structure, chemical composition, surface area, surface chemistry, surface charge, and porosity (Oberdorster *et al.*, 2005a). These properties are unique for each manufactured nanostructure and dictate the resulting interactions that can occur with the biological environment.

In particular, fullerenes (C_{60}) have unique physiochemical properties and a highly hydrophobic nature that could be of biological importance for their use in medicinal applications. The use of fullerenes for biological purposes, however, is limited by their poor solubility. Chemical modification of fullerenes allows for hydrophilic covalent attachments to increase solubility without disrupting the desired chemical and physical properties of the fullerene. Additionally, the attachment of such entities as amino acids provides a means by which the fullerene can be incorporated into proteins, peptides, or even antibodies. When introduced into the biological environment, the hydrophobic fullerene core allows for transport across the cellular membrane. Therefore, the fullerene-based amino acid represents a potentially potent vehicle for intracellular drug delivery (Yang *et al.*, 2007b).

Additionally, quantum dots and fullerenes are capable of interacting with the biological environment by penetrating intact skin (Ryman-Rasmussen *et al.*, 2006; Monteiro-Riviere, *et al.*, 2006). Quantum dots were shown to penetrate the stratum corneum barrier and localize within the epidermal and dermal layers within 8 h of exposure. Regardless of their physiochemical properties (size, shape, and surface coatings), quantum dots appeared to penetrate skin by the same intercellular mechanism. These findings suggest that nanoparticles' unique ability to traverse intact skin may be significantly due to their small size. The ability of amino acid-derived fullerenes to penetrate intact skin has also recently been demonstrated and the use of 1% Pluronic® F127 surfactant shown to increase the rate and magnitude of fullerene penetration (Monteiro-Riviere *et al.*, 2006). These studies show that skin is an important portal of entry for nanoparticle exposure that occurs in occupational and consumer settings as well as a potential route for transepidermal drug delivery.

The structure and composition of skin contributes to its protective barrier function, however, the reports by Ryman-Rasmussen *et al.*, 2006 and Monteiro-Riviere et al, 2006 prove that skin is not impervious to nanomaterials. If nanoparticles are capable of penetrating the epidermis without the aid of mechanical stressors or skin abrasion, then it is possible that external and internal mechanical stimulation are capable of intensifying this phenomenon. Although many studies have been done to examine the biological activities that occur in response to mechanical stimuli, minimal work has been done to examine how changes in structural integrity due to mechanical loads effect the penetration of substances through the body's first line of defense against foreign substances. Additionally, investigations are needed to determine whether mechanical stimuli at the tissue level can also produce mechanotransduction signals that alter the permeability of individual cellular membranes. If so, then repetitive stresses applied to cutaneous tissue could be transmitted to individual epidermal and dermal cells and, thus, lead to increased cellular uptake of nanoparticles.

Cytotoxicity

Ideally, the unique behavior of nanoparticles is advantageous for the invention of new medical applications and other developments that involve biological interactions. However, many researchers have recently reported the potential hazardous effects associated with *in vitro* nanoparticle exposure. For example, Monteiro-Riviere *et al.* (2005) revealed that exposure of human epidermal keratinocytes (HEK) to multi-walled carbon nanotubes (MWCNT) initiated a pro-inflammatory response, indicated by the release of IL-8. Cell toxicity was shown to be both dose- and time-dependent throughout the exposure period, and TEM verified cellular uptake of the MWCNT (Monteiro-Riviere *et al.*, 2005). Similarly, HEK exposed to amino acid functionalized single-walled carbon nanotubes (SWCNT)

showed a decrease in viability and exhibited increased levels of IL-8 and IL-6 (Zhang *et al.*, 2007). Additionally, it has been shown that *in vitro* exposure of immortalized HEK (HaCaT) to SWCNT caused oxidative stress and cellular toxicity as indicated by the formation of free radicals, accumulation of peroxidative products, anti-oxidant depletion, and loss of cell viability. Cell viability significantly decreased with higher concentrations of SWCNT dose and longer exposure times (Shvedova *et al.*, 2003). Research involving fullerenes suggests that the underivatized C_{60} is cytotoxic to human liver carcinoma cells and fibroblasts (Sayes *et al.*, 2004) and can induce oxidative stress in juvenile largemouth bass (Oberdorster, 2004). Moreover, MWCNTs, carbon nanofibers, and carbon black have been shown to inhibit proliferation and initiate cell death in human lung tumor cell cultures and that chemical surface treatment increases the cytotoxicity (Magrez *et al.*, 2006).

The need for safety regulations to govern nanomaterial manufacturing, research, and consumer processes is solidified by the overwhelming amount of literature that reports the cytotoxic effects of nanoparticle exposure. Although no guidelines or regulations currently exist, several steps have been taken to raise awareness about the increasing threats of nanoparticle exposure and to begin deliberations about how to conduct nanoparticle risk assessments and safety evaluations (Thomas and Sayre, 2005; Oberdorster *et al.* 2005a, Holsapple, et al, 2005; Colvin, 2003). Understanding the mechanisms through which nanoparticles interact with biological and environmental systems is essential for the development of safety regulations. Ultimately, the ability to safely manufacture and apply nanomaterials will permit the use of these nanostructures in pharmaceutical and biomedical applications that will revolutionize the industrial world.

7. REFERENCES

Agache, P.G.; Monneur, C.; Leveque, J.L.; De Rigal, D. (1980) Mechanical properties and Young's modulus of human skin *in vivo*. *Archives of Dermatological Research*, 269: 221-232.

Allen, D.G.; Riviere, J.E.; Monteiro-Riviere, N.A. (2000) Identification of early biomarkers of inflammation produced by keratinocytes exposed to jet fuels Jet A, JP-8, and JP-8(100), *Journal of Biochemical Molecular Toxicology,* 14: 231–237.

Allen, D.G.; Riviere, J.E.; Monteiro-Riviere, N.A. (2001a) Analysis of interleukin-8 release from normal human epidermal keratinocytes exposed to aliphatic hydrocarbons: Delivery of hydrocarbons to cell cultures via complexation with α-cyclodextrin, *Toxicology In Vitro*, 15: 663–669.

Allen, D.G.; Riviere, J.E.; Monteiro-Riviere, N.A. (2001b) Cytokine induction as a measure of cutaneous toxicity in primary and immortalized porcine keratinocytes exposed to jet fuels and their relationship to normal human epidermal keratinocytes, *Toxicology Letters*, 119: 209–217.

Arroyo, C.M.; Schafer, R.J.; Kurt, E.M.; Broomfield, C.A.; Carmichael, A.J. (2000) Response of normal human keratinocytes to sulfur mustard: cytokine release. *Journal of Applied Toxicology*, 20: S63-S72.

Barkhausen, T.; van Griensven, M.; Zeichen, J.; Bosch, U. (2003) Modulation of cell functions of human tendon fibroblasts by different repetitive cyclic mechanical stress patterns. *Experimental Toxicology and Pathology*, 55(2-3): 153-158.

Bartek, M.J.; LaBudde, J.A.; Maibach, H.I. (1972) Skin permeability *in vivo*: Comparison in rat, rabbit, pig, and man. *Journal of Investigative Dermatology*, 58: 114-123.

Berg, D.J.; Leach, M.W.; Kuhn, R.; Rajewsky, K.; Muller, W.; Davidson, N.J.; Rennick D. (1995) Interleukin 10 but no interleukin 4 is a natural suppressant of cutaneous inflammatory responses. *Journal of Experimental Medicine*, 182: 99-108.

Bernstein, I.A.; Vaughan, F.L. (1999) Cultured keratinocytes in *in vitro* dermatotoxicological investigation: a review. *Journal of Toxicology and Environmental Health, Part B*, 2: 1-30.

Biswas, P.; Wu, C.Y. (2005) Nanoparticles and the environment. *Journal of Air & Waste Management Association*, 55: 708-746.

Bronaugh, R.L. (2006) *In vitro* diffusion cell studies. In *Dermal Absorption Models in Toxicology and Pharmacology*, Ed: J.E. Riviere, pp 21-27.

Bronaugh, R.L.; Stewart, R.F. (1985) Methods for *in vitro* percutaneous absorption studies IV: the flow-through diffusion cell. *Journal of Pharmaceutical Sciences*, 74: 64-67.

Bronaugh, R.L.; Stewart, R.F.; Storm, J.E. (1989) Extent of cutaneous metabolism during percutaneous absorption of xenobiotics. *Toxicology and Applied Pharmacology*, 99: 534-543.

Cartwright, J.E.; Whitley, G.S.; Johnstone, A.P. (1995) The expression and release of adhesion molecules by human endothelial cell lines and their consequent binding of lymphocytes. *Experimental Cell Research*, 217: 329-335.

Cassee, F.; Muijser, H.; Duistermaat, E.; Freijer, J.; Geerse, K.; Marijnissen, J. (2002) Particle size-dependent total mass deposition in lungs determines inhalation toxicity of cadmium chloride aerosols in rats. Application of a multiple path dosimetry model. *Archives of Toxicology*, 76: 277–286.

Chabot-Fletcher, M.; Breton, J.; Lee, J.; Young, P.; Griswold, D.E. (1994) Interleukin-8 production is regulated by protein kinase C in human keratinocytes. *Journal of Investigative Dermatology*, 103: 509–515.

Chang, S.K.; Riviere, J.E. (1991) Percutaneous absorption of parathion *in vitro* in porcine skin: effects of dose, temperature, humidity, and perfusate composition on absorptive flux. *Fundamental and Applied Toxicology*, 17: 494-504.

Charlier, J.C.; Issi, J.P. (1998) Electronic structure and quantum transport in carbon nanotubes. *Applied Physiology*, A67: 79-87.

Chen, C.S.; Mrksich, M.; Huang, S.; Whitesides, G.M.; Ingber, D.E. (1997) Geometric control of cell life and death. *Science*, 276(5317): 1425-1428.

Chen, J.L.; Lapiere, J.C.; Sauder, D.N.; Peavey, C.; Woodley, D.T. (1995) Interleukin-1 alpha stimulates keratinocyte migration through an epidermal growth factor/transforming growth factor-alpha-independent pathway. *Journal of Investigative Dermatology*, 104: 729-733.

Chou, C.; Riviere, J.E.; Monteiro-Riviere, N.A. (2003) The cytotoxicity of jet fuel aromatic hydrocarbons and dose-related interleukin-8 release from human epidermal keratinocytes. *Archives of Toxicology*, 77: 384–391.

Colvin, V.L. (2003) The potential environmental impact of engineered nanomaterials. *Nature Biotechnology*, 21(10): 1166-1170.

Cooper, E.R.; Merritt, E.W.; Smith, R.L. (1985) Effect of fatty acids and alcohols on the penetration of acyclovir across human skin *in vitro*. *Journal of Pharmaceutical Sciences*, 74: 688-689.

D'Addario, M.; Arora, P.D.; Fan, J.; Ganss, B.; Ellen, R.P.; MecCulloch, C.A.G. (2001) Cytoprotection against mechanical forces delivered through β1 integrins requires induction of filamin A. *Journal of Biological Chemistry*, 276: 31969-31977.

de Waal Malefyt R.; Abrams J.; Bennett B.; Figdor C.; de Vries J. (1991) IL-10 inhibits cytokine synthesis by human monocytes: an autoregulatory role of IL-10 produced by monocytes. *Journal of Experimental Medicine*, 174: 1209–1220.

Dunn, M.G.; Silver, F.H. (1983) Viscoelastic behavior of human connective tissues: relative contribution of viscous and elastic components. *Connective Tissue Research*, 12: 59-70.

Elias, P.M. (1983) Epidermal lipids, barrier function, and desquamation. *Journal of Investigative Dermatology*, 80: 44-49.

Enk, A.H.; Katz, S.I. (1992) Identification and induction of keratinocyte-derived IL-10. *Journal of Immunology*, 149: 92-95.

Feldmann, R.J.; Maibach, H.I. (1970) Absorption of some organic compounds through the skin in man. *Journal of Investigative Dermatology*, 54: 399-404.

Fiorentino D.F.; Zlotnik A.; Mosmann T.R.; Howard M.H.; O'Garra A. (1991) IL-10 inhibits cytokine production by activated macrophages. *Journal of Immunolology*, 147: 3815–3822.

Freedberg, I.M.; Tomic-Canic, M.; Komine, M.; Blumenberg, M. (2001) Keratins and the keratinocyte activation cycle. *Journal of Investigative Dermatology,* 116(5): 633-640.

Frommel, D.; Ayranci, B.; Pfeifer, H.R.; Sanchez, A.; Frommel, A.; Mengistu, G. (1993) Podoconiosis in the Ethiopian rift valley. Role of beryllium and zirconium. *Tropical and Geographical Medicine*, 45(4): 165-167.

Fusenig, N. E.; Worst, P. K. M. (1975) Mouse epidermal cell cultures: II. Isolation, characterization and cultivation of epidermal cells from perinatal mouse skin. *Experimental Cell Research*, 93: 443–457.

Grahame, R.; Holt, P.L.J. (1969) The influence of ageing on the *in vivo* elasticity of human skin. *Gerontologia*, 15: 121-139.

Granstein, R.D.; Sauder, D.N. (1987) Whole-body exposure to ultraviolet radiation results in increased serum interleukin-1 activity in humans. *Lymphokine Research*, 3: 187-193.

Grinnell, F. (2000) Fibroblast-collagen-matrix contraction: growth-factor signaling and mechanical loading. *Trends in Cell Biology*, 10:362-365.

Grone, A. (2002) Keratinocytes and cytokines. *Veterinary Immunology and Immunopathology*, 88: 1-12.

Grossman, R.M.; Krueger, J.; Yourish, D.; Granelli-Piperno, A.; Murphy, D.P.; May, L.T.; Kupper, T.S.; Sehgal, P.B.; Gottlieb, A.B. (1989) Interleukin 6 is expressed in high levels in psoriatic skin and stimulates proliferation of cultured human keratinocytes. *Proceedings of the National Academies of Science USA*, 86: 3637-6371.

Hadgraft, J. (2001) Modulation of the barrier function of skin. *Skin Pharmacology and Applied Skin Physiology*, 14(suppl 1): 72-81.

Hauser, C.; Saurat, J.H.; Schmitt, A.; Fabienne, J.; Dayer, J.M. (1986) Interleukin 1 is present in normal human epidermis. *Journal of Immunology*, 136(9): 3317-3323.

Hengge, U.R.; Chan, E.F.; Hampshire, V.; Foster, R.A.; Vogel, J.C. (1996) The derivation and characterization of pig keratinocyte cell lines that retain the ability to differentiate. *Journal of Investigative Dermatology*, 106(2): 287-293.

Holsapple, M.P.; Farland, W.H.; Landry, T.D.; Monteiro-Riviere, N.A.; Carter, J.M.; Walker, N.J.; and Thomas, K.V. (2005) Research strategies for safety evaluation of nanomaterials, Part II: Toxicological and safety evaluation of nanomaterials, current challenges and data needs. *Toxicological Sciences*, 88(1): 12-17.

Huang, M.; Khor, E.; Lim, L. (2004) Uptake and cytotoxicity of chitosan molecules and nanoparticles: Effects of molecular weight and degree of deacetylation, *Pharmacological Research*, 21: 344–353.

Huang, S.; Ingber, D.E. (1999) The structural and mechanical complexity of cell-growth control. *Nature Cell Biology*, 1(5): E131-E138.

Ingber, D.E. (1998) Cellular basis of mechanotranduction. *Biological Bulletin*, 194: 323-327.

Jaiswal, J.K.; Simon, S.M. (2004) Potentials and pitfalls of fluorescent quantum dots for biological imaging. *Trends in Cell Biology*, 14(9): 497-502.

Kaspar, D.; Seidl, W.; Neidlinger-Wilke C.; Ignatius, A.; Claes, L. (2000) Dynamic cell stretching increases human osteoblast proliferation and CICP synthesis but decreases osteocalcin synthesis and alkaline phosphatase activity. *Journal of Biomechanics*, 33(1): 45-51.

Kittelson, D.B. (1998) Engines and nanoparticles: a review. *Journal of Aerosol Science*, 29(5): 575-588.

Kolde, G.; Schulze-Osthoff, K.; Meyer, H.; Knop, J. (1992) Immunohistological and immunoelectron microscopic identification of TNF-α in normal human and murine epidermis. *Archives of Dermatology*, 284: 154-158.

Kroto, H.W.; Heath, J.R.; O'Brien, S.C.; Curl, R.F.; Smalley, R.E. (1985) C_{60}: Buckminsterfullerene. *Nature*, 318(6042): 162-163.

Kroto, H.W. (1992) C60, Buckminsterfullerene: the celestial sphere that fell to Earth. *Angewandte Chemie International Edition*, 31: 111-129.

Kupper, T.S. (1990) The activated keratinocyte: a model for inducible cytokine production by non-bone marrow-derived cells in cutaneous inflammatory and immune responses. *Journal of Investigative Dermatology*, 94: 146S-150S.

Kupper, T.S.; Ballard, D.W.; Chua, A.O.; McGuire, J.S.; Flood, P.M.; Horowitz, M.C.; Langdon, R.; Lightfoot, L.; Gubler, U. (1986) Human keratinocytes contain mRNA indistinguishable from monocyte interleukin 1 alpha and beta mRNA. Keratinocyte epidermal cell-derived thymocyte activating factor is identical to interleukin 1. *Journal of Experimental Medicine*, 164: 2095-2100.

Kupper, T.S.; Groves, R.W. (1995) The interleukin-1 axis and cutaneous inflammation. *Journal of Investigative Dermatology*, 105: 62S-66S.

Lardot, C.; Dubois, V.; Lison, D. (1999) Sulfur mustard upregulates the expression of interleukin-8 in cultured human keratinocytes. *Toxicology Letters*, 110: 29-33.

Lee, R.T.; Briggs, W.H.; Cheng, G.C.; Rossiter, H.B.; Libby, P.; Kupper, T.S. (1997) Mechanical deformation promotes secretion of IL-1α and IL-1 receptor antagonist. *Journal of Immunology*, 5084-5088.

Liu, S.C.; Karasek, M. (1978) Isolation and growth of adult human epidermal keratinocytes in cell culture *Journal of Investigative Dermatology*, 71: 157–162.

Liu, S.C.; Eaton, M.J.; Karasek, M. A. (1979) Growth characteristics of human epidermal keratinocytes from newborn foreskin in primary and serial cultures. *In Vitro*, 15: 813–822.

Loboa, E.G.; Fang, T.D; Warren, S.M.; Lindsey, D.P.; Fong, K.D.;Longaker, M.T.; Carter, D.R. (2004) Mechanobiology of mandibular distraction osteogenesis: experimental analyses with a rat model. *Bone*, 34(2), 336-343.

Mackenzie, I.C. (1975) Ordered structure of the epidermis. *Journal of Investigative Dermatology*, 65(1): 45-51.

Magrez, A.; Kasas, S.; Salicio, V.; Pasquier, N.; Seo, J.; Celio, M.; Catsicas, S.; Schwaller, B.; Forro, L. (2006) Cellular toxicity of carbon-based nanomaterials. *Nano Letters*, 6(6): 1121-1125.

Maibach, H.I.; Feldmann, R.J.; Milby, T.H.; Serat, W.F. (1971) Regional variation in percutaneous penetration in man, *Archives of Environmental Health*, 23: 208-211.

Menton, D.N. (1976) A liquid film model of tetrakaidecahedral packing to account for the establishment of epidermal cell columns. *Journal of Investigative Dermatology*, 66(5): 283-291.

Meyer, W., Schwarz, R., and Neurand, K. (1978) The skin of domestic mammals as a model for the human skin with special reference to the domestic pig. *Current Problems in Dermatology*, 7:39-52.

Meyer, W.; Gorgen, S.; Schlesinger, C. (1986) Structural and histochemical aspects of epidermis development of fetal porcine skin. *American Journal of Anatomy*, 176: 207-219.

Mizutani, H.; Black, R.; Kupper, T.S. (1991) Human keratinocytes produce but not process pro-IL-1 beta: different strategies and processing in monocytes and keratinocytes. *Journal of Clinical Investigation*, 87: 1066-1071.

Mizutani, H.; May, L.T.; Sehgal, P.B.; Kupper, T.S. (1989) Synergistic interactions of IL-1 and IL-6 in T cell activation. *Journal of Immunology*, 143(3): 896-901.

Montagna, W.; Yun, J.S. (1964) The skin of the domestic pig. *Journal of Investigative Dermatology*, 43: 11-21.

Monteiro-Riviere, N.A. (1986) Ultrastructural evaluation of the porcine integument. *In: Swine in Biomedical Research.* Ed. M.E. Tumbleson, Plenum Press, New York, pp. 641-655.

Monteiro-Riviere, N.A. (1991) Comparative anatomy, physiology, and biochemistry of mammalian skin. *In: Dermal and Ocular Toxicology: Fundamentals and Methods.* Ed. D Hobson, CRC Press, London. pp. 3-17.

Monteiro-Riviere, N.A. (2001a) Dermatotoxicology. *In: Introduction to Biochemical Toxicology.* Eds. E. Hodgson and R.C. Smart, Wiley-Interscience. pp. 509-537.

Monteiro-Riviere, N.A. (2001b) Integument. *In: Biology of the Domestic Pig.* Ed. W.G. Pond and H.J. Mersmann, Comstock Publishing. pp. 625-652.

Monteiro-Riviere, N.A. (2004) Anatomical factors affecting barrier function. *In: Dermatotoxicology*. Eds. H. Zhai and H.I. Maibach, CRC Press. pp. 43-70.

Monteiro-Riviere, N.A. (2006) Structure and function of skin. *In: Dermal Absorption Models in Toxicology and Pharmacology.* Ed. J.E. Riviere, Taylor and Francis. pp. 1-19.

Monteiro-Riviere, N.A.; Baynes, R.; Riviere, J.E. (2003) Pyridostigmine bromide modulates topical irritant-induced cytokine release from human epidermal keratinocytes and isolated perfused porcine skin, *Toxicology*, 183: 15–28.

Monteiro-Riviere, N.A.; Inman, A.O. (2006) Challenges for assessing carbon nanomaterial toxicity to the skin. *Carbon*, 44: 1070-1078.

Monteiro-Riviere, N.A.; Inman, A.O.; Mak, V.; Wertz, P.; Riviere, J.E. (2001) Effect of selective lipid extraction from different body regions on epidermal barrier function. *Pharmaceutical Research*, 18: 992-998.

Monteiro-Riviere, N.A.; Nemanich, R.; Inman, A.O.; Wang, Y.; Riviere, J.E. (2005) Multi-walled carbon nanotube interactions with human epidermal keratinocytes, *Toxicology Letters,* 155: 377–384.

Monteiro-Riviere, N.A.; Riviere, J.E. (1996) The pig as a model for cutaneous pharmacology and toxicology research. *In: Advances in Swine in Biomedical Research*. Eds. M.E. Tumbleson and L.B. Schook, Plenum Publishing Corp., New York, NY, Vol. II 38, pp. 425-458.

Monteiro-Riviere, NA, Stinson, AW, Calhoun, HL (1993) Integument. *In: Textbook of Veterinary Histology.* Ed. H.D. Dellmann, Lea and Febiger. pp. 285-312.

Monteiro-Riviere, N.A.; Stromberg, M.W. (1985) Ultrastructure of the integument of the domestic pig (*Sus scrofu*) from one through fourteen weeks of age. *Zbl. Veterinary Medicine of Comparative Anatomy, Histology, and Embryology*, 14:97-115.

Monteiro-Riviere, N. A.; Yang, J.; Inman, A. O.; Ryman-Rasmussen, J. P.; Barron, A. R.; Riviere, J. E. Skin penetration of fullerene substituted amino acids and their interactions with human epidermal keratinocytes, 827, *The Toxicologist CD – An official Journal of the Society of Toxicology*, Volume 90, Number S-1, March 2006.

Nickoloff, B.J. (1991) The cytokine network in psoriasis. *Archives of Dermatology*, 127: 871-883.

Nickoloff, B.J.; Karabin, G.D.; Barker, J.N.W.N.; Griffiths, C.E.M.; Sarma, V.; Mitra, R.S.; Elder, J.T.; Kunkel, S.L.; Dixit, V.M. (1991) Cellular localization of interleukin-8 and its inducer, tumor necrosis factor-alpha in psoriasis. *American Journal of Pathology*, 138(1): 129-140.

Nickoloff, B.J.; Turka, L.A. (1993) Keratinocytes: key immunocytes of the integument. *American Journal of Pathology*, 143(2): 325-331.

Oberdorster, G. (1996) Significance of particle parameters in the evaluation of exposure-dose–response relationships of inhaled particles, *Inhalation Toxicology*, 8(Supplementary): 73–89.

Oberdorster, E. (2004) Manufactured nanomaterials (fullerenes, C_{60}) induce oxidative stress in the brain of juvenile largemouth bass, *Environmental Health Prospective*, 112: 1058–1062.

Oberdorster, G.; Maynard, A.; Donaldson, K.; Castranova, V.; Fitzpatrick, J.; Ausman, K.; Carter, J.; Karn, B.; Kreyling, W.; Lai, D.; Olin, S.; Monteiro-Riviere, N.; Warheit, D.; Yang, H. (2005a) Principles for characterizing the potential human health effects from exposure to nanomaterials: elements of a screening strategy. *Particle and Fibre Toxicology*, 2: 1–35.

Oberdorster, G.; Oberdorster, E.; Oberdorster, J. (2005b) Nanotoxicology: An emerging discipline evolving from studies of ultrafine particles, *Environmental Health Perspectives*, 113: 823–839.

Oxlund, H.; Maschot, J.; Vidiik, A. (1988) The role of elastin in the mechanical properties of skin. *Journal of Biomechanics*, 21: 213-218.

Rivas, J.M. ; Ullrich, S.E. (1992) Systemic suppression of delayed-type hypersensitivity by supernatants by UV-irradiated keratinocytes. *Journal of Immunology*, 149: 3865-3871.

Riviere, J.E. (1990) Biological factors in absorption and permeation. *Cosmetics and Toiletries*, 105: 85-93.

Romero, L.I.; Zhang, D.N.; Herron, G.S.; Karasek, M.A. (1997) Interleukin-1 induces major phenotypic changes in human skin microvascular endothelial cells. *Journal of Cell Physiology*, 173: 84-92.

Ryman-Rasmussen, J.P.; Riviere, J.E.; Monteiro-Riviere, N.A. (2006) Penetration of intact skin by quantum dots with diverse physiochemical properties. *Toxicological Sciences*, 9(1): 159-165.

Sayes, C.; Gobin, A.; Ausman, K.; Mendez, J.; West, J.; Colvin, V. (2005) Nano-C_{60} cytotoxicity is due to lipid peroxidation, *Biomaterials*, 26: 7587–7595.

Scheuplein, R.J. (1967) Mechanisms of percutaneous absorption, II. Transient diffusion and the relative importance of various routes of skin penetration. *Journal of Investigative Dermatology*, 48: 79-88.

Scheuplein, R.J.; Blank, I.H. (1971) Permeability of the skin. *Physiological Reviews*, 51(4): 702-743.

Shvedova, A.; Castranova, V.; Kisin, E.; Schwegler-Berry, D.; Murray, A.; Gandelsman, V.; Maynard, A.; Baron, P. (2003) Exposure to carbon nanotube material: Assessment of nanotube cytotoxicity using human keratinocytes cells. *Journal of Toxicology and Environmental Health*, 66: 1909–1926.

Silver, F.H. (1987) Biological materials: structure, mechanical properties, and modeling of soft tissues. New York: N.Y.U. Press, 1987; pp. 75-79, 164-195.

Silver, F.H.; Christiansen, D.L.; Snowhill, P.B.; Chen, Y. (2001) Transition from viscous to elastic-based dependency of mechanical properties of self-assembled type I collagen fibers. *Journal of Applied Polymer Science*, 79: 134-142.

Silver, F.H.; Siperko, L.M.; Seehra, G.P. (2003) Mechanobiology of force transduction in dermal tissue. *Skin Research and Technology*, 9: 3-23.

Skinner, C.S.; Kilgore, W.W. (1982) Percutaneous penetration of [^{14}C]parathion in the mouse: Effect of anatomic region. *Journal of Toxicology and Environmental Health*, 9: 483-490.

Smack, D.P.; Korge, M.D.; James, W.D. (1994) Keratin and keratinization. *Journal of the American Academy for Dermatology*, 30: 85-102.

Sumanasinghe, R.D.; Bernacki, S.H.; Loboa, E.G. (2006) Osteogenic differentiation of human mesenchymal stem cells in collagen matrices: effect of uniaxial cyclic tensile strain on bone morphogenetic protein (BMP-2) mRNA expression. *Tissue Engineering*, 12(12), in press.

Takei, T.; Kito, H.; Du, W.; Mills, I.; Sumpio, B.E. (1998) Induction of interleukin (IL)-1α and β gene expression in human epidermal keratinocytes exposed to repetitive strain: their role in strain-induced proliferation and morphological change. *Journal of Cellular Biochemistry*, 69: 95-103.

Takei, T.; Rivas-Gotz, C.; Delling, C.A.; Koo, J.T.; Mills, I.; McCarthy, T.L.; Centrella, M.; Sumpio, B.E. (1997) Effect of strain on human keratinocytes *in vitro*. *Journal of Cellular Physiology*, 173:64-72.

Taylor, C.; Scogna, K.H.; Ajello, J.P. (Eds). (2006) *Histology: A Text and Atlas*. Baltimore: Lippencott Williams & Wilkins. pp. 98-138; 442-463.

Terrones, M.; Terrones, H. (2003) The carbon nanocosmos: novel materials for the twenty-first century. *Philosophical Transactions of the Royal Society of London,* A361: 2789-2806.

The Royal Society, London (2004) *Nanoscience and nanotechnology: opportunities and uncertainties*, http://www.nanotec.org.uk/finalReport.htm.

Thomas, K.; Sayre, P. (2005) Research strategies for safety evaluation of nanomaterials. Part I: Evaluating the human healthy implications of exposure to nanoscale materials, *Toxicological Science*, 87(2): 316–321.

Tinkle, S. S.; Antonini, J. M.; Rich, B. A.; Roberts, J. R.; Salmen, R.; DePree, K.; Adkins, E. J. (2003) Skin as a route of exposure to sensitization in chronic beryllium disease. *Environmental Health Perspectives*, 111: 1202-1208.

Tomic-Canic, M.; Komine, M.; Freedberg, I.M. (1998) Epidermal signal transduction and transcription factor activation in activated keratinocytes. *Journal of Dermatology Science*, 17: 167-181.

Urbanski, A.; Schwarz, T.; Neuner, P. (1990) Ultraviolet light induces increased circulating interluekin-6 in humans. *Journal of Investigative Dermatology*, 94: 808-811.

Vandenburgh, H.H. (1992) Mechanical forces and their second messengers in stimulating cell growth *in vitro*. *American Journal of Physiology*, 262: R350-R355.

Wang, J.H.-C.; Thampatty, B.P. (2006) An introductory review of cell mechanobiology. *Biomechanics and Modeling in Mechanobiology*, 5: 1-16.

Wertz, P.W. (2004) Percutaneous absorption: role of lipids. *In: Dermatotoxicology.* Eds. H. Zhai and H.I. Maibach, CRC Press. pp. 71-81.

Woolina, U.; Berger, U.; Mahrle, G. (1991) Immunohistochemistry of porcine skin, *Acta Histochema*, 90: 87-91.

Yang, J.; Alemany, L.B.; Driver, J.; Hartgerink, J.D.; Barron, A.R. (2007a) Fullerene-derivatized amino acids: synthesis, characterization, antioxidant properties, and solid-phase peptide synthesis. *Chemistry - A European Journal*, in press.

Yang, J.; Wang, K.; Driver, J.; Yang, J.; Barron, A.R. (2007b) The use of fullerene substituted phenylalanine amino acid as a passport for peptides through cell membranes. *Organic & Biomolecular Chemistry*, 5: 260-266.

Yang, L.; Watts, D. (2005) Particle surface characteristics may play an important role in phytotoxicity of alumina nanoparticles, *Toxicology Letters*, 158: 122–132.

Yang, X.C.; Sachs, F. (1993) Mechanically sensitive, non-selective cation channels. *EXS*, 66: 79-92.

Yano, S.; Komine, M.; Fujimoto, M.; Okochi, H.; Tamaki, K. (2004) Mechanical stretching *in vitro* regulates signal transduction pathways and cellular proliferation of human epidermal keratinocytes. *Journal of Investigative Dermatology*, 122: 783-790.

Zhang, L.W.; Zeng, L.; Barron, A.R.; Monteiro-Riviere, N.A. (2007) Biological interactions of functionalized single-wall carbon nanotubes in human epidermal keratinocytes. *Journal of International Toxicology*, in press.

CHAPTER 3: FULLERENE-BASED AMINO ACID INTERACTIONS WITH HUMAN EPIDERMAL KERATINOCYTES

J.G. Rouse, J. Yang, A.R. Barron, and N.A. Monteiro-Riviere

Published in *Toxicology In Vitro* 20: 1313-1320, 2006.

ABSTRACT

The functionalization of C_{60} with such complexes as amino acids has the potential to provide greater interaction between the fullerene and the biological environment yielding potential new medical and pharmacological applications. Although scientific research in the past decade has revealed much about the chemical and physical properties of C_{60}, the biological activities of this compound and its derivatives are still relatively unclear. In an attempt to understand the biological activity of functionalized C_{60}, human epidermal keratinocytes (HEK) were exposed to fullerene-based amino acid (Baa) solutions ranging in concentrations of 0.4–0.00004 mg/mL in a humidified 5% CO_2 atmosphere at 37 °C. MTT cell viability after 48 h significantly decreased ($p < 0.05$) for concentrations of 0.4 and 0.04 mg/mL. In an additional study, human cytokines IL-6, IL-8, TNF-α, IL-1β, and IL-10 were assessed for concentrations ranging from 0.4–0.004 mg/mL. Media was harvested at 1, 4, 8, 12, 24 and 48 h for cytokine analysis. IL-8 concentrations for the 0.04 mg/mL treatment were significantly greater ($p < 0.05$) than all other concentrations at 8, 12, 24, and 48 h. IL-6 and IL-1β activities were greater at the 24 h and 48 h for 0.4 and 0.04 mg/mL. No significant TNF-α or IL-10 activity existed at any time points for any of the concentrations. These results indicate that concentrations lower than 0.04 mg/mL initiate less cytokine activity and maintain cell viability. In HEK, Baa concentrations of 0.4 and 0.04 mg/mL decrease cell viability and initiate a pro-inflammatory response.

1. INTRODUCTION

Engineered nanomaterials have structural features with at least one dimension in the 1–100 nm range. These materials possess unique chemical, mechanical, electrical, optical, magnetic, and biological properties that make them ideal candidates for a variety of novel commercial and medical applications. Engineered nanomaterials are commonly produced in a wide variety of types, including fullerenes (C_{60} or Bucky balls), carbon nanotubes (CNT), metal and metal oxide particles, polymer nanoparticles, and quantum dots. Each type of nanoparticle exhibits different characteristics that are desirable for widespread applications such as drug delivery systems, energy conservation, and consumer products. The rapidly developing commercialization of nanoparticles arouses the need for toxicological and safety evaluations to be conducted in order to assess the biological risks associated with nanomaterial exposure (Colvin, 2003, Holsapple *et al.*, 2005, Oberdorster *et al.*, 2005a, Oberdorster *et al.*, 2005b and Thomas and Sayre, 2005).

Exposure to nanomaterials could occur through oral, dermal, inhalation, and injection routes, all of which could potentially initiate an adverse biological response. The unique physiochemical properties of nanomaterials (i.e., shape, particle size, agglomeration state, crystal structure, chemical composition, surface area, surface chemistry, surface charge, and porosity) are most likely responsible for the biological activity that occurs in response to nanoparticle exposure (Colvin, 2003 and Oberdorster *et al.*, 2005a). Specifically, nanoparticles of smaller size have a greater potential for biological interaction because these particles have a greater surface area per unit mass (Cassee *et al.*, 2002, Oberdorster, 1996, Oberdorster *et al.*, 2005b, Huang *et al.*, 2004 and Yang and Watts, 2005). The exact

interactions that occur between nanoparticles and the biological environment, however, are poorly understood and the mechanistic pathways relatively unknown.

Although little is known about the biological effects induced by exposure to nanoparticles, past research provides useful information for evaluating the potential hazards associated with nanoparticle exposure. Monteiro-Riviere *et al.* (2005b) reported that exposure of human epidermal keratinocytes (HEK) to multi-walled carbon nanotubes (MWCNT) initiated a pro-inflammatory response, indicated by the release of IL-8. Cell toxicity was shown to be both dose- and time-dependent throughout the 1–48 h exposure period. Transmission electron microscopy (TEM) verified cellular uptake of the MWCNT, in intracytoplasmic vacuoles of the HEK (Monteiro-Riviere *et al.*, 2005b). Additionally, it has been shown that *in vitro* exposure of immortalized HEK to single-walled carbon nanotubes (SWCNT) caused oxidative stress and cellular toxicity as indicated by the formation of free radicals, accumulation of peroxidative products, anti-oxidant depletion, and loss of cell viability. Cell viability significantly decreased with higher concentrations of SWCNT dose and longer exposure times (Shvedova *et al.*, 2003). Research involving fullerenes suggests that the underivatized C_{60} is cytotoxic to human liver carcinoma cells and fibroblasts (Sayes *et al.*, 2004) and can induce oxidative stress in juvenile largemouth bass (Oberdorster, 2004).

Analysis of cytokine activity is useful for determining the response of HEK to nanoparticles. Keratinocytes produce cytokines that serve as mediators for inflammatory and immunologic reactions in skin exposed to irritants (Allen *et al.*, 2000, Allen *et al.*, 2001a, Allen *et al.*, 2001b, Corsini and Galli, 1998, Monteiro-Riviere *et al.*, 2003, Monteiro-Riviere *et al.*, 2005b, Barker *et al.*, 1991 and Nickoloff, 1991). Consequentially, cytokine production by keratinocytes can influence the migration of inflammatory cells, have systemic effects on

the immune system, influence keratinocyte proliferation and differentiation, and affect the production of other cytokines by keratinocytes (Grone, 2002). The pro-inflammatory cytokines IL-8, IL-6, TNF-α, and IL-1β have been very well studied and characterized and are regularly used as indicators of cytotoxicity (Grone, 2002, Barker *et al.*, 1991 and Nickoloff, 1991). Although different toxicants elicit various responses in keratinocytes, several previous studies in our laboratories have shown cytokine release by HEK in response to jet fuel exposure (Allen *et al.*, 2000, Allen *et al.*, 2001a, Allen *et al.*, 2001b, Chou *et al.*, 2003 and Monteiro-Riviere *et al.*, 2003) and multi-walled carbon nanotube exposure (Monteiro-Riviere *et al.*, 2005b). IL-10 is an anti-inflammatory cytokine and has been shown to be a natural suppressant of irritant responses and to limit the immunopathologic damage caused by toxicants (Enk and Katz, 1992 and Berg *et al.*, 1995). The presence of IL-10 is indicative of immune suppression, a common sequel to dermal irritation (Berg *et al.*, 1995 and Grone, 2002).

The poor water solubility of fullerenes has limited research evaluating their biological interactions, since the water insolubility restricts pristine C_{60} from naturally interacting with biological substances (Tabata and Ikada, 1999). However, the functionalization of C_{60} (i.e., the addition of amino acids, hydroxyl groups, carboxyl groups, etc.) can increase the nanoparticles' ability to interact with the biological environment (Yang and Barron, 2004 and Colvin, 2003). The purpose of this study was to investigate the effects of dermal exposure to fullerene substituted phenylalanine derivatives by analyzing cell viability and cytokine activity in HEK.

2. MATERIALS AND METHODS

2.1 Baa Synthesis

N-Boc–Baa (compound 1) was synthesized and purified by our previous method (Yang and Barron, 2004). Compound 1 (100 mg, 0.1 mmol) was mixed with 10 mL trifluoroacetic acid (TFA) in a 20 mL scintillation vial. The solution was sonicated for 2 h and stirred overnight. The product precipitated out shortly after sonication. The brown precipitate (Baa, compound 2) was centrifuged out and washed with Et_2O for 3 cycles, and then lyophilized to dryness with a 99% yield (98 mg) (see Scheme 1).

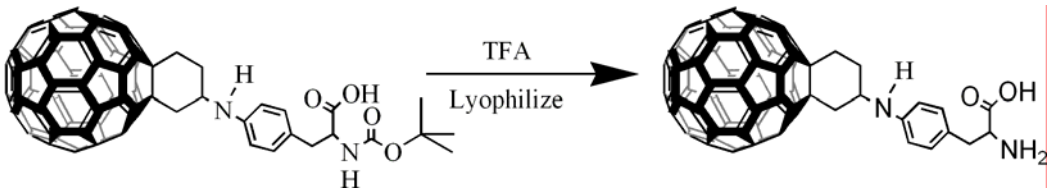

Compound 1 **Compound 2**

Scheme 1. Synthesis of C_{60}-Phe-OH (Baa)

2.2 Cell Culture

Cryopreserved neonatal HEK were purchased from Clonetics, Corp. (San Diego, CA). In order to assess the biological effect of fullerene-based amino acid (Baa), HEK were plated in 96-well culture plates (0.32 cm^2 growth area) at a density of ≈7000 cells per well and grown in a humidified environment of 5% CO_2 at 37 °C. Cells were maintained in keratinocyte growth media (KGM-2), consisting of serum-free keratinocyte basal media supplemented with human epidermal growth factor, insulin, bovine pituitary extract, hydrocortisone, transferrin, epinephrine and GA-1000 (Clonetics, Corp.).

2.3 Dose Response

Baa was added to the growth media to create a stock solution of 0.4 mg/mL. The stock solution was vortexed for ≈3 min, then sonicated for 10 min to break up aggregates and form a suspension. From this stock, serial dilutions of 0.04, 0.004, 0.0004, and 0.00004 mg/mL Baa were prepared and used to treat the cells ($n = 4$ wells/treatment). After reaching 70% confluency, each 96-well plate was exposed to the Baa solutions and to media alone (control). At 24 h and 48 h, HEK viability was determined by the MTT (3-[4,5-dimethyl-2-thiazol]-2,5-diphenyl-2 H-tetrazolium bromide) assay (Mosmann, 1983). Since the residual Baa containing carbon can affect the absorbance values (Monteiro-Riviere and Inman, 2006), the solution in each well was pipetted into a new 96-well plate. Absorbance, directly proportional to cell viability, was determined spectrophotometrically at 550 nm in an ELISA plate reader (Multiskan RC, Labsystems, Helsinki, Finland). The results from this study were used to determine the range of Baa concentrations that would not initiate a toxic response in HEK.

2.4 Time Response

Once a dose response of Baa was determined, HEK ($n = 4$ wells/treatment) were treated for 1, 4, 8, 12, 24, and 48 h in 96-well culture plates with 0.4, 0.04 and 0.004 mg/mL of Baa and in media alone (the control). After each treatment time, the media was pooled, aliquotted, and stored at −80 °C until future cytokine assays. At the termination of the 48 h experiment, HEK viability was determined as described above.

2.5 Cytokine Assay

The human cytokines IL-1β, IL-6, IL-8, IL-10, and TNF-α were quantitated with the Bio-Plex suspension array system (Bio-Rad Laboratories, Hercules, CA). This system utilizes multi-plexing to simultaneously assay for cytokines. Customized beads (5.6 μm diameter) conjugated to a capture antibody that is specific to each cytokine, IL-1β, IL-6, IL-8, IL-10, or TNF-α, and possessing a unique spectral address were mixed with culture media and incubated in a 96-well plate. The beads were rinsed and then incubated with a fluorescent-labeled reporter molecule that specifically bound to the analyte. The contents of each well were analyzed in the Bio-Plex array reader. As the beads flow into the reader, one laser identifies the spectral address of each cytokine and the other laser excites the reporter molecule to quantitate the specific cytokine relative to the standard curve. The average concentration (pg/mL) of each cytokine for each treatment and time point were calculated in order to determine the time dependency of the toxicity on HEK.

2.6 TEM

Transmission electron microscopy (TEM) was conducted on the exposed HEK to visualize cellular uptake of Baa by the HEK. Cell culture flasks (25 cm^2) were seeded with HEK (100 000 cells/flask) and grown to 80% confluency. Cells were treated with either 0.4, 0.04, or 0.004 mg/mL of Baa for 24 h and 48 h, rinsed in Hank's balanced salt solution, fixed in Trump's fixative at 4 °C for 24 h, and then harvested by gently scraping. The cells were then rinsed in 0.1 M phosphate buffer (pH 7.2), pelleted in a microcentrifuge tube, and embedded in 3% molten agar. The cells pelleted in the agar were post-fixed in osmium tetroxide and dehydrated through graded ethanol solutions, cleared in acetone, and infiltrated and embedded in Spurr's resin. Thin sections (800–1000 Å) were stained with uranyl acetate

and lead citrate and then mounted on copper grids and examined on a Philips EM208S transmission electron microscope. Unstained sections were also used to visualize Baa in the cells.

2.7 Statistical Analysis

HEK viability and cytokine concentrations (normalized to viability) were statistically compared using ANOVA (SAS 9.1 for Windows, Cary, NC). For each exposure time, multiple comparisons were made between different treatments using the Student's *t*-test at $p < 0.05$.

3. RESULTS

3.1 Dose Response and HEK Viability

HEK viability assessed by the MTT assay significantly decreased ($p < 0.05$) in a dose-dependent manner after 24 h and 48 h (data not shown). Baa at 0.004 mg/mL concentration was the highest concentration that did not show a significant decrease in viability. The time-study conducted on Baa at 0.004, 0.04, and 0.4 mg/mL also depicted a dose-dependent decrease in cell viability at 48 h (Fig. 3.1).

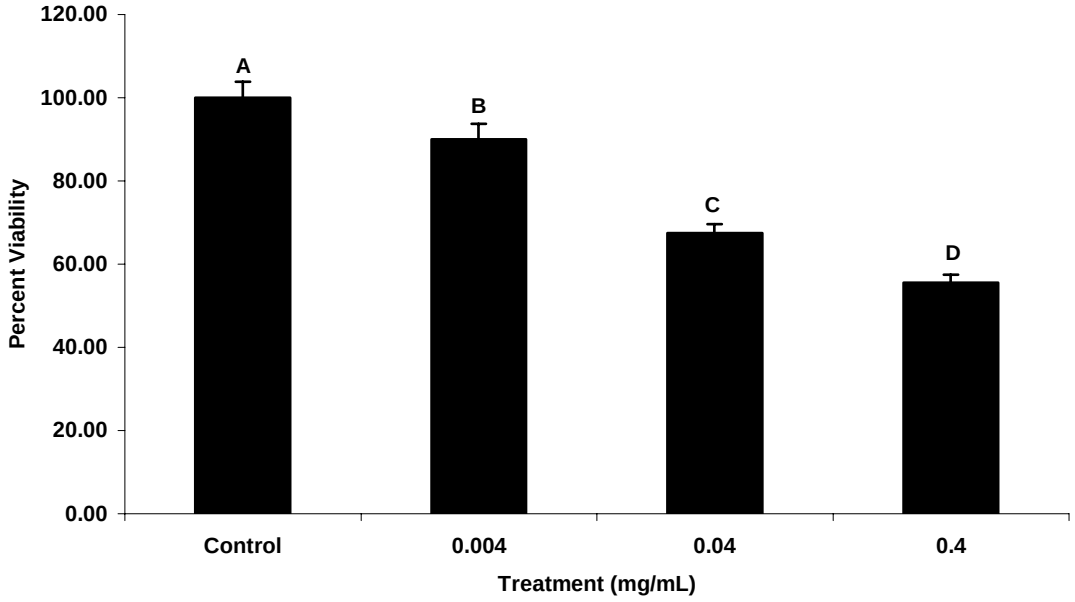

Figure 3.1. Effect of Baa on HEK viability. Mean viability (±SEM) of MTT 48 h after exposure to Baa. Histogram with different letters (A, B, C, D) denote mean values that are statistically different at $p < 0.05$.

3.2 Time Response and Cytokine Expression

IL-8 release increased with time (Fig. 3.2). At 8 h, IL-8 concentration for Baa treatment of 0.04 mg/mL peaked and was statistically different ($p > 0.05$) from control and all other treatments and continued to be higher through 48 h. HEK release of IL-6 increased with time for the Baa concentrations of 0.4 and 0.04 mg/mL but were not significantly different ($p < 0.05$) from one another (Fig. 3.3). In comparison to control levels, significantly greater ($p < 0.05$) concentrations of IL-6 release were detected in the 0.04 mg/mL Baa at both 24 h and 48 h. Likewise at 48 h, the IL-6 concentration of the 0.4 mg/mL Baa was significantly greater ($p < 0.05$) than control levels. The release of IL-1β by HEK treated with 0.04 mg/mL of Baa peaked at 12 h compared to control and other treatments (Fig. 3.4). At 48 h, 0.4 mg/mL had statistically greater ($p < 0.05$) concentrations of IL-1β than controls and

0.004 mg/mL. No significant differences occurred between treatments and controls for the cytokines IL-10 or TNF-α (data not shown).

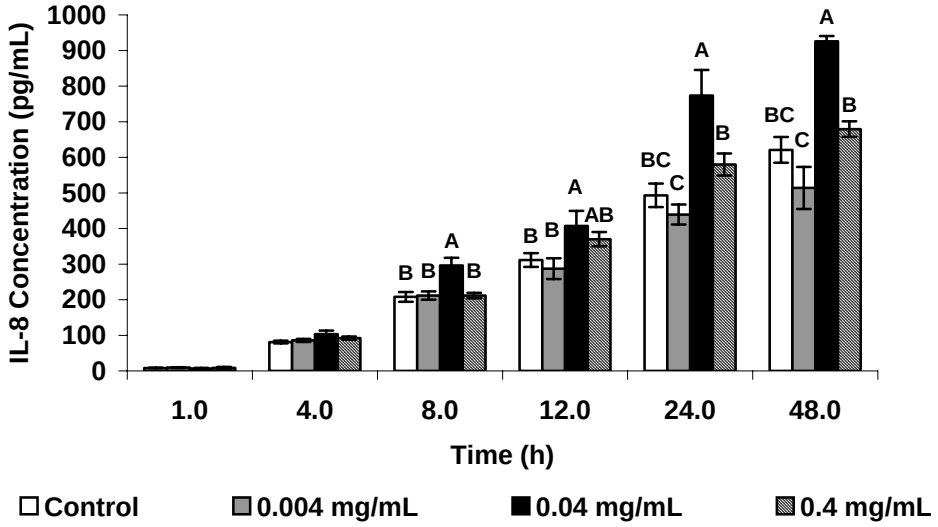

Figure 3.2. IL-8 release in HEK exposed to Baa. Mean IL-8 concentration (±SEM) increases with exposure time. Histogram with different letters (A, B, C) denote mean values that are statistically different at $p < 0.05$.

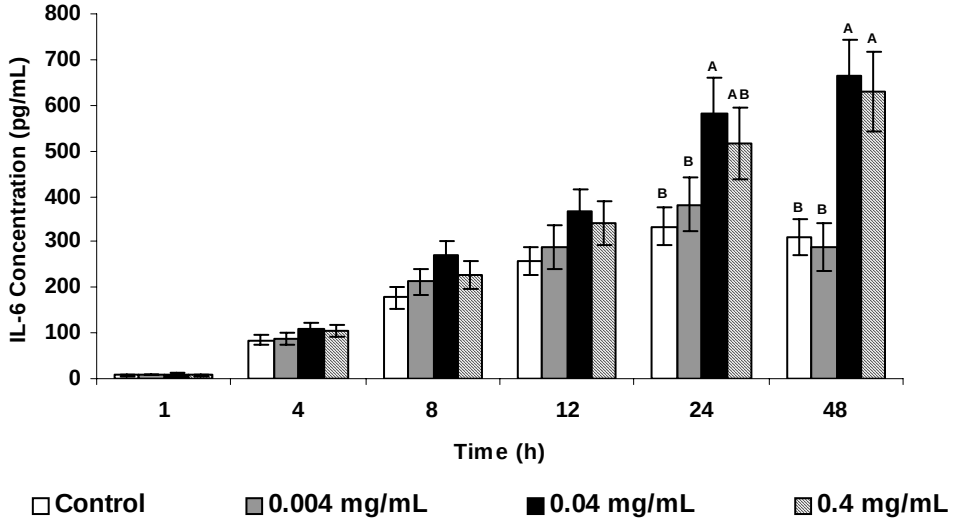

Figure 3.3. Mean IL-6 concentration (±SEM). Histogram with different letters (A, B) denote mean IL-6 values that are significantly different at $p < 0.05$.

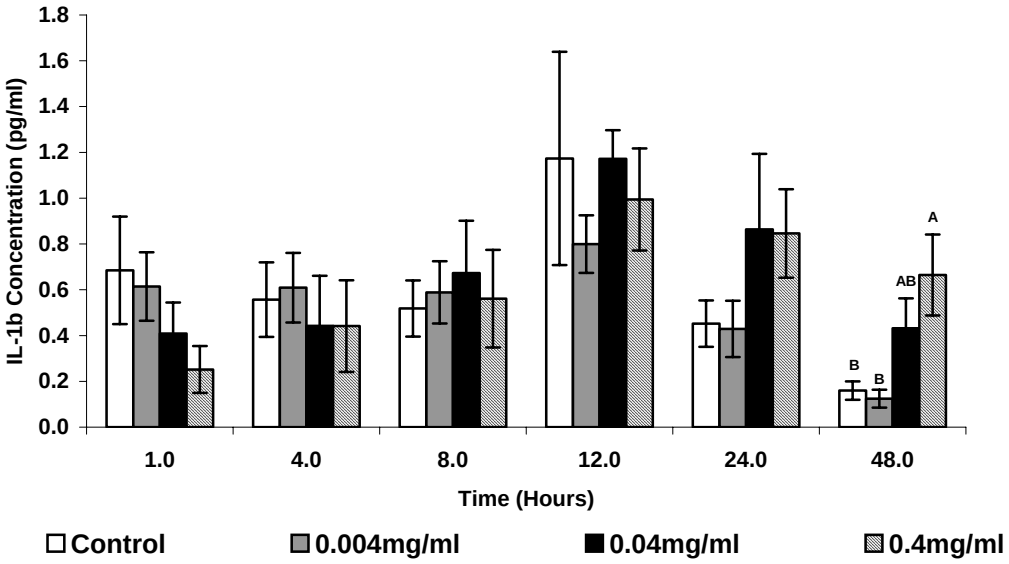

Figure 3.4. Mean IL-1β concentration (±SEM). Histogram with different letters (A, B) denote mean values that are significantly different at $p < 0.05$.

3.3 TEM

At 24 h, the TEM of the HEK treated with 0.00004 mg/mL Baa, the lowest concentration, did not show uptake of the Baa. The 0.0004 mg/mL concentration rarely depicted particles in the cytoplasm of the HEK, while few particles were found in the cytoplasm of HEK treated with 0.004 mg/mL. Unstained TEM of the HEK treated with 0.04 mg/mL at 24 h demonstrates several cells containing a few Baa particles in many vacuoles (Fig. 3.5). Since Fig. 3.5 is unstained, large agglomerates of Baa nanoparticles can be easily identified. At the 0.4 mg/mL Baa treatment, which was the highest concentration, numerous cells containing many cytoplasmic vacuoles that had Baa nanoparticles located within were depicted (Fig. 3.6). By 48 h, TEM observations showed an increase in the number of Baa nanoparticles and a further increase in the number of cells containing the Baa, especially at the 0.4 mg/mL dose (Fig. 3.7 and Fig. 3.8). Many of the keratinocytes were

necrotic (Fig. 3.7) but at other times appeared normal except for the presence of cytoplasmic extensions suggesting phagocytosis of the Baa nanoparticles (Fig. 3.8).

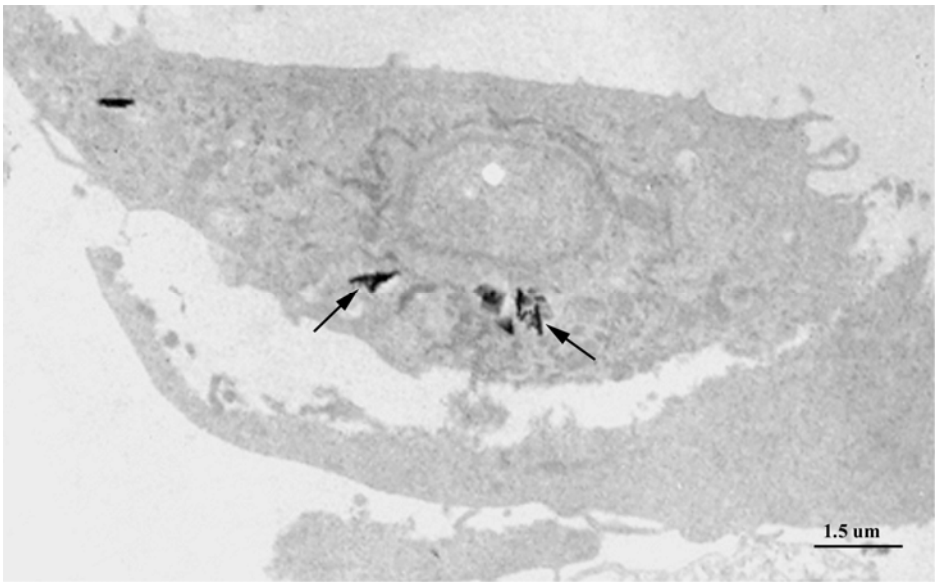

Figure 3.5. TEM micrograph depicting intracytoplasmic vacuole localization of 0.04mg/mL Baa (arrows) after 24 h (unstained).

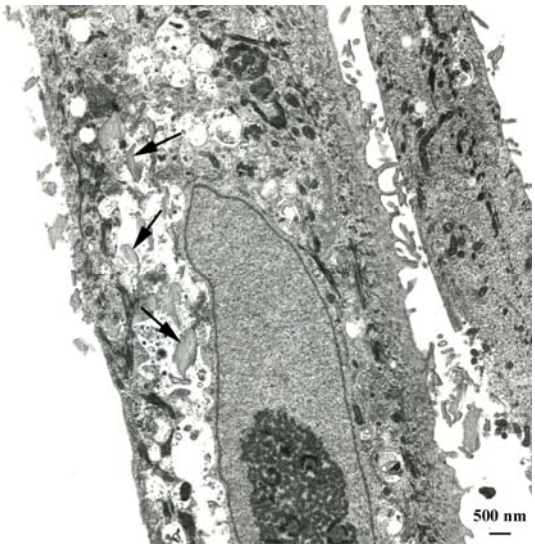

Figure 3.6. TEM micrograph that shows the localization of 0.4 mg/mL Baa (arrows) after 24 h (post-stained).

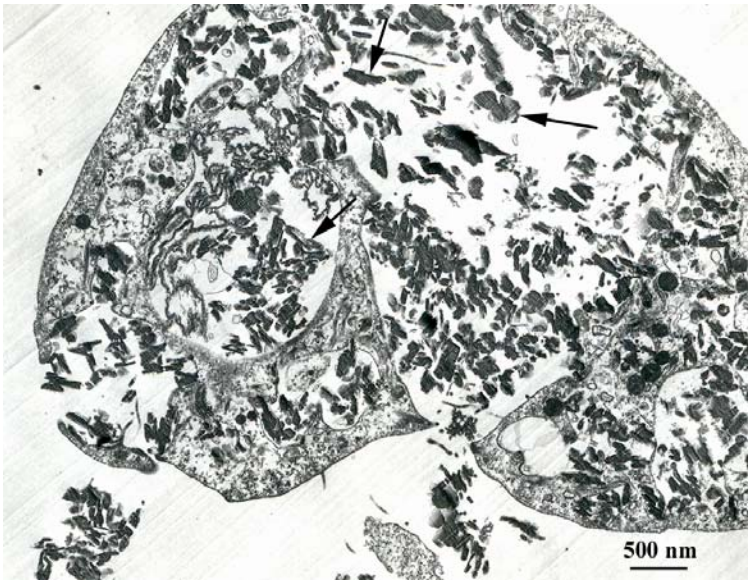

Figure 3.7. TEM micrograph of necrotic HEK as a result of 48 h exposure to 0.4 mg/mL Baa (arrows) (post-stained).

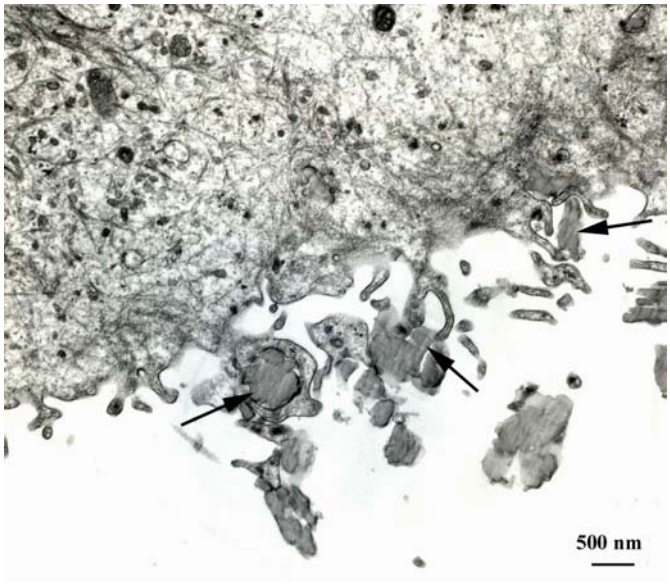

Figure 3.8. TEM micrograph of HEK treated with 0.4 mg/mL Baa (arrows) for 48 h (post-stained).

4. DISCUSSION

The aim of this study was to investigate the biological response of amino acid-derivatized fullerenes in HEK. This is the first study to investigate cytotoxicity of fullerenes in HEK by evaluating cytokine viability and pro-inflammatory potential. The decrease in cell viability and elevated levels of the pro-inflammatory cytokines IL-8, IL-6, and IL-1β indicate that the functionalized C_{60}, Baa, can initiate a toxic response in HEK at specific concentrations. TEM verified that the fullerene-based amino acids are capable of entering into HEK in the absence of a vehicle or surfactant. The presence of IL-8, IL-6, and IL-1β coincide with reports of dermal irritation in humans (Barker *et al.*, 1991, Corsini and Galli, 1998, Grone, 2002 and Nickoloff, 1991).

Healthy HEK quickly respond to injury by activating molecules that are capable of promptly signaling the need for tissue repair (Freedberg *et al.*, 2001). TNF-α and IL-1β are two of the most common initiators of keratinocyte activation (Barker *et al.*, 1991 and Freedberg *et al.*, 2001). In response to injury or irritation, keratinocytes process and release TNF-α and IL-1β that are capable of stimulating the production of IL-8 in a time-dependent manner (Allen *et al.*, 2000, Allen *et al.*, 2001a, Allen *et al.*, 2001b, Chou *et al.*, 2003, Monteiro-Riviere *et al.*, 2003 and Monteiro-Riviere *et al.*, 2005b). IL-8 is not found in normal skin, but rather plays a potentially significant role in dermal injuries and inflammatory skin diseases (Chabot-Fletcher *et al.*, 1994). IL-6 is also a major pro-inflammatory mediator that is produced by keratinocytes in response to skin irritants, contact allergens, viruses, UV irradiation, and thermal damage (Sugawara *et al.*, 2001). In this experiment, detectable levels of IL-1β indicate that the keratinocytes had entered an activation state in response to certain concentrations of Baa exposure. In turn, HEK

responded by initiating a pro-inflammatory response, indicated by the increased concentrations of IL-8 and IL-6 in the HEK culture medium.

This study also successfully identified concentrations of Baa that do not initiate a pro-inflammatory response in HEK. Knowledge of these non-cytotoxic concentrations is important for the development of therapeutic nanomaterial applications, such as those involving drug delivery systems and consumer products. As explained by Sayes *et al.*, 2004 and Sayes *et al.*, 2005, the cytotoxicity of fullerenes is largely dependent on the functionalization of the compound. For example, increasing the number of hydroxyl or carboxyl groups on the surface of the fullerene initiates less cytotoxicity than unfunctionalized. The non-cytotoxicity of certain Baa concentrations as shown in this experiment provides evidence that this functionalized C_{60} has the potential to be used for various nanoparticle applications in which adverse biological responses are not desirable.

In addition to cytotoxicity, the transport and mobility of nanoparticles are important issues to evaluate when considering the biological and environmental impacts (Anderson and Barron, 2005). Studies by Lecoanet *et al.* (2004) have determined that the fullerene with the highest cytotoxicity, unfunctionalized C_{60} (nano-C_{60}), has the lowest mobility in aqueous environments, whereas fullerenes that are relatively non-cytotoxic, such as those functionalized with hydroxyl groups ($C_{60}(OH)_n$), are the most mobile. The mobility of a nanoparticle in the biological environment is an important parameter that could contribute to the cytotoxic/non-cytotoxic effects of the fullerene. Despite the relatively low cytotoxicity, some concerns have addressed the possibility that the high mobility of functionalized fullerenes may result in the accumulation of these nanoparticles resulting in adverse biological reactions. Recent research, however, has shown that the mobility of the

hydroxyfullerenes is limited by the formation of cross-linkages between the fullerene and metal salts (Anderson and Barron, 2005). Thus, based on this research, it is possible to conclude that functionalized fullerenes, such as Baa, at certain concentrations react rapidly and irreversibly to form stable, cross-linked aggregates that do not initiate cytotoxicity. Additionally, the aggregation of nanoparticles can be avoided by the use of surfactants, such as Pluronic F127, which has been shown to reduce the aggregation of MWCNT without increasing the cytotoxicity or pro-inflammatory response of HEK (Monteiro-Riviere *et al.*, 2005a).

This study is the first *in vitro* study to depict the localization and inflammatory potential of fullerene derived amino acids in HEK. The pro-inflammatory cytokine activity identified a range of concentrations of the functionalized fullerene Baa that did not initiate a cytotoxic response in HEK. Identifying the cytotoxicity of fullerenes is an important preliminary step in understanding the mechanisms through which nanoparticles interact with the biological environment. These results are inline with previous research that has characterized the activity of fullerenes based on the physical and chemical properties of the nanoparticle. Before furthering the commercialization of nanomaterials it is imperative that more investigations be conducted in order to evaluate the cytotoxicity of the nanoparticle in use and to fully understand the interactions that can occur between the nanoparticle and the biological environment. Furthermore, this research should be expanded to include analysis of nanoparticle interactions with intact skin, a topic that is currently under investigation in our laboratories.

5. REFERENCES

D. Allen, J. Riviere and N. Monteiro-Riviere, Identification of early biomarkers of inflammation produced by keratinocytes exposed to jet fuels Jet A, JP-8, and JP-8(100), *Journal of Biochemical Molecular Toxicology* **14** (2000), pp. 231–237.

D. Allen, J. Riviere and N. Monteiro-Riviere, Analysis of interleukin-8 release from normal human epidermal keratinocytes exposed to aliphatic hydrocarbons: Delivery of hydrocarbons to cell cultures via complexation with α-cyclodextrin, *Toxicology In Vitro* **15** (2001a), pp. 663–669.

D. Allen, J. Riviere and N. Monteiro-Riviere, Cytokine induction as a measure of cutaneous toxicity in primary and immortalized porcine keratinocytes exposed to jet fuels and their relationship to normal human epidermal keratinocytes, *Toxicology Letters* **119** (2001b), pp. 209–217.

R. Anderson and A. Barron, Reaction of hydroxyfullerene with metal salts: A route to remediation and immobilization, *Journal of the American Chemical Society* **127** (2005) (30), pp. 10458–10459.

J. Barker, R. Mitra, C. Griffiths, V. Dixit and B. Nickoloff, Keratinocytes as initiators of inflammation, *The Lancet* **337** (1991), pp. 211–214.

D. Berg, M. Leach, R. Kuhn, K. Rajewsky, W. Muller, N. Davidson and D. Rennick, Interleukin 10 but not interleukin 4 is a natural suppressant of cutaneous inflammatory responses, *Journal of Experimental Medicine* **182** (1995), pp. 99–108.

F. Cassee, H. Muijser, E. Duistermaat, J. Freijer, K. Geerse and J. Marijnissen, Particle size-dependent total mass deposition in lungs determines inhalation toxicity of cadmium chloride aerosols in rats. Application of a multiple path dosimetry model, *Archives of Toxicology* **76** (2002), pp. 277–286.

M. Chabot-Fletcher, J. Breton, J. Lee, P. Young and D. Griswold, Interleukin-8 production is regulated by protein kinase C in human keratinocytes, *Journal of Investigative Dermatology* **103** (1994), pp. 509–515.

C. Chou, J. Riviere and N. Monteiro-Riviere, The cytotoxicity of jet fuel aromatic hydrocarbons and dose-related interleukin-8 release from human epidermal keratinocytes, *Archives of Toxicology* **77** (2003), pp. 384–391.

V. Colvin, The potential environmental impact of engineered nanomaterials, *Nature Biotechnology* **10** (2003), pp. 1166–1170.

E. Corsini and C. Galli, Cytokines and contact dermatitis, *Toxicology Letters* (1998), pp. 277–282.

H. Enk and S. Katz, Identification and induction of keratinocyte-derived IL-10, *Immunology* **149** (1992), pp. 92–95.

I. Freedberg, M. Tomic-Canic, M. Komine and M. Blumenberg, Keratins and the keratinocyte activation cycle, *Journal of the Investigative Dermatology* **116** (2001), pp. 633–640.

A. Grone, Keratinocytes and cytokines, *Veterinary Immunology and Immunopathology* **88** (2002), pp. 1–12.

M. Holsapple, W. Farland, T. Landry, N. Monteiro-Riviere, J. Carter, N. Walker and K. Thomas, Research Strategies for safety evaluation of nanomaterials, Part II: Toxicological and safety evaluation of nanomaterials, current challenges and data needs, *Toxicological Sciences* **88** (2005) (1), pp. 12–17.

M. Huang, E. Khor and L. Lim, Uptake and cytotoxicity of chitosan molecules and nanoparticles: Effects of molecular weight and degree of deacetylation, *Pharmacological Research* **21** (2004), pp. 344–353.

H. Lecoanet, J. Bottero and M. Wiesner, Laboratory assessment of the mobility of nanomaterials in porous media, *Environmental Science Technology* **20** (2004), pp. 5164–5169.

N. Monteiro-Riviere and A. Inman, Challenges for assessing carbon nanomaterial toxicity to the skin, *Carbon* **44** (2006), pp. 1070–1078.

N. Monteiro-Riviere, R. Baynes and J. Riviere, Pyridostigmine bromide modulates topical irritant-induced cytokine release from human epidermal keratinocytes and isolated perfused porcine skin, *Toxicology* **183** (2003), pp. 15–28.

N. Monteiro-Riviere, A. Inman, Y. Wang and R. Nemanich, Surfactant effects on carbon nanotube interactions with human keratinocytes, *Nanomedicine: Nanotechnology, Biology and Medicine* **1** (2005), pp. 293–299.

N. Monteiro-Riviere, R. Nemanich, A. Inman, Y. Wang and J. Riviere, Multi-walled carbon nanotube interactions with human epidermal keratinocytes, *Toxicology Letters* **155** (2005b), pp. 377–384.

T. Mosmann, Rapid colorimetric assay for cellular growth and survival: Application to proliferation and cytotoxicity assays, *Journal of Immunology Methods* **65** (1983), pp. 55–63.

B. Nickoloff, The cytokine network in psoriasis, *Archives of Dermatological Research* **127** (1991), pp. 871–884.

G. Oberdorster, Significance of particle parameters in the evaluation of exposure-dose–response relationships of inhaled particles, *Inhalation Toxicology* **8** (1996) (Supplementary), pp. 73–89.

E. Oberdorster, Manufactured nanomaterials (fullerenes, C_{60}) induce oxidative stress in the brain of juvenile largemouth bass, *Environmental Health Prospectives* **112** (2004) (10), pp. 1058–1062.

G. Oberdorster, A. Maynard, K. Donaldson, V. Castranova, J. Fitzpatrick, K. Ausman, J. Carter, B. Karn, W. Kreyling, D. Lai, S. Olin, N. Monteiro-Riviere, D. Warheit and H. Yang, Principles for characterizing the potential human health effects from exposure to nanomaterials: Elements of a screening strategy, *Particle and Fibre Toxicology* **2** (2005a) (8), pp. 1–35.

G. Oberdorster, E. Oberdorster and J. Oberdorster, Nanotoxicology: An emerging discipline evolving from studies of ultrafine particles, *Environmental Health Perspectives* **113** (2005b), pp. 823–839.

C. Sayes, J. Fortner, W. Guo, D. Lyon, A. Boyd, K. Ausman, Y. Tao, B. Sitharaman, J. Wilson, J. Hughes, J. West and V. Colvin, The differential cytotoxicity of water-soluble fullerenes, *Nano Letters* **4** (2004) (10), pp. 1881–1887.

C. Sayes, A. Gobin, K. Ausman, J. Mendez, J. West and V. Colvin, Nano-C_{60} cytotoxicity is due to lipid peroxidation, *Biomaterials* **26** (2005) (36), pp. 7587–7595.

A. Shvedova, V. Castranova, E. Kisin, D. Schwegler-Berry, A. Murray, V. Gandelsman, A. Maynard and P. Baron, Exposure to carbon nanotube material: Assessment of nanotube cytotoxicity using human keratinocytes cells, *Journal of Toxicology and Environmental Health* **66** (2003), pp. 1909–1926.

T. Sugawara, R. Gallucci, P. Simeonova and M. Luster, Regulation and role of interleukin 6 in wounded human epithelial keratinocytes, *Cytokine* **15** (2001) (6), pp. 328–336.

Y. Tabata and Y. Ikada, Biological function of fullerene, *Pure Applied Chemistry* **77** (1999), pp. 2047–2053.

K. Thomas and P. Sayre, Research strategies for safety evaluation of nanomaterials. Part I: Evaluating the human healthy implications of exposure to nanoscale materials, *Toxicological Science* **87** (2005) (2), pp. 316–321.

J. Yang and A. Barron, A new route to fullerene substituted phenylalanine derivatives, *Chemical Communications* (2004), pp. 2884–2885.

L. Yang and D. Watts, Particle surface characteristics may play an important role in phytotoxicity of alumina nanoparticles, *Toxicology Letters* **158** (2005), pp. 122–132.

CHAPTER 4: EFFECTS OF MECHANICAL FLEXION ON THE PENETRATION OF FULLERENE AMINO ACID-DERIVATIZED PEPTIDE NANOPARTICLES THROUGH SKIN

J.G. Rouse, J. Yang, J.P. Ryman-Rasmussen, A.R. Barron, and N.A. Monteiro-Riviere

Published in *Nano Letters* 7(1): 155-160, 2007.

ABSTRACT

In the occupational setting, activities that involve repetitive motion can intensify mechanical loads that are applied to the skin. Processes, such as constant hand movements, can alter the permeability barrier of skin and thus increase risks associated with exposure to nanoparticles. In order to investigate the relationship between mechanical stressors and nanoparticle exposure, a flexing apparatus was designed to simulate repetitive wrist motion. Dermatomed porcine skin (400 μm; n=3/time point) was fixed to the flexing device and topically dosed with 33.5 mg/mL of a fullerene substituted phenylalanine derivative (Baa-Lys(FITC)-NLS). Skin was flexed for 60 or 90 min or left unflexed (control). Percutaneous absorption was assessed using a flow-through diffusion cell system for 8 h and 24 h. After each time point, samples were bisected and either frozen or processed for transmission electron microscopy (TEM). Frozen tissues were sectioned at 20 μm to visualize Baa-Lys(FITC)-NLS penetration by confocal microscopy. TEM was used to detect the fullerene within skin at the ultrastructural level. Skin flexed for 60 and 90 min depicted dermal penetration at 8 h, whereas Baa-Lys(FITC)-NLS did not penetrate into the dermis of unflexed skin until 24 h. TEM analysis revealed nanoparticle localization within the intercellular spaces of the stratum granulosum, suggesting that penetration of the derivatized fullerene occurs through intercellular lipid moieties. These results suggest that external factors, such as a repetitive flexing motion and the associated mechanical stressors, can influence interactions that occur between nanoparticles and skin. These results are important for risk assessment of nanoparticles because they indicate that skin is an important route of exposure.

1. INTRODUCTION

The ability of quantum dots and fullerenes to penetrate intact skin[1,2] provides potential benefits for the development of nanomaterial applications involving drug delivery. For these developments to occur, it is important to fully understand the mechanisms through which nanoparticles traverse skin and to determine external factors that contribute to increased penetration. Many processes in the occupational environment, for example, involve repetitive motions that accentuate naturally occurring biomechanical forces and alter the body's ability to perform certain physiological functions.[3] Mechanical stimulation that occurs during these repetitive motions may alter the structural organization of skin and lead to increased penetration of nanoparticles by compromising the permeability barrier of the epidermis.

The high prevalence of podoconiosis in the African rift valleys due to exposure of unprotected feet to soils with high concentrations of beryllium and zirconium[4,5] led Tinkle *et al.* to investigate the relationship between particle penetration and mechanical stressors.[6] These results showed a direct correlation between particle penetration and a flexing movement used to simulate pressure applied by walking barefoot[6] and suggest that forces applied to skin during standard physiological processes, such as walking, can influence dermal exposure and lead to increased penetration. To investigate the relationship between nanoparticle penetration and biomechanical loading, a fullerene-substituted peptide, Baa-Lys(FITC)-NLS was synthesized, and its penetration through flexed and unflexed skin was observed.

2. MATERIALS AND METHODS

2.1 Baa-Lys(FITC)-NLS Synthesis

We have previously reported the synthesis of the phenylalanine-based fullerene amino acid, Bucky amino acid[7] (Baa, Figure 4.1a), and the uptake and interaction of Baa with human epidermal keratinocytes (HEK).[8] The presence of the fullerene substituent has a significant effect on the intracellular transport of peptides containing Baa. The addition of a fullerene-derived amino acid to a cationic peptide results in the peptide showing cellular uptake, whereas the same peptide sequence in the absence of Baa shows no transport across the cell membrane.[9] One peptide sequence that shows particular facile intracellular transport is based on the nuclear localization sequence (NLS, primary sequence H-Pro-Lys-Lys-Lys-Arg-Lys-Val-OH). The stability of the fullerene linkage and the ability to prepare peptides with a fluorescent tag allows for investigation of the transport of a bio-nano conjugate through skin.

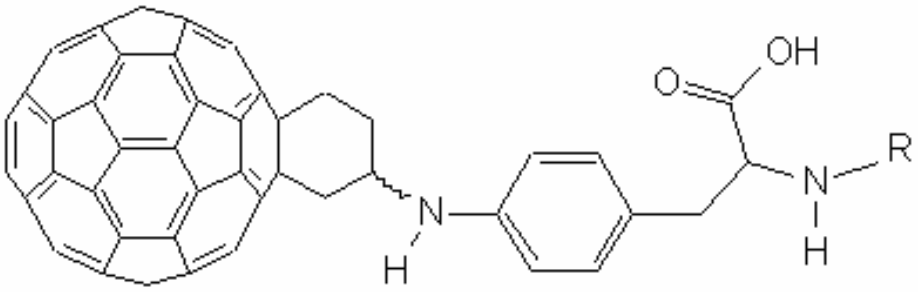

R = H (Baa, **1a**); C(O)O ^{t}Bu (N-Boc-Baa, **1b**)

Figure 4.1. Schematic representation of Bucky amino acid (Baa)

The couplings of normal amino acid sequence without Baa was carried out on an automated peptide synthesizer using preloaded Fmoc-Val-Wang resin as the solid phase.[10] After the NLS sequence (Pro-Lys-Lys-Lys-Arg-Lys-Val) was completed, a Lys(Mtt) residue was coupled to the end to allow attachment of the fluorescein isothiocyanate (FITC) fluorescent marker. The coupling with N-Boc-Baa (Figure 4.1b)[11] was performed manually.[10] Cleavage from the resin followed by RP-HPLC purification yielded the fullerene substituted peptide, Baa-Lys(FITC)-NLS (Figure 4.2).[12] Before functionalization, the individual fullerenes were, on average, 0.7 nm in size. Individual Baa-Lys(FITC)-NLS particles are *ca.* 3.5 nm.

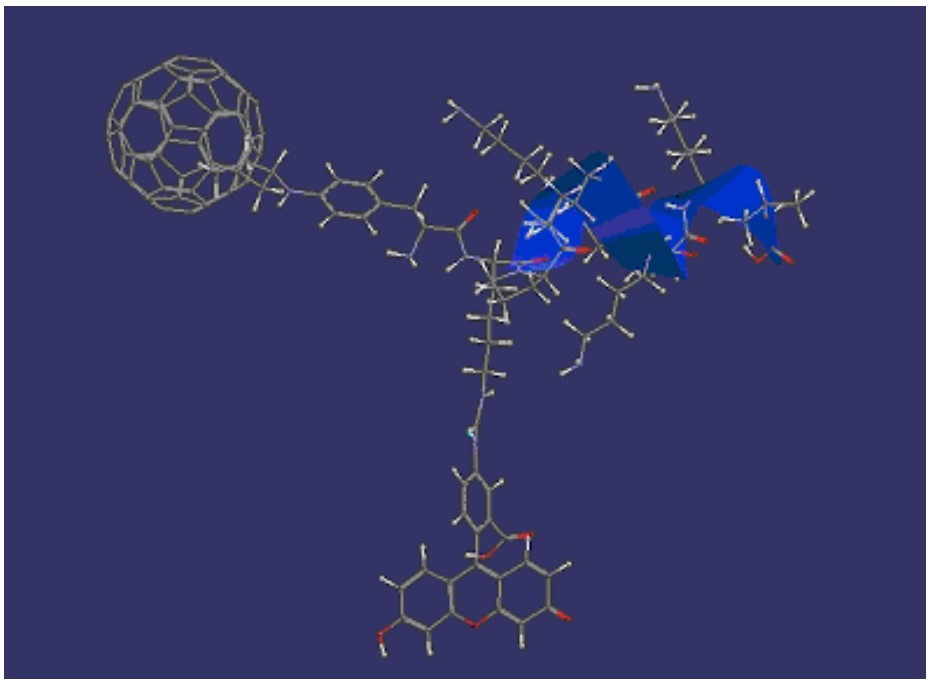

Figure 4.2. Calculated structure of Baa-Lys(FITC)-NLS showing the special relationship between the C_{60}.

2.2 Animal Care

Because of its physiological and structural similarities to human skin,[13-16] porcine skin was used a model for human skin in this study. The care and experimental use of all pigs were in accordance with the North Carolina State University Institutional Animal Care and Use Committee (IACUC). Pigs were sacrificed by intravenous injection of 100 mg/kg Euthasol (Delmarva Laboratories, Inc., Midlothian, VA), and the skin was dermatomed at a thickness of 400 μm. The dermatomed skin was fixed to a flexing apparatus designed to flex skin at ± 45° and at a frequency of 20 flexes·min^{-1}.

2.3 Flexing Apparatus

The flexing device consists of two rectangular platforms approximately 9 x ¾ inches connected to a 3-inch hinge. One side of the hinge is attached to a rotational motor and the other is fixed to a drawer slider. As the motor rotates, the whole system moves horizontally back and forth and the edge of the hinge that is fixed to the motor moves vertically up and down. When the skin is fixed to the platforms, tensile and compressive forces are applied along the flex line that runs along the center of the two platforms. Prior to attaching the skin, the platforms were covered in Parafilm®, and tissue wipes (Kimberly-Clark®, Wypall X70) soaked in saline to keep the dermal side of the skin hydrated throughout the duration of flexing.

2.4 Flow-Through Diffusion Cell System

To determine the effects of flexing on skin penetration, the dermatomed skin was dosed with 20 μL of Baa-Lys(FITC)-NLS in 1% PBS (33.5 mg·mL^{-1}), and the dosed areas were subsequently flexed for 60 or 90 min or left unflexed (control). In pilot studies, skin

flexed for either 15 or 30 min and dosed with radiolabeled methyl parathion showed no evidence of increased penetration in comparison to unflexed samples. Therefore, flex of times of 60 and 90 min were chosen to investigate nanoparticle penetration. After the allotted flexing time, percutaneous absorption was assessed using a flow-through diffusion cell system.[17,18] Temperature and pH of the perfusate (1.2 mM KH_2PO_4, 32.7 mM $NaHCO_3$, 2.5 mM $CaCl_2$, 4.8 mM KCl, 1.2 mM $MgSO_4 \cdot 7H_2O$, 118 mM NaCl, 1200 $mg.L^{-1}$ D-glucose, 4.5% BSA, 5 U/mL heparin, 30 $\mu g \cdot mL^{-1}$ amikacin, and 12.5 $U \cdot mL^{-1}$ penicillin G) were monitored and kept constant at 37 °C and pH 7.4. The diffusion cells were run at 1.75 $mL \cdot min^{-1}$ for either 8 h or 24 h. Immediately after each time point, the samples were bisected along the flex line and either frozen at -80 °C for later sectioning or placed in Trump's fixative at 4 °C for transmission electron microscopy (TEM). Confocal microscopy and TEM were used to visualize Baa-Lys(FITC)-NLS penetration. At least three diffusion cells were run for each flex time and exposure time.

2.5 Confocal Microscopy

Prior to imaging, the skin was sectioned at 20 μm using a cryostat (Reichert-Jung, Cryocut 1800). To avoid surface contamination from the sectioning knife, the blade was wiped off using cotton swabs between every section and the blade was frequently moved laterally to expose unused areas. The FITC-labeled fullerenes were imaged using a Nikon C1 confocal laser scanner connected to a Nikon Eclipse 2000E inverted fluorescence microscope with a 40X Plan Fluor extra long working distance (dry) objective (0.6 NA). The fullerenes were excited with a 488 nm Ar laser line and the fluorescence was detected in a 500-545 nm channel. A 633 nm HeNe laser line was used to obtain differential interference contrast

(DIC) images of the sectioned skin. Images were captured using Nikon EZ-C1 software (version 2.01.152).

2.6 Transmission Electron Microscopy

At each experimental time point, half of each skin sample was placed in Trump's fixative at 4° C for 24 h for TEM. Each sample was rinsed in 0.1 M phosphate buffer (pH 7.2) and post-fixed in buffered 1% osmium tetroxide for 1 h. After rinsing in phosphate buffer, the skin was dehydrated through graded ethanol solutions, cleared in acetone, and infiltrated and embedded in Spurr's resin. Thin sections (800-1000 Å) were mounted on copper grids and left unstained to visualize the fullerenes in the tissue.

2.7 Dynamic Light Scattering

Previously, we have observed that the parent amino acid, Baa, aggregates in aqueous solution as a consequence of the presence of both hydrophobic and hydrophilic groups within the same molecule. It is reasonable to suppose that the peptides that are soluble in water would also form aggregates. In order to understand the transport of the Baa-Lys(FITC)-NLS the particle size in solution was determined by dynamic light scattering (DLS). Solutions in the range of 0.125–2.0 $mg.mL^{-1}$ were prepared in PBS buffer

2.8 Cryo-TEM

To further examine the actual aggregate size and morphology, cryo-TEM experiments were performed (1.0 $mg.mL^{-1}$). Samples for cryo-TEM studies were prepared by dipping a copper grid coated with amorphous carbon-holey film into the sample solution. The TEM images were mainly taken in the hole region of the TEM grid to minimize the artificial effect from the samples or ice.

3. RESULTS

3.1 Penetration of Baa-Lys(FITC)-NLS

For each experimental treatment, Baa-Lys(FITC)-NLS had penetrated the skin by 8 h (Figure 4.3). The fullerenes were localized primarily in the epidermal layers of non-flexed (control) skin, whereas the 60 and 90 min flexed samples showed evidence of greater epidermal (60 min) and dermal (90 min) penetration (Figure 4.3, middle row). Skin flexed for 90 min had a substantially greater amount of Baa-Lys(FITC)-NLS dermal penetration than non-flexed skin (control) and 60 min flexed skin. The DIC images (Figure 4.3, top row) depict an intact stratum corneum, which provides evidence that nanoparticle penetration did not occur as a result of skin abrasion. The fluorescence of Baa-Lys(FITC)-NL as it moves through the skin can be seen in Figure 4.3, middle row. The fluorescence intensity maps (Figure 4.3, bottom row) reveal a concentration gradient of the Baa-Lys(FITC)-NLS, ranging from a high concentration of particles in the epidermis (white) to a low concentration in the dermal layers (blue). Images are representative of two separate experiments performed in triplicate.

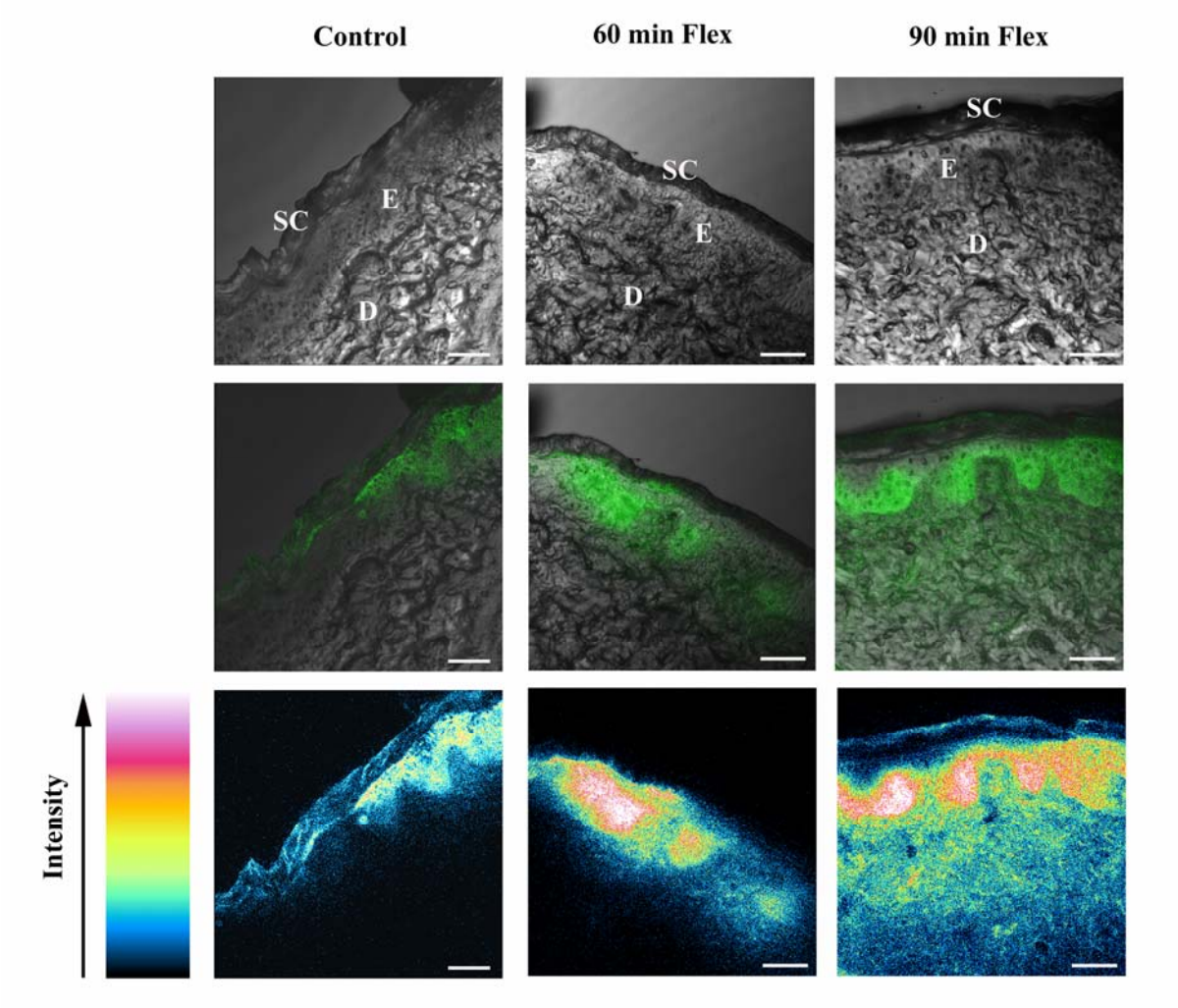

Figure 4.3. Confocal scanning microscopy images of intact skin dosed with Baa-Lys(FITC)-NLS for 8 h. Top row: confocal-DIC channel image shows an intact stratum corneum (SC) and underlying epidermal (E) and dermal layers (D). Middle row: Baa-Lys(FITC)-NLS fluorescence channel (green) and con focal-DIC channel shows fullerene penetration through the epidermal and dermal layers of skin. Bottom row: fluorescence intensity scan showing Baa-Lys(FITC)-NLS penetration. All scale bars represent 50 μm.

After 24 h of Baa-Lys(FITC)-NLS treatment, skin penetration was greater in all experimental groups (Figure 4.4). Again, the DIC images reveal a thick, intact stratum corneum and the intensity maps show the highest concentration of particles in the upper epidermal layers and a lower concentration as the fullerenes penetrate into the dermis. Skin flexed for 90 min showed the greatest amount of dermal penetration, evident by the higher

fluorescence intensity of the nanoparticles in this group (Figure 4.4, bottom row). It is important to note that for all treatments nanoparticle penetration was non-homogeneous probably due to a nonuniform distribution of the dose over the dose region and/or differences in the thickness of the epidermis. The images presented are representative of the trends seen for each set of treatments.

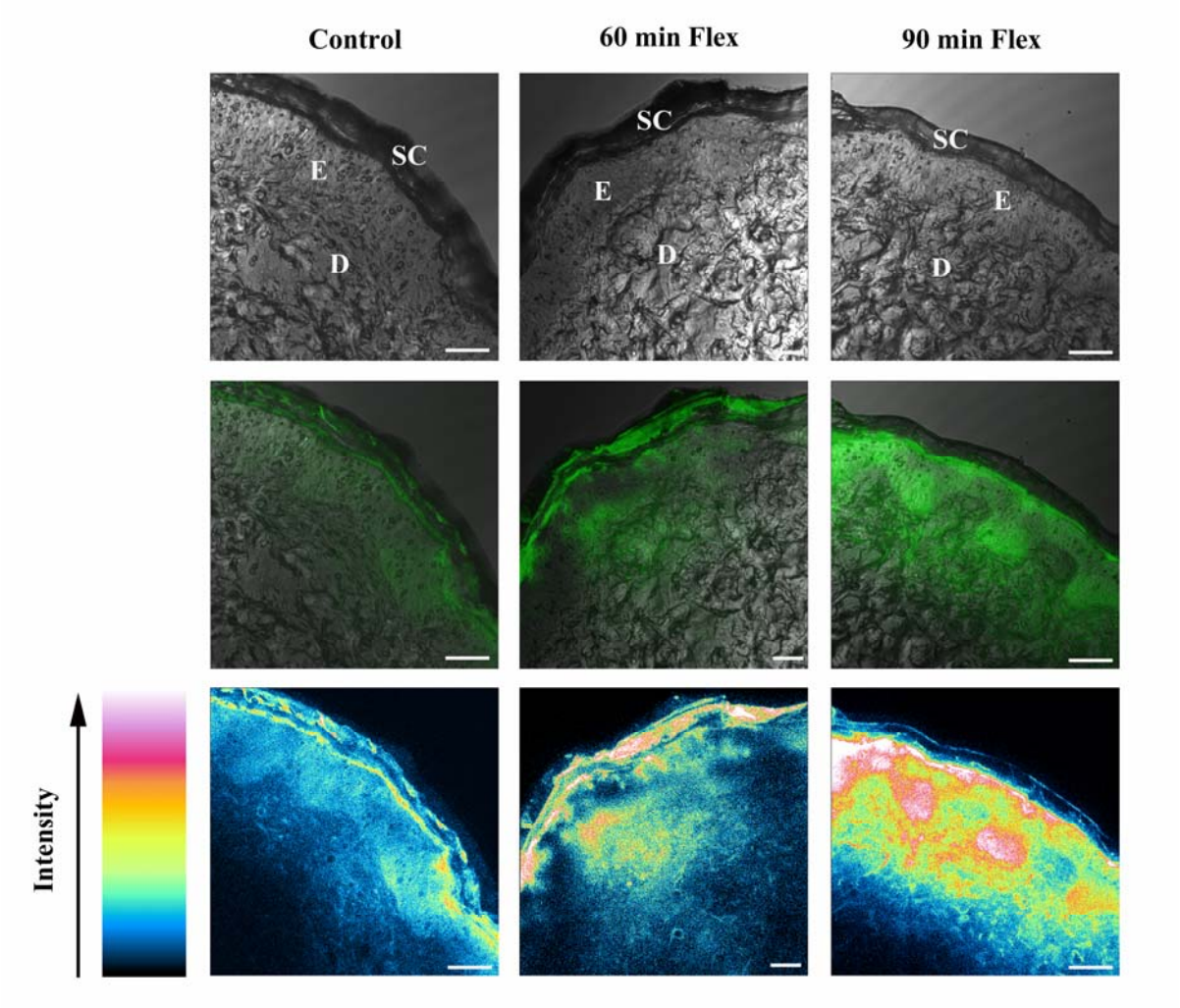

Figure 4.4. Confocal scanning microscopy images of skin dosed with Baa-Lys(FITC)-NLS for 24 h. Top row: confocal-DIC channel image shows an intact stratum corneum (SC) and underlying epidermal (E) and dermal layers (D). Middle row: Baa-Lys(FITC)-NLS fluorescence c hannel (green) and confocal-DIC channel shows fullerene penetration through the skin. Bottom row: fluorescence intensity scan of Baa-Lys(FITC)-NLS. All scale bars represent 50 μm.

3.2 TEM

TEM further verifies that Baa-Lys(FITC)-NLS is capable of penetrating intact skin and localizing between keratinocytes. Figure 4.5 is a representative image of skin flexed for 90 min that depicts localization of the fullerene within the intercellular space of the stratum granulosum cell layer at 24 h.

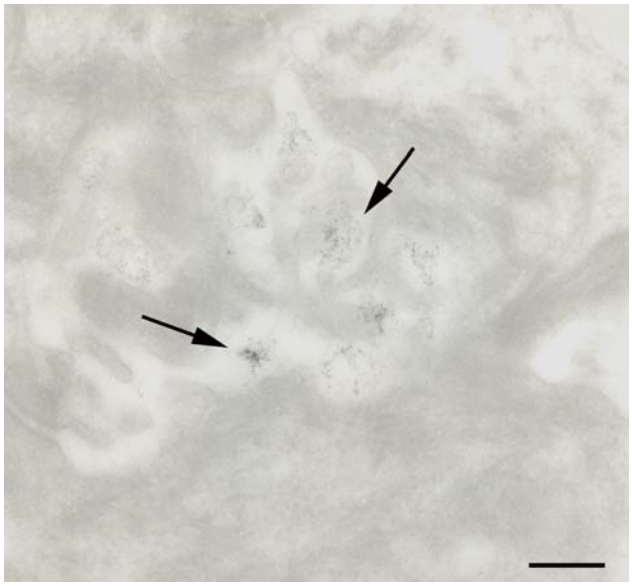

Figure 4.5. Unstained transmission electron microscopy image of Baa-Lys(FITC)-NLS (arrows) localization at 24 h in skin flexed for 90 min. The fullerenes are present within the intercellular space of the stratum granulosum cell layer (shown by the arrows). The scale bar represents 300 nm.

3.3 Dynamic Light Scattering

Baa-Lys(FITC)-NLS show aggregation in aqueous solution across the concentration ranges measured (0.125-2.0 $mg.mL^{-1}$). At 0.5 $mg.mL^{-1}$ there appears to be two distinct types of aggregate; the major species (*ca*. 80%) is *ca*. 250 nm while the minor content is a smaller aggregate (*ca*. 40 nm). As may be seen from Figure 4.6, above 1.0 $mg.mL^{-1}$ a third distinct

aggregate is observed of *ca*. 800 nm. It would appear that the solution species for Baa-Lys(FITC)-NLS are aggregates of increasing sizes with increasing concentration, suggesting that the 40 nm aggregates will become the greater component at the concentrations studied herein.

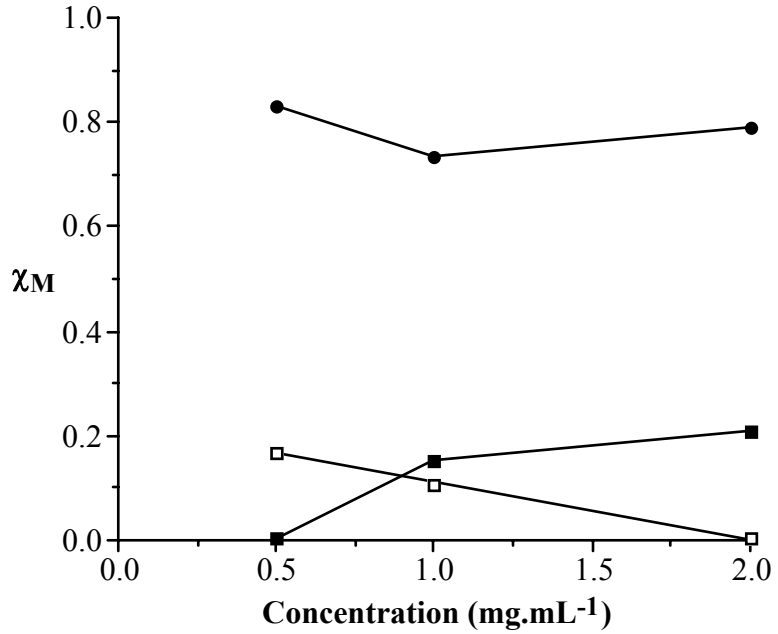

Figure 4.6. Plot of the fraction of aggregates for Baa-Lys(FITC)-NLS as a function of solution concentration. Average aggregate size = 40 nm (□), 250 nm (●), and 800 nm (■).

3.4 Cryo-TEM

The result of the cryo-TEM experiments showed that fullerene peptides exhibited strong aggregation behavior in aqueous solution, a similar phenomenon demonstrated by other water-soluble fullerene derivatives.[1] Baa-Lys(FITC)-NLS forms spherical and ellipsoidal clusters (Figure 4.7), with an average aggregate sizes of 50 – 150 nm, which are generally smaller than the diameters observed by DLS.

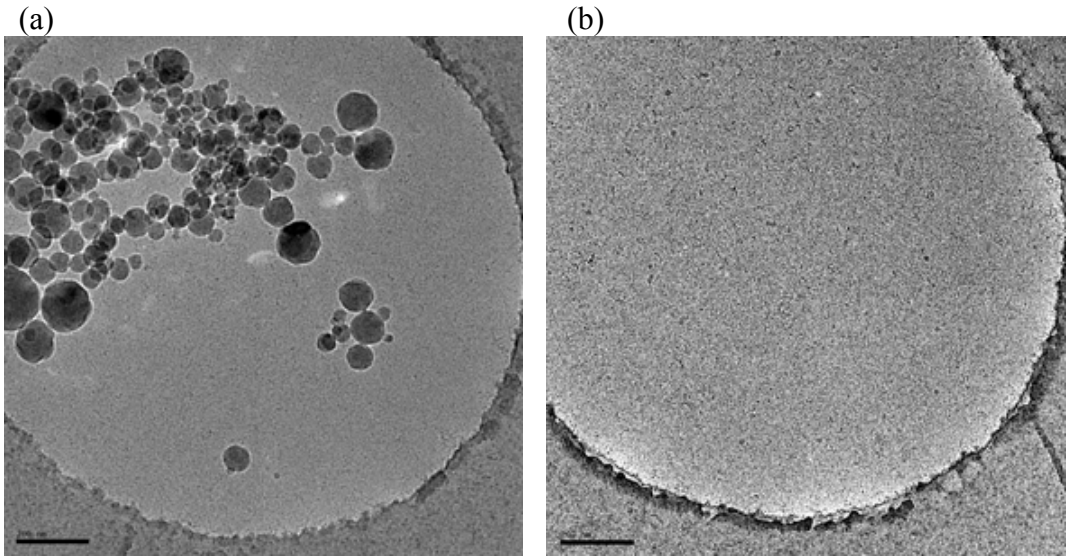

Figure 4.7. Vitreous ice cryo-TEM micrograph of the large aggregates (a) and small aggregates (b) formed by Baa-Lys(FITC)-NLS in PBS buffer (1.0 mg.mL-1 @ pH = 7).

4. DISCUSSION

This study investigated the effects of mechanical flexion on the penetration of fullerenes through intact skin. In developing new applications involving nanomaterials and nanoparticles, it is important to adequately assess all factors that can lead to increased nanoparticle exposure. Previous research has already demonstrated that nanoparticles can penetrate skin cells[8,19] and intact skin;[1,2] the aim of this study is to identify factors that can lead to increased penetration and/or rate of penetration. Evaluation of these factors is of interest for the development of nanodrug delivery applications and in identifying occupational hazards that arise during manufacturing processes and repeated exposure to nanoparticles. Since recent research has identified the potential toxicity of some nanoparticles,[8,19-23] these results could have profound implications for researchers, manufacturers and medical personnel alike.

The mechanical loading regimes used in this study attempt to mimic physiological forces that can occur during nanoparticle manufacturing processes or conditions involved in consumer use. The external forces applied to the skin while flexing proves to have a significant effect on both the rate and extent of fullerene penetration. Skin flexed for 90 min shows evidence of dermal penetration after 8 h of nanoparticle exposure, whereas control specimens show evidence of fullerenes primarily localized in the epidermis and only a slight amount in the dermis after the 24 h treatment. These results suggest that the action of a flexing procedure increases the rate at which fullerenes can penetrate through the skin. Furthermore, flexing increased the amount of fullerenes that were capable of penetrating into the dermal layers of skin, indicated by the higher fluorescence intensity of fullerenes for both 60 and 90 min flexed skin.

The route of nanoparticle penetration through the skin is of great interest, especially in the nanomedicine field. In this study, TEM depicted derivatized fullerenes localized within intercellular spaces of the epidermis, suggesting that migration through the skin occurs intercellularly as opposed to movement through cells. Additionally, the concentration gradients of fullerenes between the epidermis and dermis shown in the fluorescence intensity maps of Figures 4.3 and 4.4 indicate that fullerene penetration occurs via a mechanism of passive diffusion. Therefore, movement of the derivatized nanoparticles through the skin is dependent on the hydrophobic lipid entities that are present between the epidermal cells. These intercellular lipids are arranged into lamellar sheets and, typically, are responsible for the permeability barrier of the skin.[24] The ability of the nanoparticles to traverse through these lipid lamellae and to enter into the dermis of skin indicates that nanomaterials could get absorbed by the capillaries of the papillary layer with the potential to localize elsewhere in

the body.[21] For drug-delivery applications, the ability of nanoparticles to have access to systemic circulation has important implications. However, because some nanoparticles have been shown to initiate adverse biological responses,[8,19-23] there are potential risks for systemic toxicity to occur and, therefore, the need arises for risk assessment and the establishment of safety regulations.

At present, the mechanisms through which flexing increases nanoparticle penetration are unknown. Dynamic light scattering and cryo-TEM analyses were conducted in order to determine the particle size in solution and to determine its relationship to transport through skin. On the basis of these techniques, it was found that in solution Baa-Lys(FITC)-NLS forms spherical and ellipsoidal clusters with average aggregate sizes of approximately 40-250 nm. On the basis of previous knowledge that the vertical and lateral gaps between corneocytes present in the stratum corneum are about 19 nm,[26] it seems likely that the larger Baa-Lys(FITC)-NLS aggregates based on conformational shape would have limited capabilities of diffusing through the epidermal layers via intercellular spaces. It is evident from the results of this study, however, that the fullerene-based peptides do penetrate through the epidermal layers via passive diffusion and that flexing increases this penetration. Since external mechanical stimuli are transmitted to individual cells,[27,28] it is possible to speculate that the forces applied to the skin during flexing cause changes in the morphology and architectural lipid organization of the upper epidermal layers. A transient increase in the size of the intercellular spaces during mechanical stimulation could be responsible for the increase in penetration seen in skin samples flexed for 60 and 90 min. Additional investigations into the mechanisms of penetration revealed that nanoparticle penetration through flexed skin did not increase when the dose was applied after 60 and 90 min of

flexing (data not shown). These findings support the aforementioned conclusions in that the flexing procedure does not induce permanent damage to the epidermal barrier, but rather causes a transient change in architectural organization that results in an increased ability of nanoparticles to diffuse through the intercellular spaces of the upper epidermis.

This study confirms that fullerene-based peptides can penetrate intact skin and that mechanical stressors, such as those associated with a repetitive flexing motion, increase the rate at which these particles traverse into the dermis. These results are important for identifying external factors that increase the risks associated with nanoparticle exposure during manufacturing or consumer processes. Future assessments of nanoparticle safety should recognize and take into account the effect that repetitive motion and mechanical stressors have on nanoparticle interactions with the biological environment. Additionally, these results could have profound implications for the development of nanoparticle use in drug-delivery, specifically in understanding mechanisms by which nanoparticles penetrate intact skin.

5. REFERENCES

1. Ryman-Rasmussen, J. P.; Riviere, J. E.; Monteiro-Riviere, N. A. *Toxicol. Sci.* **2006**, *91*, 159-165.

2. Monteiro-Riviere, N. A.; Yang, J.; Inman, A. O.; Ryman-Rasmussen, J. P.; Barron, A. R.; Riviere, J. E. *Toxicol. Sci.* **2006**, *90*, 168.

3. Barr, A. E. *Man. Therapy* **2006**, *11*, 173-174.

4. Blundell, G.; Henderson, W. J.; Price, E. W. *Ann. Trop. Med. Parasitol.* **1989**, *83*, 381-385.

5. Corachan, M.; Tura, J. M.; Campo, E.; Soley, M.; Traveria, A. *Trop. Geogr. Med.* **1988**, *40*, 359-364.

6. Tinkle, S. S.; Antonini, J. M.; Rich, B. A.; Roberts, J. R.; Salmen, R.; DePree, K.; Adkins, E. J. *Environ. Health Perspect.* **2003**, *111*, 1202-1208.

7. Yang, J.; Barron, A. R. *Chem. Commun.* **2004**, 2884-2885.

8. Rouse, J. G.; Yang, J.; Barron, A. R.; Monteiro-Riviere, N. A. *Toxicol. In Vitro* **2006**, *20*, 1313-1320.

9. Yang, J.; Wang, K.; Driver, J.; Yang, J.; Barron, A. R. *Org. Biomol. Chem.* **2007**, in press.

10. Using preloaded Fmoc-Val-Wang resin (491 mg, 0.30 mmol) as solid phase, each coupling used 4 fold amino acid excess, and HBTU, HOBT as activators and DIEA as base in a 1:1:1:3 ratio. Fmoc deprotection was performed using 25% perperidine in DMF solution. After the NLS sequence (Pro-Lys-Lys-Lys-Arg-Lys-Val) was completed, a Lys(Mtt) residue was coupled to the end. One sixth of the resin was placed in a 25 mL fritted glass tube, swollen with DMF. A 3-fold excess of N-Boc-Baa (157 mg, 0.15 mM) dissolved in DMF/DCM (9 mL, 2:1) was activated with PyBOP/HOBt/DIEA (1:1:1:3) for 2 minutes, then mixed with the resin in the fritted glass tube, and shaken on an automated shaker for 1 day at room temperature. The resin was washed thoroughly with DMF and DCM to remove any unreacted N-Boc-Baa. The resin was washed with DCM for complete removal of DMF. To achieve the maximum cleavage of Mtt protecting group, the resin was shrunk with MeOH twice. When the resin was treated with 1% TFA and 5% TIPS in DCM 2 minutes for three times. The resin was washed again with DCM thoroughly, and swelled in DMF for 1 hour. Afterward the resin was shaken with a solution of FITC (65 mg) in DMF (8 mL) and DIEA (130 mL) overnight. At the end of the synthesis, the FITC labeled fullerene peptides was washed repeatedly with DMF, DCM and shrunk with MeOH. The resin was thoroughly dried over Dryrite in a vacuum oven overnight. The cleavage of the peptide was achieved with TFA/TIPS/H_2O (95:2.5:2.5) cocktail for 4 hr. After filtration, the peptide solution was concentrated by Rotavap at room temperature and precipitated

with cold Et_2O. The crude was washed with diethyl ether two more times and, after centrifugation of the final wash, it was frozen and lyophilized. RP-HPLC purification was carried out on a Phenomenex Luna C5 column using an isocratic gradient of (A) 0.1% TFA in water and (B) 0.1% TFA in 2-propanol, 70% B, at 5.0 $mL \cdot min^{-1}$ flow rate. The elution time was 37 min. After purification 59.1 mg (50.6%) was recovered.

11. Yang, J.; Alemany, L. B.; Driver, J.; Hartgerink, J. D.; Barron, A. R. *Chem.-Eur. J.* 2006, in press.

12. MALDI-MS: *m/z* calculated 2337 [M^+ + H], 1948 [M^+ + H-FITC]; found 2337, 1948.

13. Chilcot, R. P.; Dalton, C. H.; Hill, I.; Davison, C. M.; Blohm, K. L.; Clarkson, E. D.; Hamilton, M. G. *Hum. Exp. Toxicol.* **2005**, *24*, 347-352.

14. Monteiro-Riviere, N. A. In *The Biology of the Domestic Pig*; Pond, W. G., Mersmann, H. G., Eds.; Cornell University Press: Ithaca, NY, 2001; pp 585-624.

15. Schmook, F. P.; Meingassner, J. G.; Billich, A. *Int. J. Pharm.* **2001**, *215*, 51-56.

16. Singh, S.; Zhao, K.; Singh, J. *Drug Chem. Toxicol.* **2002**, *25*, 83-92.

17. Chang, S. K.; Riviere, J. E. *Fundam. Appl. Toxicol.* **1991**, *17*, 494-504.

18. Bronaugh, R. L.; Stewart, R. F. *J. Pharm. Sci.* **1985**, *74*, 64-67.

19. Monteiro-Riviere, N. A.; Nemanich, R.; Inman, A. O.; Wang, Y.; Riviere, J. E. *Toxicol. Lett.* **2005**, *155*, 377-384.

20. Magrez, A.; Kasas, S.; Salicio, V.; Pasquier, N.; Seo, J. W.; Celio, M.; Catsicas, S.; Schwaller, B.; Forro, L. *Nano Lett.* **2006**, *6*, 1121-1125.

21. Shvedova, A.; Castranova, V.; Kisin, E.; Schwegler-Berry, D.; Murray, A.; Gandlelsman, V.; Maynard, A.; Baron, P. *J. Toxicol. Environ. Health* **2003**, *66*, 1909-1926.

22. Oberdorseter, E. *Enivron. Health Perspect.* **2004**, *112*, 1058-1062.

23. Sayes, C. M.; Fortner, J. D.; Guo, W.; Lyon, D.; Boyd, A. M.; Ausman, K. D.; Tao, Y. J.; Sitharaman, B.; Wilson, L. J.; Hughes, J. B.; West, J. L.; Colvin V. L. *Nano Lett.* **2004**, *4*, 1881-1887.

24. Monteiro-Riviere, N. A.; Riviere, J. E. In *Dermal Absorption Models in Toxicology and Pharmacology*; Riviere, J. E., Ed.; Taylor & Francis: New York, 2006; pp 1-8.

25. Monteiro-Riviere, N. A.; Inman, A. O.; Riviere, J. E.; McNeill, S. C.; Francoeur, M. L. *Pharm. Res.* **1993**, *10*, 1326-1331.

26. van der Merwe, D.; Brooks, J. D.; Gehring, R.; Baynes, R. E.; Monteiro-Riviere, N. A.; Riviere, J. E. *Toxicol. Sci.* **2006**, *89*, 188-204.

27. Zahalak, G. I.; Wagenseil, J. E.; Wakatsuki, T.; Elson, E. L. *Biophys. J.* **2000**, *79*, 2369-2381.

28. Guilak, F.; Mow, V. C. *J. Biomech.* **2000**, *33*, 1663-1673.

CHAPTER 5: EFFECTS OF CYCLIC STRAIN ON AMINO ACID-DERIVATIZED FULLERENE PEPTIDE NANOPARTICLE INTERACTIONS WITH HUMAN EPIDERMAL KERATINOCYTES

Jillian G. Rouse, Elizabeth G. Loboa, Andrew R. Barron, Nancy A. Monteiro-Riviere

1. INTRODUCTION

Mechanobiology is the study of a cell's biological response to mechanical loads and the mechanotransduction mechanisms used in transforming the loads into signaling cascades and cellular events (Ingber, 1998; Wang and Thampatty, 2006). During wound healing and in response to physiological applied loads, cells are capable of sensing and responding to the applied stress by altering patterns of protein expression and remodeling their extracellular matrix (ECM) (Chiquet et al, 1996; Trachslin *et al.*, 1999). The ECM is a substrate on which cells can adhere, grow, migrate, and differentiate. Additionally, the ECM has been elucidated as the location at which forces are transmitted to and from cells. Mechanical stimuli are transduced from the extracellular matrix components to cytoskeletal elements via integrin adhesion receptors that are present at the attachment sites. Following ligand binding to an adhesion receptor, integrins mediate signal transduction into the cell and results in cytoskeletal reorganization, gene expression, and differentiation. Similarly, signals can be transferred from within the cell to the integrin receptor to alter ligand-integrin binding affinity (Liu *et al.*, 2000; Ingber, 1991).

Once transmitted to the cellular level, a mechanical force can elicit several different biochemical transduction signals that result in a wide variety of cellular responses. These mechanotransduction signals are dependent on the magnitude, frequency, direction, and distribution of the mechanical stimuli and have been shown to promote cellular growth, differentiation, migration, and apoptosis in a variety of cell types (Barkhausen *et al.* 2003; Chen *et al.*, 1997; Huang and Ingber, 1999; Loboa *et al.*, 2004; Kaspar *et al.*, 2000; Sumanasinghe *et al.* 2006). Relatively unknown, however, is if signal transduction pathways

that are activated by mechanical deformation play a role in cell membrane permeability or effect the ability of ions and particles to move into and out of cells.

Lee *et al.*, 1997 demonstrated increased cellular uptake of fluorescent microspheres by keratinocytes in response to cellular straining. These results suggest that the applied mechanical stimulation induces transient membrane injury that permits the micro-sized particles to move into the cell and allows intracellular proteins, such IL-1, to be released out of the cell and into the extracellular environment (Lee *et al.*, 1997). Although the aim of this study was not to investigate the effects of cellular straining on membrane permeability but rather to relate strain-induced deformation to keratinocyte proliferation and cytokine release, these findings imply that mechanical stimulation may influence the ability of drugs and other particle-like entities to interact at the cellular level.

Other studies have investigated the effects of mechanical stimulation in cultured keratinocytes and have shown that in response to cyclic tensile strain, keratinocytes increase cell proliferation, DNA synthesis, elongation, and protein synthesis (Takei, *et al.* 1997). Yano et al, 2004 verified that mechanical stretching of keratinocytes induces proliferative signals that could contribute to the normal hyperproliferative nature of the epidermis. Others attribute strain-induced proliferation to increased production and release of IL-1 (Takei et al, 1998; Lee *et al.*, 1997). These studies provide insight into the mechanotransduction signals that may occur in keratinocytes as a result of mechanical stimulation at the tissue level.

Understanding how nanoparticles interact with the biological environment at the cellular level is crucial for the development of nano-drug delivery systems. Currently, many peptide- and nucleic acid-based drugs are limited by their inability to enter the cell and reach their therapeutic target. The use of cell penetrating peptides (CPPs) improves the drug's

pharmacological properties; however, the range of available CPP sequences and their potential for toxicity limits their use. Incorporation of fullerenes, specifically Bucky amino acid (Baa), into therapeutic peptide sequences facilitates transport across the cell membrane and, thus, allows for effective delivery of otherwise membrane impermeable molecules (Yang et al, 2007b). Additionally, Baa demonstrates low cytotoxicity since HEK viability is maintained with exposure of Baa concentrations of less than 0.04 mg/mL (Rouse *et al.*, 2006).

The potential use of fullerene derivatized amino acids for drug delivery is strengthened by the ability of the particles to penetrate intact skin (Monteiro-Riviere et al, 2006; Rouse *et al.*, 2007). Transdermal drug delivery offers a non-invasive alternative for systemic administration of therapeutic agents. This mechanism of drug delivery is beneficial in that it avoids the potential first-pass gastrointestinal and hepatic metabolism, which affords the use of lower dosages at reduced frequencies (Tsai *et al.*, 1995). The development of such drug delivery systems, however, is dependent on understanding the mechanisms that contribute to percutaneous absorption *in vivo.* Therefore, the use of *in vitro* models should consider the fact that the biological environment is a dynamic, not static, system. Biophysical forces, both from the internal and external milieus, and how these forces are mechanotransduced at the cellular level should be considered when evaluating biological interactions.

The results reported herein were obtained from a pilot study aimed at evaluating how repetitive tensile strain applied to HEK effects cell membrane permeability and consequent interactions with fullerene-derivatized amino acids (Baa-Lys(FITC)-NLS). The ability of mechanical stimuli to influence cellular interactions with nanoparticles is pivotal for the

developmental of nano-drug delivery systems, especially for those involving transepidermal delivery. Additionally, understanding the mechanism involved in cellular interactions with nanoparticles can aid in the development of health and safety regulations to minimize the risks involved with nanoparticle exposure during manufacturing processes and consumer use.

2. MATERIALS AND METHODS

2.1 Baa-Lys(FITC)-NLS Synthesis

Synthesis of the fullerene substituted amino acid with the nuclear localization sequence (NLS) and fluorescein isothiocyanate (FITC) label was conducted as previously described (Yang and Barron, 2004; Yang *et al.*, 2007a). Briefly, the coupling of the amino acid sequences without Baa were carried out on an automated APEX 396 Multiple Peptide Synthesizer using preloaded Fmoc-Lys(Boc) Wang resin as the solid phase. Separately, N-Boc-Baa was synthesized (Yang and Barron, 2004) and then mixed with the resin and shaken for 1 day. Afterwards, the resin was shaken with a solution of FITC, dried, and cleaved from the peptide. The final concentrated and purified product, Baa-Lys(FITC)-NLS, had an isolated yield of 50.6% (Yang *et al.*, 2007a). Figure 5.1 depicts the predicted structure of Baa-Lys(FITC)-NLS.

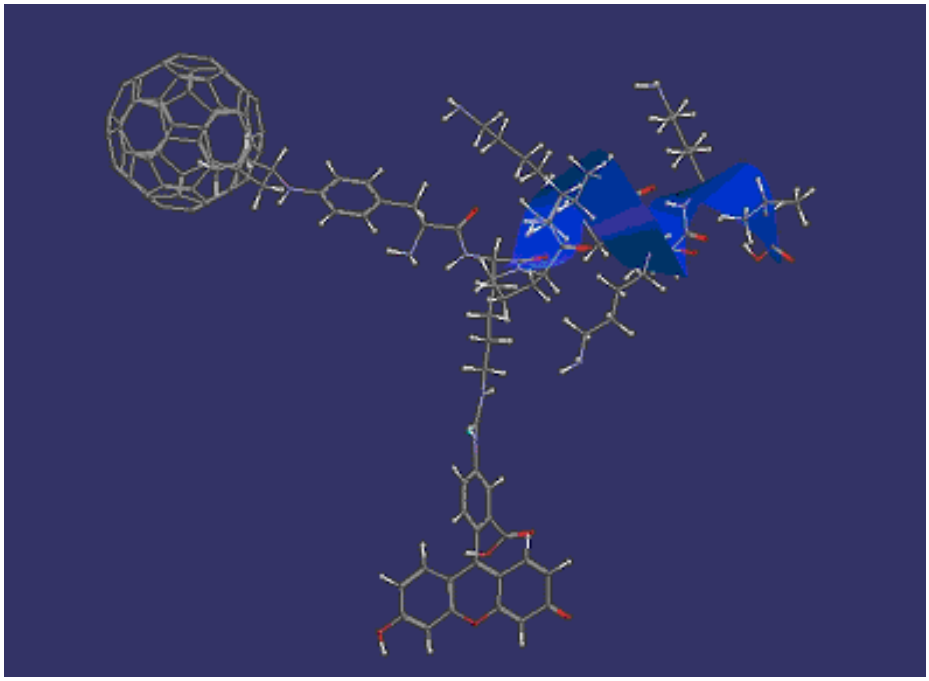

Figure 5.1. Calculated structure of Baa-Lys(FITC)-NLS showing the special relationship between the C60.

2.2 Cell Culture

Cryopreserved neonatal HEK were purchased from Clonetics, Corp. (San Diego, CA). HEK were plated in 6-well, collagen I-coated Flexcell culture plates (9.625 cm^2 growth area) at a density of ≈150,000 cells per well and grown in a humidified environment of 5% CO_2 at 37 °C (Flexcell Interational Corp., Hillsborough, NC). Cells were maintained in keratinocyte growth media (KGM-2), consisting of serum-free keratinocyte basal media supplemented with human epidermal growth factor, insulin, bovine pituitary extract, hydrocortisone, transferrin, epinephrine and GA-1000 (Clonetics, Corp.).

2.3 Baa-Lys(FITC)-NLS Treatment

As previously described, a dose response study was conducted to determine Baa concentrations that initiate a toxic response in HEK (Rouse *et al.*, 2006). Based on these

results a Baa-Lys(FITC)-NLS concentration of 0.04 mg/mL was chosen as a low toxic dose for this study. Baa-Lys(FITC)-NLS was added to growth media to create the desired concentration. After reaching about 80% confluency, the cells were dosed with the Baa-Lys(FITC)-NLS treatment and subsequently exposed to either 4 h or 8 h of cyclic strain. Control plates were also dosed with Baa-Lys(FITC)-NLS, but were not exposed to tensile strain. Cell proliferation, lactate dehydrogenase (LDH) release, and cytokine release were assessed at 4, 8, 12, and 24 h time points after the application of the Baa-Lys(FITC)-NLS dose.

2.4 Mechanical Strain

Uniaxial strain (10%; cyclic) was applied at a frequency of 1 Hz to the cell cultures using a Flexercell® Tension Plus™ System from Flexcell International Corp. (Hillsborough, NC). This bioreactor applies strain through a vacuum pressure to cells grown on flexible membrane plates. Flexing began immediately after application of the dose and continued for either 4 h or 8 h. Strain was not applied to cells in the control plates.

2.5 Cell Proliferation Assay

Cellular proliferation was assessed using the CytoTox-ONE™ Homogenous Membrane Integrity Assay (Promega, Madison, WI). This is a fluorescence-based assay that measures LDH release with an enzymatic process that results in the conversion of resazurin into the fluorophore resorufin. LDH is a cytoplasmic enzyme present in a wide variety of cell types that catalyzes the conversion of lactate to pyruvate. After lysing the cells, the amount of fluorescence produced is proportional to the number of lysed cells (Decker and Lohmann-

Matthes, 1988; Korzeniewski and Callewaert, 1983). Therefore, this assay is a convenient method for determining cell proliferation.

At each time point, cells in each treatment plate (4 h strain, 8 h strain, no strain) were rinsed with HBSS and lysed with a 9% solution (weight/volume) of Triton X-100 in water. Medium from the lysed cells was sampled and stored at –80 °C. Later, 100 µL aliquots of cell medium were transferred to black 96-well plates with microclear bottoms (Corning/Costar USA). To begin the enzymatic reaction, 100 µL of the CytoTox-ONE™ reagent was added to each well and the plate was incubated at 22 °C for 10 minutes. Following the incubation period, 50 µL of Stop Solution was added to each well and the fluorescence was determined using a tunable Molecular Dynamics Gemini EM™ microplate reader with an excitation wavelength 560 nm and an emission wavelength of 590 nm. The fluorescence from the culture medium of the lysed cells, referred to herein as the maximum fluorescence, corresponds to the number cells in each well and is used to monitor cell proliferation.

2.6 Membrane Integrity Assay

The CytoTox-ONE™ Homogenous Membrane Integrity Assay was also used to assess membrane integrity as indicated by LDH release. The membrane of healthy cells is mostly impermeable to LDH, whereas LDH is released out of cells with a compromised cell membrane. Therefore, the presence of LDH in culture media can be used an indicator of cellular cytotoxicity (Decker and Lohmann-Matthes, 1988; Korzeniewski and Callewaert, 1993). To test for the presence of LDH in cells exposed to mechanical stimulation and Baa-Lys(FITC)-NLS, medium was sampled at each time point prior to cell lysis and stored at –80 °C until fluorescence readings were recorded similarly to as described above.

2.7 Cytokine Assay

At each time point, growth medium was sampled to quantitate human cytokines IL-1β, IL-6, IL-8, IL-10, and TNF-α using the Bio-Plex suspension array system (Bio-Rad Laboratories, Hercules, CA). This system utilizes multi-plexing to simultaneously assay for cytokines. Customized beads (5.6 μm diameter) conjugated to a capture antibody that is specific to each cytokine, IL-1β, IL-6, IL-8, IL-10, or TNF-α, and possessing a unique spectral address were mixed with culture media and incubated in a 96-well plate. The beads were rinsed and then incubated with a fluorescent-labeled reporter molecule that specifically bound to the analyte. The contents of each well were analyzed in the Bio-Plex array reader. As the beads flow into the reader, one laser identifies the spectral address of each cytokine and the other laser excites the reporter molecule to quantitate the specific cytokine relative to the standard curve. The average concentration (pg/mL) of each cytokine for each treatment and time point were calculated in order to determine the time dependency of the toxicity on HEK.

2.8 Statistical Analysis

HEK proliferation and cytokine concentrations (normalized to proliferation) were statistically compared using ANOVA (SAS 9.1 for Windows, Cary, NC). For each exposure time, multiple comparisons were made between different treatments using the Student's *t*-test at $p < 0.05$.

3. RESULTS

The effects of tensile strain on cellular proliferation are shown in Figure 5.2. The maximum fluorescence corresponds to the levels of LDH present in growth medium after cell

lysis and is a measure of the number of cells in a given well at each time point. Application of mechanical strain for 8 h significantly decreased ($p < 0.05$) HEK proliferation in comparison to 4 h strained and unstrained cells at 12 h and 24 h. By 24 h, HEK exposed to 4 h of strain also statistically decreased ($p < 0.05$) cell proliferation in comparison to control cells.

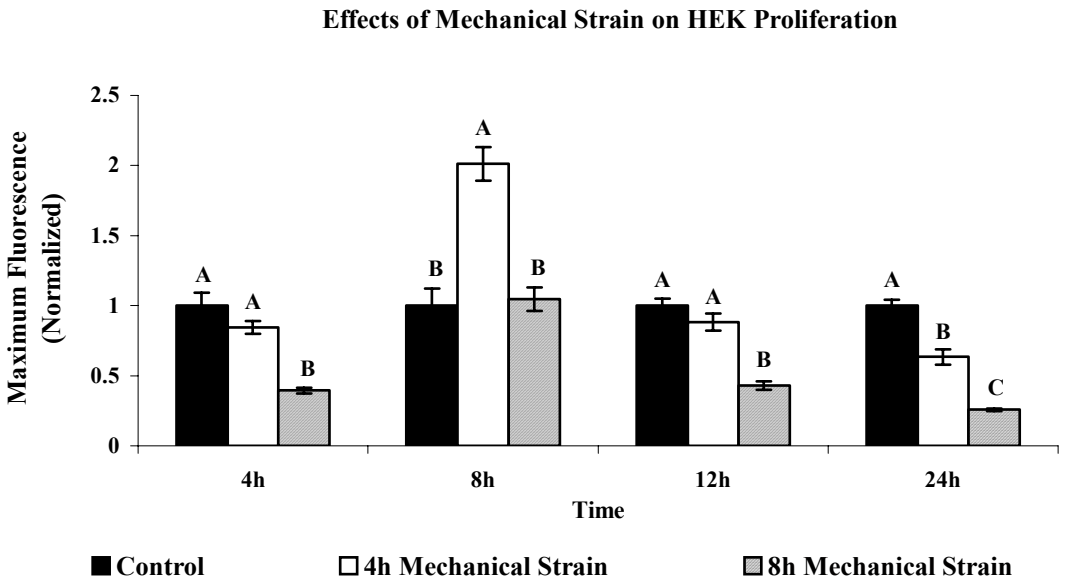

Figure 5.2. HEK proliferation, corresponding to LDH content in the medium of lysed cells. Histogram with different letters (A, B, C) denote fluorescence values that are significantly different at $p < 0.05$

LDH release by HEK was used to examine changes in cellular membrane integrity in response to mechanical stimulation (Figure 5.3). At 12 h and 24 h, cell medium of HEK that had been exposed to 8 h of mechanical strain contained a significantly ($p < 0.05$) higher amount of LDH than that of unstrained cells and cells exposed to only 4 h of strain.

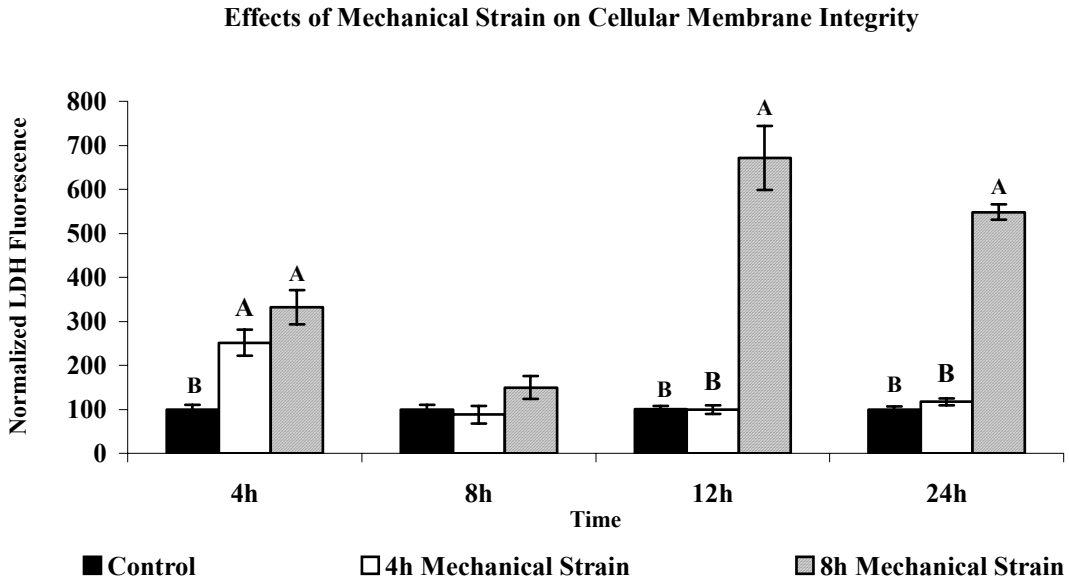

Figure 5.3. LDH release by HEK was monitored throughout the 24 h time period and used as an indicator of cell membrane integrity. Histogram with different letters (A, B) denote fluorescence values that are significantly different at $p < 0.05$

IL-8 release increased slightly with time (Figure 5.4). At 12 h, IL-8 concentration for cells exposed to 8 h of strain peaked and was statistically different ($p < 0.05$) from control and all other treatments and continued to be higher through 24 h. Beginning at the 8 h time point, HEK release of IL-6 increased with time for control and strained cells (Figure 5.5). HEK exposed to tensile strain for 8 h, however, showed a statistically greater ($p < 0.05$) amount of IL-6 than 4 h strained and unstrained cells at 12 h and 24 h. Similarly, IL-1β release was significantly greater ($p < 0.05$) for cells strained for 8 h at the 12 h and 24 h time points (Figure 5.6).

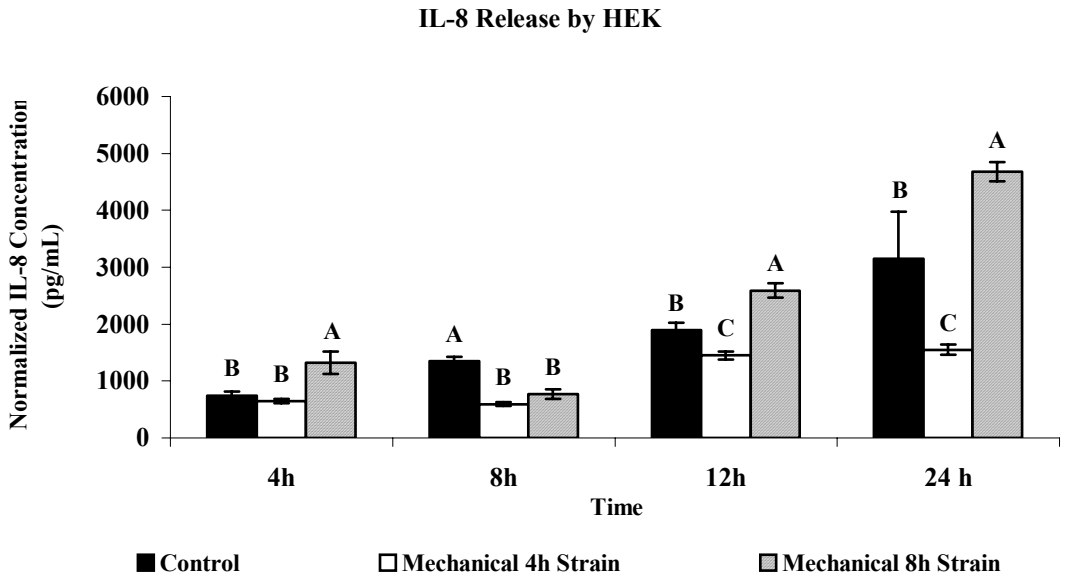

Figure 5.4. IL-8 release in HEK exposed to Baa-Lys(FITC)-NLS and mechanical strain. Histogram with different letters (A, B, C) denote mean values that are statistically different at $p < 0.05$.

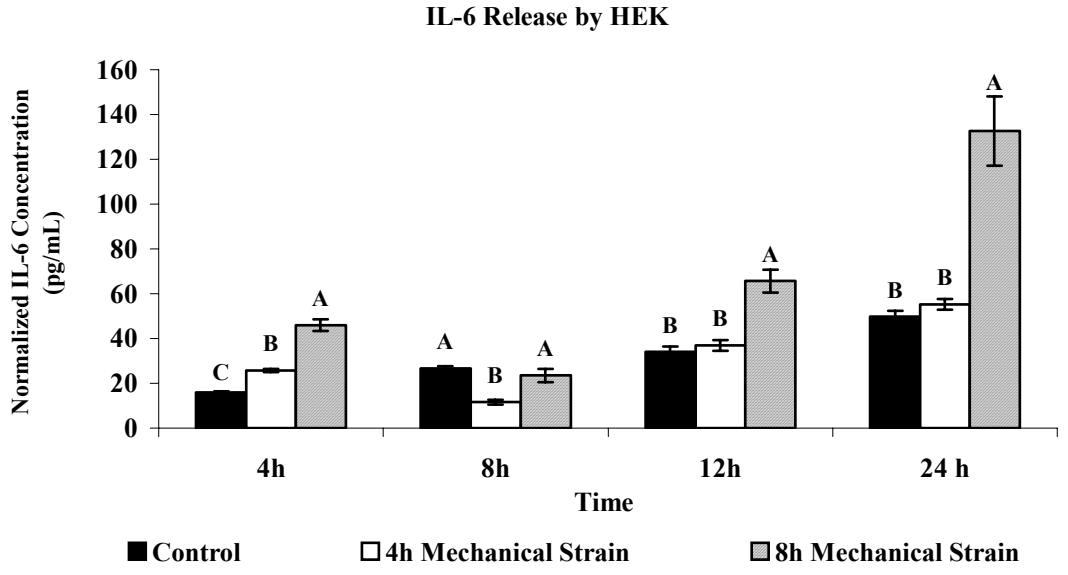

Figure 5.5. IL-6 release in HEK exposed to Baa-Lys(FITC)-NLS and mechanical strain. Histogram with different letters (A, B, C) denote mean values that are statistically different at $p < 0.05$.

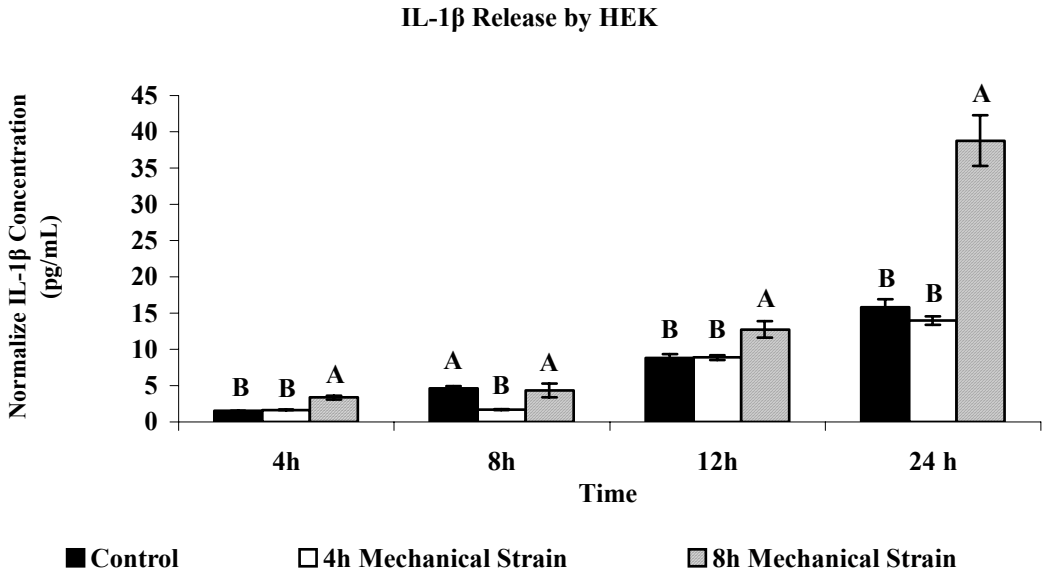

Figure 5.6. IL-1β release in HEK exposed to Baa-Lys(FITC)-NLS and mechanical strain. Histogram with different letters (A, B, C) denote mean values that are statistically different at $p < 0.05$.

4. DISCUSSION

The unique interactions between nanostructures and the biological environment afford them great potential for use in novel pharmaceutical and biomedical applications. Understanding the mechanisms that are involved with nano-drug delivery systems and external factors that influence their cellular interactions are essential for the development of these applications. According to the results of this study, exposure of HEK to cyclic tensile strain for 8 h decreased cellular proliferation and membrane integrity in comparison to unstrained cells. Additionally, cells strained for 8 h showed an increase in the proinflammatory cytokines IL-8, IL-6, and IL-1β release by 12 h. HEK strained for 4 h also exhibited a decrease in cellular proliferation at 24 h in comparison to controls; however, decreased proliferation was not accompanied by an increased release of LDH or cytokines. These results suggest that long-term exposure of HEK to 10% cyclic tensile strain and Baa-

Lys(FITC)-NLS are capable of decreasing cellular proliferation and initiating an inflammatory response over a 24 h time period.

Previous studies have recently reported the interactions between HEK and fullerene-based amino acid nanoparticles (Monteiro-Riviere *et al.*, 2006; Rouse *et al.*, 2006). In both of these investigations, cytotoxicity and inflammatory responses were shown to increase with increasing concentration of nanoparticle dose, similarly to the findings reported here where exposure of HEK to mechanical strain and Baa-Lys(FITC)-NLS decreased cell proliferation and increased cytokine release. However, cells exposed to 8 h of mechanical strain and Baa-Lys(FITC)-NLS showed an approximate five-fold increase in IL-8 and a ten-fold increase in IL-1β production in comparison to the previously reported results. Contrastingly, IL-6 up-regulation was substantially less in the present study than in the studies reported by Monteiro-Riviere and Rouse. Since IL-6 can be indicative of cellular proliferation, the relatively smaller increase in production of this cytokine suggests that fullerene exposure in combination with mechanical strain inhibits cellular growth and development more than exposure to fullerenes alone. Additionally, the significantly greater production of IL-8 and IL-1β suggests that together mechanical strain and fullerene exposures initiate a stronger inflammatory response than the response initiated solely by fullerene exposure.

Although the results of this study indicate that treatment with Baa-Lys(FITC)-NLS and mechanical strain can decrease cell proliferation, decrease membrane integrity, and increase the release of proinflammatory cytokines, it is not clear as to whether these responses are caused by the direct effects of mechanical stimulation or the ability of mechanical stimulation to increase cellular interactions with the fullerene nanoparticles. In order to clarify the factors responsible for the cellular responses seen in this study, it is

necessary to first examine the effects that tensile strain alone have on HEK proliferation, membrane integrity, and cytokine release. Knowing how cyclic tensile strain affects these cellular activities, one can then determine if mechanical loading effects cellular interactions with nanoparticles.

The fluorophores resorufin, whose production is catalyzed by the presence of LDH, and fluorescein isothiocyanate (FITC), which is used to fluorescently label Baa, have overlapping excitation and emission spectra. Therefore, it is possible that the fluorescence data collected by setting the excitation and emission wavelengths for resorufin may contain interfering signals due to the simultaneous excitation and emission of FITC. Presently, it is unclear what percentage of maximum FITC fluorescence occurs at the excitation and emission wavelengths used in the CytoTox-ONE^{TM} Homogeneous Membrane Integrity Assay; however, future studies should either account for the overlapping spectra of the two fluorophores or determine an alternative method for evaluating cell proliferation or viability.

Despite the aforementioned drawbacks of this study, it is possible to speculate about the cellular interactions between HEK and Baa-Lys(FITC)-NLS nanoparticles in the presence of mechanical stimulation based on these and previously reported results. It seems likely that the decreased proliferation of cells exposed to 8 h of tensile strain at 12 and 24 h (evident in Figure 5.3 by significantly decreased maximum fluorescence values) is primarily the result of mechanical stimulation acting to amplify interactions between HEK and Baa-Lys(FITC)-NLS. Previous studies done to investigate the effects of tensile strain on keratinocyte proliferation have shown opposite results to the ones presented in this study, in that exposure of cell cultures to strain-induced deformation increases proliferation (Takei *et al.*, 1997; Yano et al, 2004). Conversely, in the absence of mechanical stimulation, Baa-Lys(FITC)-

NLS has been shown to decrease cell viability and initiate an inflammatory response in HEK (Monteiro-Riviere *et al.*, 2006; Rouse *et al.*, 2006). Taken together, these results allow one to postulate that the decrease in cell proliferation and membrane integrity reported in this study are due to the combined effects of tensile strain and Baa-Lys(FITC)-NLS exposure. It seems quite possible that exposure of HEK to tensile strain for an 8 h time period is capable of increasing cellular uptake of fullerene nanoparticles, which at toxic concentrations leads to an up-regulation of cytokine synthesis and release. These results are applicable to a lesser extent for cells exposed to 4 h of mechanical stimulation. As previously mentioned, however, these conclusions are based on pilot studies and are merely speculations. Further testing is needed to clearly solidify the effects that mechanical loading have on nanoparticle interactions with keratinocytes (see *Future Directions*).

Although the results of this study are somewhat inconclusive in determining the effects of strain-induced deformation on nanoparticle interactions with HEK, these preliminary findings do provide sufficient evidence that exposure to mechanical stimulation and fullerene-derivatized amino acids, in combination, alters normal cellular activities. Furthermore, these findings warrant future investigations to further analyze the effects of mechanotransduction on cellular membrane permeability and subsequent interactions with nanoparticles. Understanding these mechanisms is crucial for the development of nano-applications with biological implications as well as for the establishment of safety guidelines to regulate the potentially harmful risks associated with over-exposure to nanoparticles.

5. REFERENCES

Barkhausen, T.; van Griensven, M.; Zeichen, J.; Bosch, U. (2003) Modulation of cell functions of human tendon fibroblasts by different repetitive cyclic mechanical stress paterns. *Experimental Toxicology and Pathology*, 55: 153-158.

Chen, C.S.; Mrksich, M.; Huang, S.; Whitesides, G.M.; Ingber, D.E. (1997) Geometric control of cell life and death. *Science*, 276(5317): 1425-1428.

Chiquet, M., Matthison, M., Koch, M., Tannheimer, M., Chiquet- Ehrismann, R., 1996. Regulation of extracellular matrix synthesis by mechanical stress. *Biochemistry and Cell Biology* 74, 737-744.

Decker, T.; Lohmann-Matthes, M.L. (1988) A quick and simple method for the quantitation of lactate dehydrogenase release in measurements of cellular cytotoxicity and tumor necrosis factor (TNF) activity. *Journal of Immunological Methods*, 15: 61-69.

Huang, S.; Ingber, D.E. (1999) The structural and mechanical complexity of cell-growth control. *Nature Cell Biology,* 1(5): E131-E138.

Ingber, D.E. (1991) Integrins as mechanochemical transducers. *Current Opinion in Cell Biology*, 3: 841-848.

Ingber, D.E. (1998) Cellular basis of mechanotranduction. *Biological Bulletin*, 194: 323-327.

Kasper, D.; Seidl, W.; Neidlinger-Wilke, C.; Ignatius, A.; Claes, L. (2000) Dynamic cell stretching increases human osteoblast proliferation and CICP synthesis but decreases osteocalcin synthesis and alkaline phosphatase activity. *Journal of Biomechanics*, 33(1): 45-51.

Korzeniewski, C.; Callewaert, D.M. (1983) An enzyme-release assay for natural cytotoxicity. *Journal of Immunological Methods*, 64: 313-320.

Lee, R.T.; Briggs, W.H.; Cheng, G.C.; Rossiter, H.B.; Libby, P.; Kupper, T.S. (1997) Mechanical deformation promotes secretion of IL-1α and IL-1 receptor antagonist. *Journal of Immunology*, 5084-5088.

Liu, S.; Calderwood, D.A.; Ginsberg, M.H. (2000) Integrin cytoplasmic domain-binding proteins. *Journal of Cell Science*, 113: 3565-3571.

Loboa, E.G.; Fang, T.D.; Warren, S.M.; Lindsey, D.P.; Fong, K.D.; Longaker, M.T.; Carter, D.R. (2004) Mechanobiology of mandibular distraction osteogenesis: experimental analyses with a rat model. *Bone*, 34(2): 336-343.

Monteiro-Riviere, N. A.; Yang, J.; Inman, A. O.; Ryman-Rasmussen, J. P.; Barron, A. R.; Riviere, J. E. Skin penetration of fullerene substituted amino acids and their interactions with

human epidermal keratinocytes, 827, *The Toxicologist CD – An official Journal of the Society of Toxicology*, Volume 90, Number S-1, March 2006.

Rouse, J.G.; Yang, J.; Barron, A.R.; Monteiro-Riviere, N.A. (2006) Fullerene-based amino acid interactions with human epidermal keratinocytes. *Toxicology In Vitro*, 20: 1313-1320.

Rouse, J.G.; Yang, J.; Ryman-Rasmussen, J.P.; Barron, A.R.; Monteiro-Riviere (2007) Effects of mechanical flexion on the penetration of fullerene amino acid-derived peptide nanoparticles through skin. *Nano Letters*, 7(1): 155-160.

Sumanasinghe, R.D.; Bernacki, S.H.; Loboa, E.G. (2006) Osteogenic differentiation of human mesenchymal stem cells in collagen matrices: effect of uniaxial cyclic tensile strain on bone morphogenetic protein (BMP-2) mRNA expression. *Tissue Engineering*, 12(12): in press.

Takei, T.; Kito, H.; Du, W.; Mills, I.; Sumpio, B.E. (1998) Induction of interleukin (IL)-1α and β gene expression in human epidermal keratinocytes exposed to repetitive strain: their role in strain-induced proliferation and morphological change. *Journal of Cellular Biochemistry*, 69: 95-103.

Takei, T.; Rivas-Gotz, C.; Delling, C.A.; Koo, J.T.; Mills, I.; McCarthy, T.L.; Centrella, M.; Sumpio, B.E. (1997) Effect of strain on human keratinocytes *in vitro. Journal of Cellular Physiology*, 173: 64-72.

Trachslin, J.; Koch, M.; Chiquet, M. (1999) Rapid and reversible regulation of collagen XII expression by changes in tensile stress. *Experimental Cell Research*, 247: 320-328.

Tsai, J.; Guy, R.H.; Thornfield, C.R.; Gao, W.N.; Feingold, K.R.; Elias, P.M. (1995) Metabolic approaches to enhance transdermal drug delivery. 1. Effect of lipid synthesis inhibitors. *Journal of Pharmaceutical Sciences*, 85: 643-648.

Wang, J.H.-C.; Thampatty, B.P. (2006) An introductory review of cell mechanobiology. *Biomechanics and Modeling in Mechanobiology*, 5: 1-16.

Yang, J. and Barron, A.R. (2004) A new route to fullerene substituted phenylalanine derivatives, *Chemical Communications*, pp. 2884–2885.

Yang, J.; Alemany, L.B.; Driver, J.; Hartgerink, J.D.; Barron, A.R. (2007a) Fullerene-derivatized amino acids: synthesis, characterization, antioxidant properties, and solid-phase peptide synthesis. *Chemistry – A European Journal*, in press.

Yang, J.; Wang, K.; Driver, J.; Yang, J.; Barron, A.R. (2007b) The use of fullerene substituted phenylalanine amino acid as a passport for peptides through cell membranes. *Organic & Biomolecular Chemistry*, 5: 260-266.

Yano, S.; Komine, M.; Fujimoto, M.; Okochis, H.; Tamaki, K. (2004) Mechanical stretching *in vitro* regulates signal transduction pathways and cellular proliferation of human epidermal keratinocytes. *Journal of Investigative Dermatology*, 122: 783-790.

CHAPTER 6: CONCLUSIONS

The biological interactions of nanoparticles, both at the tissue and cellular levels, are dictated by the unique physiochemical properties inherent of nano-sized structures. These characteristics afford nanomaterials the ability to be used in a variety of pharmaceutical and biomedical applications involving drug-delivery, imaging, and diagnostic agents. The development of these potentially revolutionizing treatments, however, is dependent on understanding the mechanisms of interaction between the nanostructures and biological environment. Additionally, since recent research has reported the potential cytotoxicity of many types of nanoparticles, it is also important to fully understand mechanisms of toxicity and to be able to establish regulations that ensure the development of safe manufacturing processes and applications for consumer use.

The first study presented in this thesis described the normal interactions that occur between Bucky amino acid (Baa) and human epidermal keratinocytes (HEK). These results showed that the fullerene-based amino acids are capable of entering keratinocytes and becoming localized in cytoplasmic vacuoles. Once in the cells, higher concentrations of Baa are capable of decreasing cell viability and initiating the release of the proinflammatory cytokines IL-8, IL-6, and IL-1β. The ability of Baa to enter cells is advantageous for the development of nano-drug delivery systems; however, these results identify the importance of nanoparticle concentration and exposure time on cytotoxicity.

Mechanical stress is an important factor in the regulation of fundamental events to maintain tissue and cellular homeostasis. When investigating interactions between nanoparticles and the biological environment, it is important to consider the presence of normal physiological mechanical stimuli that are capable of altering tissue and cellular

activities. These concepts are portrayed by the research presented in Chapter 4. This study showed that repetitive mechanical flexion applied to skin can increase the penetration of Baa-Lys(FITC)-NLS. This compound contains the Bucky amino acid, Baa, with a nuclear localization sequence (NLS) marker, which targets the fullerene to the cell nucleus, and a fluorescein isothiocyanate (FITC) label, which allows for tracking and visualization of the particle via fluorescence microscopy. The ability of Baa-Lys(FITC)-NLS to penetrate intact skin and the discovery that external mechanical stimulation can increase the rate and extent of dermal penetration has profound implications for the development of this particle for use in transepidermal drug delivery systems. Especially important for pharmaceutical applications, is the mechanism by which nanoparticles traverse the epidermal barrier, which according to this study appears to occur via passive diffusion through the intercellular lipids. Additional testing, however, is needed to clearly define the mechanisms by which nanoparticles penetrate into skin cells and the physical and chemical parameters that are responsible for compromising the barrier function of the epidermis. The results from this research also exposed the risks that are associated with nanoparticle manufacturing and consumer processes that involve repetitive motion. Until risk assessments are conducted to determine biological tolerance levels and regulations are established to set safety limits on nanoparticle exposure, caution should be used when encountering repetitive exposure to nanomaterials.

The discovery that repetitive flexing increases the penetration of fullerene-derived amino acids through intact skin led way to an investigation to determine cellular responses prompted by mechanical stimulation. The pilot study, reported in Chapter 5, attempted to establish a relationship between the application of cyclic tensile strain and nanoparticle

interactions with HEK. Although these were preliminary findings, results showed that exposure of HEK to Baa-Lys(FITC)-NLS and tensile strain decreased cellular proliferation and initiated an inflammatory response. However, it was not possible to determine whether these responses were caused by the direct effects of mechanical stimulation or by the ability of tensile strain to increase cellular interactions with the fullerene nanoparticles. Further studies are needed to delineate how mechanotransduction signaling pathways alter cellular viability and the inflammatory response in HEK and how these biochemical processes effect the biological interactions of nanoparticles at the cellular level.

Future Directions

In order to clearly define the mechanisms by which repetitive mechanical flexion increases nanoparticle penetration, further investigations should be conducted to quantitate the levels of stress and strain that are responsible for increased penetration. The flexing apparatus used in the current study attempted to simulate repetitive wrist movement; however, no measures were taken to quantitate the actual forces applied to the skin as a result of the motion. Knowledge of the applied forces, in combination with the physical parameters of the skin, could permit the development of a mathematical model to predict the level of stress required to compromise the barrier function of skin. Another limiting factor of the current study was the inability to quantitate the amount of fullerene nanoparticles that penetrated the intact skin. The data collected consisted of qualitative data, both from confocal and TEM images; however, attempts to quantitatively measure the fluorescence of the absorbed FITC-labeled fullerene were unsuccessful. The inability to detect Baa-Lys(FITC)-NLS in the perfusate of the flow-through diffusion cells suggests that only a small amount of fullerenes were actually absorbed through the skin and that most of the nanoparticles

remained lodged in the epidermal and dermal layers. Increased exposure time may increase the ability of nanoparticles to be absorbed through skin; however, construction of a model to predict the dependence of nanoparticle penetration on mechanical loading is largely reliant on the ability to quantitatively measure the percentage of the dose that penetrates the epidermal barrier.

Further investigations are also needed to evaluate the effects of mechanical loading on nanoparticle interactions at the cellular level. The pilot study reported above shows that tensile strain does exert some effect on cellular proliferation, membrane integrity, and cytokine release; however, it is unclear as to whether these altered activities are the direct result of tensile strain or due to the increased ability of fullerenes to interact with HEK in the presence of mechanical stimulation. To delineate the two possibilities, future studies should first determine the effects that different magnitudes of tensile strain (i.e. 10%, 12%, etc.) alone have on cellular viability and cytokine expression. Subsequent investigations can then compare proliferation/viability, membrane integrity, and cytokine regulation of cells treated with Baa-Lys(FITC)-NLS to determine if tensile strain is responsible for the altered interactions of nanoparticles with HEK. Additionally, studies should include new assays and TEM to compare cellular uptake of the Baa-Lys(FITC)-NLS in the presence and absence of mechanical stimulation. The ability of tensile strain to increase cellular uptake of nanoparticles could have profound effects on the ability of pharmaceutical drugs to interact with their therapeutic targets.

For the development of nanoparticle applications involving biological interactions, it is necessary to completely understand the basic mechanisms of interaction that occur between nanomaterials and the biological environment. The research presented in this thesis

identifies important factors that contribute to biological interactions with nanoparticles that are important for the development of nano-applications as well as for the establishment of safety regulations to govern nanoparticle manufacturing and consumer processes. Eventually, these studies and those of similar nature will lead way to *in vivo* investigations of nanomaterial interactions with the biological environment. Such knowledge is necessary for the advancement of nanotechnology and will lead way for the discovery and development of biomedical applications that will ultimately transform the medical and pharmaceutical worlds.